RESONANT TERAHERTZ (THz) GENERATION BY INTERACTION OF HIGH-POWER LASER IN PLASMA

Thesis Submitted for the Award of the Degree of

DOCTOR OF PHILOSOPHY

in

Physics

By

Hitesh Kumar Midha

Registration Number: 41900652

Supervised By

Dr. Vishal Thakur (17014)

Department of Physics (Professor)

Lovely Professional University, Punjab

Co-Supervised by

Dr. Niti Kant

Department of Physics (Associate Professor)

University of Allahabad, Prayagraj

Co-Supervised by

Dr. Alka

Research Associate, THz Sources Group,

Secondary Sources Division,

ELI-ALPS, ELI-HU Non-Profit Ltd.,

Wolfgang Sandner Utca 3., Szeged 6728,

Hungary

LOVELY PROFESSIONAL UNIVERSITY, PUNJAB

2025

DECLARATION

I, hereby declared that the presented work in the thesis entitled "Resonant Terahertz (THz) generation by interaction of high-power laser in plasma." in fulfilment of degree of **Doctor of Philosophy (Ph. D.)** is outcome of research work carried out by me under the supervision of **Dr. Vishal Thakur**, working as Professor, in the Department of Physics, School of Chemical and Physical Sciences of Lovely Professional University, Punjab, India, and under the co-supervision of **Dr. Niti Kant**, Associate Professor, University of Allahabad, Prayagraj, Uttar Pradesh, India, and **Dr. Alka Mehta**, Research Associate, THz Sources Group, Secondary Sources Division, ELI-ALPS, ELI-HU Non-Profit Ltd., Wolfgang Sandner Utca 3., Szeged 6728, Hungary. In keeping with general practice of reporting scientific observations, due acknowledgements have been made whenever work described here has been based on findings of another investigator. This work has not been submitted in part or full to any other University or Institute for the award of any degree.

(Signature of Scholar)

Name of the scholar: Hitesh Kumar Midha

Registration No.: 41900652

Department/school: Department of Physics, School of Chemical and Physical Sciences

Lovely Professional University,

Punjab, India

CERTIFICATE

This is to certify that the work reported in the Ph. D. thesis entitled "Resonant Terahertz (THz) generation by interaction of high-power laser in plasma" submitted in fulfillment of the requirement for the award of degree of **Doctor of Philosophy (Ph.D.)** in the Department of Physics, School of Chemical and Physical Sciences, is a research work carried out by **Hitesh Kumar Midha**, 41900652, is bonafide record of his original work carried out under my supervision and that no part of thesis has been submitted for any other degree, diploma or equivalent course.

Signature of Supervisor

Dr. Vishal Thakur (17014)

Department of Physics (Professor)

Lovely Professional university, Phagwara, Punjab, India.

Signature of Co-Supervisor

Dr. Niti Kant

Department of Physics (Associate Professor)

University of Allahabad, Prayagraj,

Uttar Pradesh, India

Signature of Co-Supervisor

Dr. Alka Mehta

Research Associate, THz Sources Group,

Secondary Sources Division, ELI-ALPS,

ELI-HU Non-Profit Ltd., Wolfgang Sandner

Utca 3., Szeged 6728, Hungary

Abstract

The "terahertz gap" refers to a portion of the electromagnetic spectrum that lies between the microwave and infrared frequency ranges, typically spanning from around 0.1 to 10 terahertz (THz), corresponding to wavelengths between 30 micro meters and 3 milli meters. This frequency range is often considered challenging to work with due to technical limitations in both generating and detecting terahertz waves.

The terahertz gap has historically been difficult to address because traditional electronic and optical techniques have limitations in this frequency range. Microwaves are typically generated and detected using electronic components such as antennas and transistors, while infrared waves are manipulated using optical techniques like lenses and mirrors. Terahertz waves require a combination of both electronic and optical methods, making their generation and detection more complex.

However, in recent years, significant progress has been made in terahertz technology, leading to new opportunities for applications and research. Advances in femtosecond laser technology, nonlinear optical processes, and new materials have enabled the development of terahertz sources and detectors. These advancements have the potential to bridge the terahertz gap and open up a wide range of applications.

In the first objective efficient THz generation by Hermite-cosh-Gaussian lasers in plasma with slanting density modulation is investigated**.** Terahertz (THz) has emerged as a significant field of study because to its extensive practical applications in various domains such as medical diagnosis, remote sensing, defence, and short-range wireless communication, among others. Numerous endeavours have been undertaken to achieve a tuneable and energy-efficient terahertz (THz) source. This study examines the co-propagation of two Hermite-cosh-Gaussian (HchG) laser pulses within an under dense plasma medium characterised by a slanting up density profile. The interaction between laser and plasma exhibits nonlinear characteristics, leading to the creation of THz radiation with high efficiency. An analytical study is conducted to examine the relationship between the conversion efficiency of terahertz (THz) waves and characteristics such as plasma frequency, Hermite polynomial mode index (s), decentred parameter (b), and electron collisional frequency (γ_{en}). The results show that as we move

in off-resonant direction, THz conversion efficiency decreases and becomes almost zero for normalized THz frequency and normalized collisional frequency values > 1.6 and > 4 respectively. THz conversion efficiency increases with increase in Hermite polynomial mode index values for $s= 0,1,2$. The suggested method is particularly useful for producing high intensity, tuneable, energy efficient THz radiation source by adjusting the value of decentred parameter and Hermite polynomial mode index values.

In the second objective the resonant terahertz radiation by p-polarized chirped laser in hot plasma with slanting density modulation is analysed. The production of terahertz (THz) radiation via the interaction between lasers and plasmas is an intriguing and swiftly progressing domain of study within the realms of optics and plasma physics. The aforementioned procedure entails the utilisation of high-intensity laser pulses to engage with a plasma, hence leading to the generation of coherent THz radiation. THz radiation, which falls within the frequency range between microwave and infrared, finds utility in various domains such as imaging, spectroscopy, and materials characterization. This study examines the interaction of two p-polarised, positively chirped laser beams, with a hot collisional plasma characterised by a slanting up density profile. This study investigates the impact of normalised THz frequency, normalised collisional frequency, chirp parameter, and incidence angle of a laser beam on the normalised THz amplitude. The amplitude of the THz signal diminishes fast in off-resonant conditions and tends towards zero as the normalised THz frequency exceeds 1.2. The normalised amplitude of the THz wave falls as the chirp parameter increases from $0.0011\ to\ 0.0099$, considering both the normalised THz frequency and the normalised slanting up density modulation parameter. The amplitude of the THz signal, after being normalised, is also influenced by the incident angle and the collisional frequency. In the off-resonant state, the normalised amplitude of the THz wave tends to approach zero when the collisional frequency exceeds 0.8. The objective of this study is to enhance the current knowledge regarding the estimation of the best incident oblique angle, chirp parameter, and collisional frequency to attain an energy-efficient THz source.

In the third objective enhanced THz generation by Hermite-cosh-Gaussian chirped laser in static magnetized plasma is studied. The investigation of tuneable and energy-efficient terahertz (THz) generation has become a prominent field of study due to its significant ramifications in various disciplines, including defence and medical research. This study

selects two co-propagating Hermite-cosh-Gaussian (HchG) laser beams with positively chirped frequencies for analysis. The laser beam exhibits interaction with a collisionless undersense plasma in the presence of a static transverse magnetic field. The interaction between laser and plasma exhibits nonlinear characteristics, leading to the creation of THz radiation with high energy efficiency. This study focuses on the analytical investigation of the relationship between THz conversion efficiency, normalised transverse distance and plasma frequency, as well as other laser parameters such as Hermite polynomial mode index (s), decentred parameter (a), and frequency chirp (b). The results show that THz conversion efficiency quickly decreases for normalised THz frequencies when the condition is off resonant. It nearly reaches zero. An increase in normalized THz amplitude and a shift in the peak towards higher normalized transverse distance values are seen as the Hermite polynomial mode index is varied from 0 to 2. As we raise the chirp parameter from 0.0011 to 0.0099 for s=0,1,2, the normalised THz amplitude increases. The proposed methodology demonstrates significant use in generating high-intensity, adjustable, and energy-efficient terahertz (THz) radiation sources through the manipulation of the decentred parameter and Hermite polynomial mode index values.

Acknowledgements

Above all, I would like to express my profound thanks to the **God** for granting me the ability to work hard and stay focused, enabling me to take full advantage of the chances presented to me and achieve academic brilliance.

I express my deep appreciation to my respected mentor and research supervisor, **Dr. Vishal Thakur**, Professor in the Department of Physics at Lovely Professional University, Punjab. I am grateful for his consistent support, invaluable guidance, and encouraging cooperation in helping me comprehend the intricacies of research and successfully completing my research project with utmost satisfaction. Their cooperative methodology and fervour for investigating novel concepts were a consistent wellspring of inspiration and drive for me.

I am grateful to my Co-supervisor **Dr. Niti Kant**, an Associate Professor in the Department of Physics at Allahabad University, Prayagraj, Uttar Pradesh. His words of support provided continuous motivation during the entire duration of my research endeavour. Their profound knowledge, unwavering perseverance, and unwavering commitment had a pivotal role in influencing the trajectory of my career and guiding me through the obstacles.

I would like to express my sincere gratitude to my Co-supervisor, **Dr. Alka Mehta**, Research Associate, THz Sources Group, Secondary Sources Division, ELI-ALPS, ELI-HU Non-Profit Ltd., Wolfgang Sandner Utca 3., Szeged 6728, Hungary for his unwavering support, and meticulous guidance throughout the entire process of my work, ensuring that I stayed on the correct path to successfully achieve my desired goal.

Lastly, I am grateful to my **family and friends** for their unwavering encouragement during the research's preparatory phase.

Hitesh Kumar Midha

Contents

List of figures

CHAPTER- 1

Introduction

1.1 Terahertz gap

In the electromagnetic spectrum, the region roughly between 0.1 THz to 10 THz is known as terahertz region which covers high frequency microwave band and long wavelength infrared region of spectrum. This zone bridges the gap between optics and electronics, so opens the wide horizons for optoelectronics stream in physics, chemistry, life sciences and applied sciences. These waves are invisible to necked human eyes and nonionizing for in nature [1].

1.2 Terahertz waves properties

Terahertz (THz) waves, alternatively referred to as T-rays or submillimeter radiation, are situated within the electromagnetic spectrum, spanning from microwaves to infrared light. The wavelengths of these entities span at around 1 millimeter to 100 micrometers, while their frequencies range from 0.3 to 3 THz. The following are essential characteristics of terahertz waves:

1.2.1 Frequency range

Terahertz waves typically have frequencies ranging from 0.3 to 3 THz, which corresponds to wavelengths ranging from 1 millimeter to 100 micrometers. Terahertz radiation possesses the ability to penetrate a diverse range of non-conducting substances, including plastics, textiles, paper, ceramics, and composites. This characteristic renders it valuable for imaging purposes in several domains such as security screening, quality control, and medical diagnostics.

1.2.2 Non-ionizing characteristic

In contrast to X-rays, terahertz radiation exhibits a non-ionizing nature, indicating that it lacks the necessary energy to induce ionisation in atoms or molecules. Compared to X-rays, this characteristic enhances the safety of imaging applications. Dielectric sensing involves the utilisation of terahertz waves to detect alterations in material composition and structure, as these waves exhibit sensitivity towards the

dielectric characteristics of materials. This characteristic renders them valuable for applications involving quality control and material characterisation.

The penetrating depth of terahertz waves is constrained in the majority of materials as a result of their absorption by water vapour and certain other compounds. The efficacy of imaging through thick or dense materials is constrained by this limitation.

1.2.3 Spectral signatures

Various materials exhibit distinct absorption spectra within the terahertz region, enabling the application of spectroscopic techniques for the purpose of substance investigation and identification. The utilisation of this characteristic is observed in various domains, including pharmaceutical analysis and security screening. The synthesis and detection of terahertz waves can be achieved by a range of methods, such as optical rectification, frequency difference generation, and the utilisation of photoconductive antennas. Sensitive electronic devices, such as Schottky diodes, field-effect transistors, or superconducting devices, are commonly employed for detection purposes.

Terahertz waves have various uses in domains such as imaging and sensing, spectroscopy, telecommunication, and security screening. Medical imaging, pharmaceuticals, semiconductor characterization, and non-destructive testing are among the various domains in which they find application.

1.3 THz wave applications

Terahertz (THz) waves, also known as submillimeter waves, occupy a unique frequency range between microwaves and infrared light. Terahertz waves possess distinctive characteristics that render them highly advantageous for a wide range of applications, especially in domains that necessitate non-destructive testing and imaging. It is anticipated that ongoing study and breakthroughs in technology will continue to enhance their applicability across several domains. They have a wide range of applications across various fields due to their ability to interact with materials in ways that other forms of radiation cannot. Some notable applications of terahertz waves include:

1.3.1 Spectroscopy

THz Spectroscopy: THz waves can reveal the vibrational and rotational transitions of molecules. This is particularly useful for identifying and characterizing chemical compounds in gases, liquids, and solids.

1.3.2 Material analysis

THz waves can penetrate various materials, allowing for non-destructive testing and quality control in industries like pharmaceuticals, agriculture, and food processing.

1.3.3 Art conservation

THz spectroscopy can help analyze the layers and composition of artworks without damaging them.

1.3.4 THz imaging

Terahertz imaging provides unique contrast for materials with varying refractive indices and absorption properties. It's used for security screening, medical imaging, and quality control in industries like aerospace and electronics manufacturing.
Medical Imaging: THz imaging has potential applications in imaging biological tissues, such as detecting skin cancer or studying teeth and bones.

1.3.5 Communication

THz waves offer the potential for extremely high data rates in wireless communication due to their wide available bandwidth. This could revolutionize wireless communication, enabling faster downloads and improved connectivity.

1.3.6 Security and defense

THz Imaging for Security Screening: THz waves can reveal hidden objects under clothing, making them useful for airport security and other screening applications.

1.3.7 Chemical detection

THz waves can identify specific chemicals or explosives by their unique spectral fingerprints.

1.3.8 Manufacturing and quality control

Pharmaceutical Industry: Terahertz waves can be employed to assess the crystallinity and composition of medicinal goods, thereby ensuring their quality and efficacy. Semiconductor Industry: THz waves can characterize the properties of semiconductor materials and devices, aiding in research and development.

1.3.9 Astronomy and space exploration

Astronomical Observation: THz waves can reveal information about the interstellar medium, star formation, and the early universe, as well as provide insights into planetary atmospheres.

Planetary Exploration: THz spectroscopy can be used to analyze the composition of planetary surfaces and atmospheres in space missions.

1.3.10 Non-destructive testing

Industrial Inspection: THz waves can detect defects, such as cracks or voids, in materials used in industries like aerospace, automotive, and construction.

1.3.11 Biological and medical research

Biological Imaging: THz waves can provide information about water content, cell structure, and other biological properties, aiding in the study of tissues and cells.
Protein Dynamics: THz waves can reveal the dynamics of proteins and biomolecules, contributing to understanding biological processes.

1.3.12 Terahertz spectroscopy for cultural heritage

Art and Artifact Analysis: THz waves can help uncover hidden layers, repairs, or alterations in historical artifacts, paintings, and sculptures.
These applications demonstrate the versatility and potential impact of terahertz waves across diverse fields. Continued research and technological advancements in terahertz technology are likely to lead to even more innovative applications in the future.

These terahertz waves (T-waves, T-light) have hidden potential for applications in the field of explosive detection[2], short distance wireless communication and sensing, remote sensing, defense[3], material characterization[4], biological and chemical imaging[5], high field condensed matter studies[6], non-destructive testing [7], ultrafast magnetic switching[7]etc. Because of wide range applications, scientists show their keen interest in research and development of THz field generation, detection and application from the last two decades.

1.4 Challenges

Terahertz technologies encounter obstacles pertaining to the efficient generation and detection of terahertz waves, addressing the constrained penetration depth, and devising practical and economically viable systems for diverse applications.

1.5 Laser plasma interaction

Laser-plasma interaction is a captivating and intricate phenomenon that transpires when a powerful laser beam engages with a plasma, an ionised gas composed of charged particles (electrons and ions). This interaction results in numerous physical processes and can produce diverse consequences, rendering it a subject of considerable research and practical applications. Here's an overview of some key aspects of laser-plasma interaction:

1.5.1 Plasma formation

A high-intensity laser beam, when concentrated on a material, can generate plasma by ionising its atoms and molecules. The intense electromagnetic field of the laser removes electrons from their atomic orbits, resulting in a mixture of free electrons and ions. This plasma can have unique properties compared to neutral matter.

1.5.2 Self-focusing and filamentation

Intense laser beams can experience self-focusing in plasma as a result of the plasma's nonlinear response to the laser field. This self-focusing can result in the creation of self-guided passageways known as "filaments." Filamentation is associated with strong

electric fields and can produce multiple secondary phenomena, including terahertz radiation and high-order harmonic production.

1.5.3 Nonlinear optics and harmonic generation

The intense laser fields within the plasma can drive nonlinear optical effects. One notable effect is high-order harmonic generation (HHG), where the plasma generates coherent, high-frequency harmonics of the incident laser beam. HHG can generate extreme ultraviolet (XUV) and even soft X-ray radiation.

1.5.4 Electron acceleration and Wakefield

The strong electric fields within the plasma can accelerate charged particles, particularly electrons. This effect can be harnessed for laser Wakefield acceleration, where electrons are "surf" on the plasma wave generated by the laser, gaining tremendous energy over a very short distance. Laser Wakefield accelerators have the potential to revolutionize particle acceleration and enable compact, high-energy particle accelerators.

1.5.5 Relativistic and nonlinear effects

At high laser intensities, relativistic and quantum effects can become significant. Electrons can be driven to relativistic velocities, leading to phenomena like radiation pressure, betatron oscillations, and even the generation of antimatter through processes like electron-positron pair creation.

Laser-plasma interaction is an interdisciplinary domain encompassing laser physics, plasma physics, optics, and particle physics. Researchers persist in investigating and utilising the potential of these interactions for applications like particle acceleration, fusion research, the generation of novel radiation sources, and the examination of matter under severe conditions.

1.6 Literature review for Laser-induced THz radiation generation in plasma

The recent time experiences rapid growth in terahertz rays' generation method, i.e., electron-based accelerator, laser nonlinear crystal interaction, laser pulse and plasma interaction, quantum cascade laser, photo excited semiconductors etc. In all these above-mentioned methods laser plasma interactions gain more attention due to its inherent properties. When intense laser (greater than 10^{11}-10^{12} w/cm^2) interact with matter (i.e., nonlinear crystals, semiconductors etc.), high-energy, broadband terahertz wave generation is constrainted by matter damage and saturation properties thus diminishing the resultant THz amplitude. When laser wave of intensity 10^{11} w/cm^2 interacted with nonlinear crystal it generates up to sub mJ terahertz wave of few GV/m via optical rectification method [8], [9], [10].

In recent years laser intensities archives higher and higher values up to pettawatt (1 billion million watts) levels, plasma is only known source to handle such high energies and open up the new avenues for more effective non ionizing terahertz waves generation. In recent study A. Gopal *et al.* [11] uses the laser intensity up to 10^{20} W/cm^2 there is no sign of saturation in intense laser plasma interaction.

Researchers shows their immense contribution in theoretical [12], [13], [14], [15], [16], [17], [18], [19], [20], [21], [22] as well as in practical [23], [24], [25], [26], [27]perspective for laser plasma interaction methods in order to achieve tunable broadband THz sources. A controllable and focused terahertz generator was found by Malik *et al.* [28] when triangle laser passes through ripple density plasma in external DC magnetic field. Two powerful dark hollow laser beams interacting with collisional plasma produce a nonlinear ponderomotive force, resulting in terahertz production. Bakhtiari *et al.* [29] studied the influence of laser and plasma parameters on effective terahertz production. Kumar and Tripathi [30] examined resonant terahertz production using optical mixing of linearly polarised two-color lasers in ripple density plasma. Suitable ripple density wave vector provides necessary condition for phase matching.

Bhasin and Tripathi [31] suggested an analytical model for the resonant terahertz generation by using x-mode picosecond laser passed through magnetized ripple density plasma. They demonstrated using optical rectification that magneto plasma enhances

the power of terahertz radiation. Pathak *et al.* [32]studies that when relativistic electron beam interacts with ripple density under dense plasma at an incidence angle produces space charge beam mode. These beam modes give velocity to the plasma electrons with density ripple results into strong THz wave radiation. The theoretical results are verified by simulations in which output frequency of radiation depends upon ripple density and electron beam energy. There is strong nonlinear coupling exists between ripple density, energy of beam, side band and electromagnetic radiation solved mathematically. Electromagnetic mode falls at high frequencies which is compensates by increase in density of plasma.

Liu and Tripathi [33]strengthen the path for tunable terahertz source by adjusting the magnetic field. For this purpose, a short laser wave passed through a tunnel plasma of ionized gas in density profile of axial square shape. As the pulse passed via tunnel generates free electrons with transverse drift and started oscillation at cyclotron frequency results into THz generation. Applied magnetic field (nearly100 KG) tune the THz frequency and density ripple controls the angular direction of THz radiation.

Bhasin and Tripathi [34] investigated that hen an amplitude modulated laser beam incident obliquely under mode conversion, excites the amplitude modulated surface plasma wave at modulation frequency over the surface free space boundary which exerts a nonlinear ponderomotive force on metal electrons results into nonlinear current and generates strong terahertz waves at modulation frequency. These surface plasma wave exhibit very week damping effect, shows good option for optical rectification and have highest amplitude at free space metal interface. This amplitude falls rapidly away from boundary.

Kumar and Tripathi [35] suggest an analytical model to achieve a tunable THz resource in which THz frequency controlled by laser wavelength. In this investigation when a relativistic electron beam interacted with wiggler magnetic field under laser modulation exerts a ponderomotive force and coherent THz radiation. The THz yield exhibits a linear relationship with the electron bunch radius and a quadratic relationship with the bunch radius, beam current, and the inverse square of the wiggler wave vector. THz power has maximum value at THz frequency equals to 1.4 THz.

Kumar and Tripathi [30] observed the effect of ripple density plasma on resonant THz generation. When finite spot sized 2 collinear laser pulses of intensities of 10^{16} w/cm^2 launched into at an angle to the density ripple wave vector produces terahertz radiation at difference frequency in unmagnetized plasma. Density ripples generates additional angular momentum for proper phase matching. They investigated the effect of pulse spot size, density ripple, laser frequency, laser amplitude on resonant terahertz radiation. Power conversion efficiency for present scheme is 2.5×10^{-5} for laser wavelength 1 μm, ripple density ≥30%, spot size=$4c/\omega_p$ and pulse duration $>$ 100 fs.

Kumar *et al.* [36] compare the TE and TM mode in semiconductor waveguide in the generation of resonant terahertz radiation. They concluded that when two laser beams of different frequency propagate through semiconductor slab ripple wave vector in transverse magnetic field generates THz radiation at beat frequency. TM mode laser beating generates higher THz yield than TE mode. In this plan ripple density provides requisite phase matching.

Kumar and Tripathi [37]ascertained that surface plasma wave (SPW) experiences low loss if glass coated with ultrathin metal foil. For resonant THz photon generation two nonlinear laser beams incident normally to metal foil surface from free space to excite the SPW. As we move into glass and in free space surface plasma wave decreases away from thin metal sheet. At laser intensity 10^{12} w/cm^2 and 1μm wavelength, The ratio of THz amplitude to laser amplitude is about 10^{-3}. In this study metal film thickness is a critical parameter.

Kumar and Tripathi [38]examined the tunable THz source adjusted with metal film thickness. They using two nonlinear laser pulses interact with optical fiber encased in a thin metallic sheet with a dielectric modulation. Laser pulses excites the surface Plasmon waves along the laser direction. A CO_2 megawatt laser source is used for this scheme to generate ratio of THz amplitude to laser amplitude of the order of 10^{-2}. At higher frequencies, coupling between surface Plasmon decreases hence decrease in THz amplitude. Dielectric grating structure of optical fiber provides required phase matching condition for resonant wave in THz domain.

When electron bunches impinged periodically on the TM mode resonators loaded with dielectric, Kumar and Tripathi [39] investigated the Cherenkov mechanism for generation of waves in THz domain. These electron bunches excite the slowly moving

forward wave via phase synchronization. THz energy conversion efficiency can be enhanced by 10% with the help of suitable parameters. THz amplitude can be enhanced by seed THz signal as every electron bunch lose significant amount of energy per unit length which is stored in the resonator. Yoshii *et al.* [40] investigated the Cerenkov wake radiations in magnetised plasma. Yugami *et al.* [41] investigated experimentally and find out that laser waves excite the Cherenkov wake in the presence of transverse magnetic field there was generation of sub terahertz radiation.

It's reported by Mori *et al.* [42] that if two non collinear laser pulses pass via Argon clustered plasma results into linearly polarized terahertz pulse with five times more terahertz yield.

Kumar *et al.* [43] examined that when two laser pulses incident obliquely at hot plasma having step density profile result into terahertz wave in reflected direction at difference frequency. When plasma density equals to critical density of difference frequency there is resonant coupling observed between plasma wave and THz wave. PCE of terahertz wave is maximum at optimum angle of incidence attributable to the robust interaction between Langmuir waves and electromagnetic waves.

Mehta *et al.* [44] mathematically investigated the terahertz generation driven by two p-polarized Gaussian electromagnetic waves incident obliquely on collision less hot plasma with density ripple on its surface. As laser pulse interacts with density profile, it generates ponderomotive force on plasma electrons. Electrons starts oscillating due to nonlinear ponderomotive force. So, at beat frequency irrotational current density arises, which generates terahertz wave. This theoretical investigation is very useful in the formation of tunable terahertz sources. In this paper researcher neglected the effect of kinetic and Landau damping. Amplitude of terahertz radiation depends not only on beating frequency of laser, angle of incidence but also on plasma density. In this study power of radiated terahertz wave fall with terahertz frequency, varies as square of ripple amplitude and obtain optimum value at an particular incidence angle.

Varshney *et al.* [45]studied the generation of terahertz waves through the interaction of two cosh - Gaussian laser beams (marginally slightly different frequency) with clustered plasma. Researcher studies the variation of resultant THz amplitude with laser decentered parameter, beam width, ripple density amplitude and plasma density. They concluded in their studies that electric field of THz amplitude is highly dependent upon

decentered parameter. Increase in decentered parameter results into increase in terahertz amplitude by order of 3 which is higher for hollow Gaussian beam (b=5) than Gaussian beam (b=0). Researcher notice the increase in terahertz amplitude with decrease in laser beam width. There is increase in terahertz amplitude due to clustered plasma. As laser interacts with cluster plasma which results into nonlinear ponderomotive force. This nonlinear force oscillates the plasma electron to maintain the plasma neutrality. This oscillatory velocity oscillates in resonance with ripple density plasma to generate transient nonlinear current. These transient current converts into strong terahertz radiation at beat frequency.

Mehta *et al.* [46] studied the effect of frequency chirp in the presence of transverse static magnetic field on terahertz amplitude. In their studies researcher shows that tunable THz source can be attained by modifying the chirp parameter and the transverse magnetic field value. The chirp parameter enhances the interaction duration between the laser and plasma electrons, leading to the generation of a broadband terahertz pulse. This approach involves the interaction of two laser beams with under dense plasma in the presence of a transverse static magnetic field. THz amplitude has maximum value when terahertz frequency approaches upper hybrid frequency at resonance. Without magnetic field there is a dip in terahertz amplitude when terahertz frequency equal to 1.36 plasma frequency because of destructive interference. By applying the sufficient magnetic field this dip disappears because of resonant condition.

Mehta *et al.* [47] examined the impact of frequency chirp in the context of ripple density plasma on THz generation. A linear correlation exists between laser pulse amplitude and terahertz amplitude. The ripple density plasma establishes the requisite phase matching conditions, facilitating optimal momentum and energy transfer from the laser pulse to the plasma, hence enhancing the efficiency of terahertz generation. Chirp parameter is inversely proportional to group delay dispersion. Increase in chirp parameter results into decrease in group delay dispersion, hence reduces the chirp. Increase in the value of density ripple amplitude results into to increase in terahertz amplitude.

Varshney *et al.* [48]investigated the generation of tunable focused intense terahertz wave by photo mixing of 2 cosh - Gaussian Laser beams impinge into corrugated plasma. A DC magnetic field is applied in transverse direction. The cosh-Gaussian laser

beams interact with coagulated plasma which generates nonlinear ponderomotive force. This nonlinear force imparts oscillatory velocity to plasma electrons. Oscillating electrons pair with ripple density, resulting in nonlinear current density and robust Terahertz wave production.

Transverse static magnetic field works in two ways. On the one hand it controls the group and phase velocity of laser beam and on the other it manages the polarizability of THz wave. The author Investigate that optimum values of Plasma and Laser parameter can enhance the resultant terahertz amplitude. The efficiency of THz waves can be enhanced through appropriate values of the decentered parameter (b), beam width parameter (a_0), corrugation factor and applied magnetic field. The efficiency of resultant THz radiation has two ranges. For b <1.5 terahertz amplitude decreases with beam width and obtain maximum value for Gaussian beam (b=0) at resonance. For $1.5 \leq b \leq 5$ resultant THz radiation enhances with decentered parameter (b) and have utmost value for hollow Gaussian wave(b=5), the reason behind this variation is that ponderomotive force varies with laser profile. Laser profile diminishes from b=0(Gaussian wave) to b=1.4(flat top) and attain the minimum value then it increases to b=5 (cosh-Gaussian wave). Efficiency of THz radiation increases with the decentered parameter b and decreases with width parameter (a_0). Varshney *et al.* attain the efficiency up to 20% for b=5, $a_0 = 3c/5w_p$ and for external magnetic field of 107 KG. In this mathematical model researcher observed that when two non-linearly mixed laser pulses incident obliquely, on the density gradient hot nano cluster plasma surface, nonlinear ponderomotive force generated in cluster and plasma electrons Which results into terahertz generation in reflected wave. Amplitude of wave depends upon laser intensity, incident angle, cluster radius and electron thermal velocity. Laser intensity increases results into increase in terahertz amplitude due to outer ionization of cluster atoms by ponderomotive force. Vij and Kant [49] observed two peaks at theta equal to 22 degree and 68 degrees. Theta equal to 22 degree is optimized value for high THz amplitude. Terahertz amplitude can be enhanced by increasing value of cluster radius and electron thermal velocity. Researcher find out the relation between THz amplitude and frequency. When terahertz frequency approaches plasma frequency then there is strong coupling between Langmuir and terahertz wave which results into high terahertz amplitude. Step density profile provides essentials for phase matching condition. In this

study terahertz conversion efficiency increases (1.4×10^{-4}) with resonant interactions between plasma and terahertz radiation. The amplitude of a terahertz wave is maximised when the laser frequency approaches one by root 3 of cluster plasma frequency and plasma frequency equals to terahertz radiation frequency. This research article studied the effect of thermal velocity of electron, cluster radius, and laser intensity on terahertz radiation generation.

These cluster structure provides efficient energy absorption capacity to enhance terahertz amplitude and energies. Clusters are studied by Jahangiri *et al.* [50], [51] to compare the terahertz radiation generation efficiency by argon cluster and argon gas. They showed experimentally that Ar cluster shows significant improvement of the order of two in magnitude in comparison with Ar gas.

1.6.1 p-polorisation

Polarisation refers to the orientation of the electric field vector of an electromagnetic wave, such as a laser beam, as it propagates across space. Understanding and controlling the polarisation of laser light is crucial in several applications within optics, communications, and material interactions. Laser polarisation can be categorised based on the orientation of the electric field vector.

P-polarization, also known as parallel polarisation or transverse magnetic (TM) polarisation, is a specific condition of polarisation for electromagnetic waves, including light. P-polarization denotes the condition in which the electric field vector oscillates parallel to the plane of incidence. The plane of incidence is defined by the trajectory of the incoming wave and the perpendicular line to the surface it strikes.

The following are the primary attributes of P-polarization:

1. Orientation: The electric field vector oscillates parallel to the plane of incidence. When a wave moves horizontally (in the same direction as the ground), the electric field also oscillates horizontally (in the same direction as the ground).

2. Magnetic Field Orientation: The magnetic field vector is at a right angle to the plane of incidence. It is orientated perpendicular to the electric field vector.

3. Reflection: When light that is polarised in the P direction encounters a reflective surface, the light that is reflected remains polarised in the P direction. However, the

phase of the reflected light may be altered as a result of the qualities of the material and the angle at which the light strikes the surface.

4. Transmission: Transparent materials allow for the transmission of P-polarized light, although its intensity and phase can be altered by factors such as absorption and scattering.

Polarizers are optical devices that have the ability to selectively allow the transmission or blockage of P-polarized light. Linear polarizers have the ability to selectively block light that is not aligned in the desired direction.

1.6.2 Frequency chirp

Frequency chirp, sometimes called chirp modulation or chirping, is the occurrence of a signal's frequency changing over time. This alteration in frequency can manifest in other forms of waveforms, such as electromagnetic waves, acoustic waves, and even in signals utilised in communication systems. Frequency chirp is a crucial factor in several applications such as radar, laser systems, and communication technologies.

Below are few essential aspects of frequency chirp:

1. Linear Chirp: A linear chirp is characterised by a consistent and continuous variation in frequency over a period of time. The derivative of frequency with respect to time is referred to as the "chirp rate" and is commonly quantified in hertz per second (Hz/s).

Linear chirps can be classified as either "up-chirps," where the frequency increases over time, or "down-chirps," where the frequency lowers over time.

2. Quadratic Chirp: In a quadratic chirp, the frequency change does not occur at a constant pace, but instead follows a quadratic function. This leads to a non-linear variation in frequency over time.

3. Frequency modulation Up-Chirp and Down-Chirp

Frequency chirp refers to the phenomena of a signal's frequency changing over time, either in the form of an up-chirp or a down-chirp. The terms "up-chirp" and "down-chirp" indicate the direction of frequency modulation. Now, let's examine these notions more thoroughly:

1. Up-Chirp: An up-chirp is a signal in which the frequency increases over time. This indicates that the frequency commences at a lower number and progressively increases.

Up-chirps are characterised by a positive chirp rate, indicating a consistent increase in frequency over time.

Up-chirps are utilised in diverse applications, such as radar systems, to aid in the measurement of target distances and the collection of Doppler information.

2. Down-Chirp: In a down-chirp, the signal's frequency lowers over time. This indicates that the frequency begins at an elevated level and progressively decreases. Down-chirps are characterised by a negative chirp rate, which means that the frequency is consistently falling over time.

1.6.3 Slanting plasma density in laser plasma interaction for terahertz generation

The inclined plasma density profile is crucial in laser-plasma interactions aimed at terahertz (THz) production. The following is the correlation:

Nonlinear optical phenomena, such as optical rectification or coherent transition radiation, possess the ability to produce terahertz (THz) radiation. These phenomena transpire when a powerful laser pulse interacts with plasma, often generated on the solid surface of the target. The efficacy and characteristics of these processes are determined by the plasma density profile.

Phase matching is a critical need for efficient conversion in nonlinear optical systems used for THz generation. It ensures that the optical and THz waves are in sync with each other. To accomplish phase matching, one can create spatial variations in the effective refractive index that the interacting waves experience by using a slanted plasma density profile. This specific form enables the synchronisation of the phase fronts of the waves that are interacting, hence improving the effectiveness of THz generation.

Under appropriate conditions, the existence of a tilted plasma density profile might facilitate quasi-phase matching, a phenomenon where the phase matching requirement is almost fulfilled across a particular contact length. This can lead to a higher level of THz generation compared to plasma density profiles that are homogeneous.

The interaction between the powerful laser pulse and the plasma can result in considerable self-focusing and compression of the pulse, which can be attributed to the nonlinearity of the plasma. Self-focusing can cause the intensity of a laser beam to be distributed unevenly along its path, which in turn increases the slanted profile of plasma

density. Enhanced concentration in the specific area can lead to successful generation of terahertz (THz).

Cherenkov radiation is produced when the plasma density profile is tilted, causing the emission of terahertz (THz) radiation at an angle with respect to the direction of laser transmission. This capability can provide advantages in specific situations where there is a requirement for precise emission targeting.

The sloped plasma density profile is essential in laser-plasma interactions for the progression of terahertz (THz) radiation. It promotes phase alignment, enhances nonlinear optical processes, and improves the efficiency and characteristics of THz radiation generation. It is crucial to understand and control the plasma density profile in order to maximise the efficiency of terahertz (THz) sources by studying the interactions between lasers and plasma.

1.7 Objectives of the proposed work

Based on the challenges faced in THz generation the following are the objectives for the work done in this thesis.

1. To investigate the efficient THz generation by Hermite-cosh-Gaussian lasers in plasma with slanting density modulation**.**

2. To investigate the resonant Terahertz radiation by p-polarized chirped laser in hot plasma with slanting density modulation.

3. To study THz generation by frequency difference of Hermite-cosh-Gaussian chirped lasers in magnetized plasma.

1.8 Research methodology

Two Hermite-Gaussian laser beam with radial polarisation are travelling in the z direction and interacting with a slanting up density plasma modulation characterised by a density profile described by the equation $n = n_0 e^{k_z z}$, where n_0 represents the plasma density at z=0 and k_z is the wave number of the plasma density. The equations provided describe the electric and magnetic fields of laser pulses.

$$\overrightarrow{\mathrm{E_J}}(\mathrm{r},\mathrm{z}) = \hat{\mathrm{r}}\mathrm{E_0}\mathrm{H_s}\left(\frac{\sqrt{2}\mathrm{r}}{\mathrm{r_0}}\right)\mathrm{e}^{-\left(\frac{\mathrm{r}^2}{\mathrm{r_0}^2}\right)}\mathrm{e}^{\mathrm{i}(\mathrm{k_J z}-\omega_\mathrm{J}\mathrm{t})} \qquad (1.1)$$

$$\overrightarrow{\mathrm{B_J}}(\mathrm{r},\mathrm{z}) = \frac{\left\{\vec{\mathrm{k}}_\mathrm{J}\times\overrightarrow{\mathrm{E}_J}(\mathrm{r},\mathrm{z})\right\}}{\omega_\mathrm{J}} \quad \text{where } J = 1,2 \qquad (1.2)$$

here, $\overrightarrow{\mathrm{B_J}}(\mathrm{r},\mathrm{z})$ is the magnetic field of laser pulse, $r = r(x,y) = \sqrt{x^2+y^2}$ is radius of Gaussian pulse, r_0 is pulse waist, E_0 is amplitude of laser pulse, s is the mode index of Hermite polynomial H_s.

Hermite function is given as $H_0(x) = 1, H_1(x) = 2x, H_2(x) = 4x^2 - 2$. It depends on the values of x also.

During the first stage, when electrons are stationary, they do not encounter any magnetic force. As laser pulses travel through the plasma, they impart oscillatory velocity to the plasma electrons.

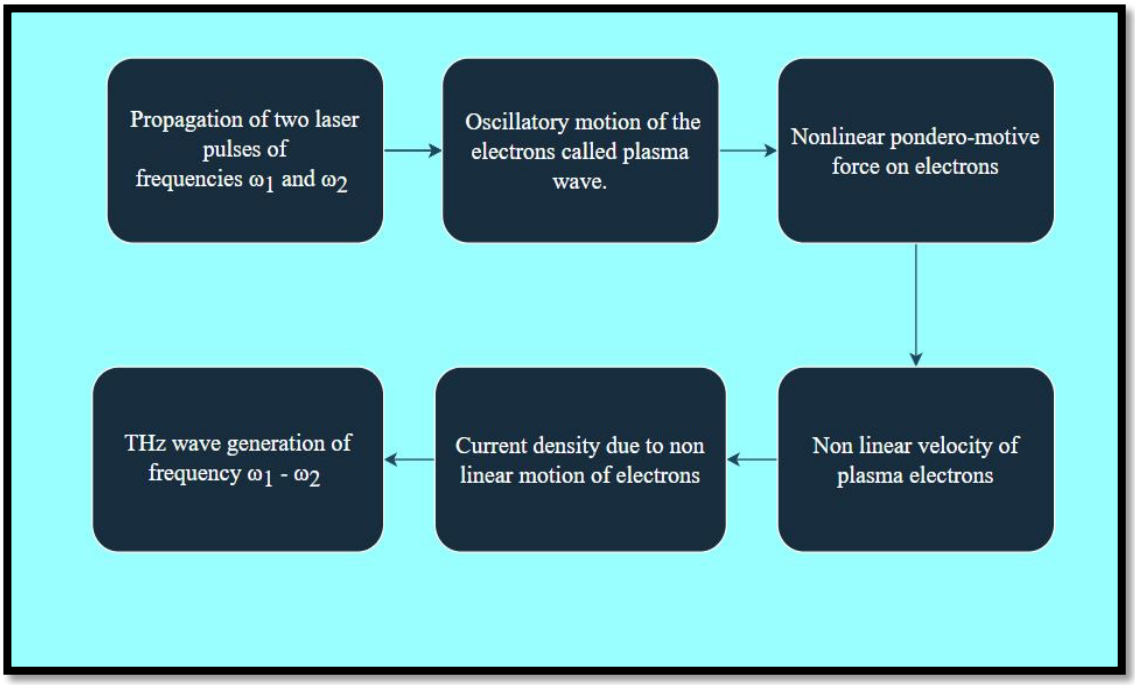

Fig 1.1 Flow chart for THz generation by laser plasma interaction

By employing the Equation of motion $m d\vec{V_J}/dt = -e\,\vec{E_J} - m\gamma_{en}\vec{V_J}$ where γ_{en}, e and m are collision frequency, charge of plasma electron and rest mass respectively. We obtain the velocity of plasma electrons as

$$\vec{V_J} = \frac{e\,\vec{E_J}}{m(i\omega_J - \gamma_{en})} \tag{1.3}$$

The oscillating velocity leads to a nonlinear ponderomotive force. This force is defined as

$$\overrightarrow{F_P}^{NL} = -\frac{m}{2}\,\vec{\nabla}\left(\vec{V_1}.\vec{V_2}^{*}\right)$$

so, we get

$$\Rightarrow \overrightarrow{F_P}^{NL} = \overrightarrow{F_{or}}^{NL} e^{i((k_1-k_2)z-(\omega_1-\omega_2)t)} = \overrightarrow{F_{or}}^{NL} e^{i(k'z-\omega' t)} \tag{1.4}$$

where, $\Delta = E_0{}^2 e^2 H_s\left(\sqrt{2}r/r_0\right) e^{-\left(2r^2/r_0{}^2\right)} e^{ik'z-\omega' t} \Big/ [2m\,(i\omega_1 - \gamma_{en})(i\omega_2 + \gamma_{en})]$, $k' = (k_1 - k_2)$, $\omega' = (\omega_1 - \omega_2)$, and

$$\overrightarrow{F_{or}}^{NL} = \Delta\left[\hat{r}\left\{s\left(4\sqrt{2}r/r_0\right) H_{s-1}\left(\sqrt{2}r/r_0\right) + \left(2b/r_0\right) H_s\left(\sqrt{2}r/r_0\right) - \left(4r/r_0{}^2\right) H_s\left(\sqrt{2}r/r_0\right)\right\} + \left\{\hat{z}ik' H_s\left(\sqrt{2}r/r_0\right)\right\}\right]$$

By calculating the equation of motion, $\partial\vec{V}_{\omega'}^{NL}/_{\partial t} = \left(\vec{F}_P^{NL}/_m\right) - \nu_{en}\vec{V}_{\omega'}^{NL}$ and equation of continuity $\partial n_{\omega'}^{NL}/_{\partial t} + \vec{\nabla}.n\vec{V}_{\omega'}^{NL} = 0$, $\vec{V}_{\omega'}^{NL}$ can be calculated by solving this equation. For slanting density profile $n = n_0 e^{k_z z}$ here, $n_0$is the initial (unperturbed) plasma density.

The equation provided yields both nonlinear oscillatory velocity and nonlinear density perturbation of plasma electrons.

$$\Rightarrow \vec{V}_{\omega'}^{NL} = \frac{i\omega'\vec{F}_P^{NL}}{m\left(\omega'^2 + i\omega'\gamma_{en}\right)} \quad (1.5)$$

$$\Rightarrow n_{\omega'}^{NL} = \frac{n_0\vec{\nabla}.(e^{k_z z})\vec{F}_P^{NL}}{m\left(\omega'^2 + i\omega'\gamma_{en}\right)} \quad (1.6)$$

In this derivation, we assume that n remains constant throughout time and is only dependent on z.

$\partial(\mathrm{n})/_{\partial \mathrm{t}} = 0.$

The presence of nonlinear density perturbation $n_{\omega'}^{NL}$ results in the formation of a self-consistent space charge potential ϕ and field, due to the separation of electrons from ions.

This gives rise to linear density perturbation as $n_{\omega'}^{L} = -\chi_P\vec{\nabla}.(\vec{\nabla}\phi)/_{4\pi e}$ where, $\chi_P = -\omega_P^2/\left(\omega'^2 + i\omega'\gamma_{en} - k'^2V_{th}^2\right)$ indicates the collisional plasma's electric susceptibility.

By the use of Poisson's equation $\nabla^2\phi = 4\pi\left(n_{\omega'}^{L} + n_{\omega'}^{NL}\right)e$, The space charge field exerts a linear force, denoted as $\vec{F}_P^L$, on the electrons such as

$$\vec{F}_P^L = \mathrm{e}\vec{\nabla}\phi = \frac{\omega_P^2\, e^{k_z z}\,\vec{F}_P^{NL}}{(1+\chi_P)\left(\omega'^2 + i\omega'\gamma_{en}\right)} \quad (1.7)$$

as, $\omega_P = \sqrt{\left(4\pi n_0 e^2/_m\right)}$ is plasma frequency.

The nonlinear oscillatory velocity of electrons may be determined by calculating the equation of motion $\partial\vec{V}^{NL}/_{\partial t} = \left(\vec{F}_P^{NL} + \vec{F}_P^L\right)/_m - \gamma_{en}\vec{V}^{NL}$, which accounts for the effects of both linear and nonlinear ponderomotive forces.

$$\Rightarrow \vec{V}^{NL} = \frac{1}{m}\left\{\frac{\omega'^2 + i\omega'\gamma_{en} - \omega_P^2 + \omega_P^2\,(e^{k_z z})}{(-i\omega' + \gamma_{en})\left(\omega'^2 + i\omega'\gamma_{en} - \omega_P^2\right)}\right\}\vec{F}_P^{NL} \qquad (1.8)$$

Nonlinear oscillatory current density is shows as

$$\vec{J}^{NL} = -\frac{1}{2}n' e\vec{V}^{NL} = -\frac{n_0 e}{2m}\left\{\frac{\omega^2 + i\omega\gamma_{en} - \omega_P^2 + \omega_P^2(e^{k_z z})}{(-i\omega + \gamma_{en})\left(\omega'^2 + i\omega\gamma_{en} - \omega_P^2\right)}\right\}\overrightarrow{F_{or}}^{NL} e^{i(kz-\omega t)} \qquad (1.9)$$

Where, the equation is given by $n' = n_0 e^{k_r z}$, The density perturbation is significantly larger than n_0, and I have $(k_1 - k_2) = k \approx k',\ (\omega_1 - \omega_2) = \omega \approx \omega'$.

k and ω represents the propagation constant and frequency, respectively, of the THz field. The vector $\vec{J}^{NL}$ leads to the generation of THz fields.

By solving Maxwell's equations $\vec{\nabla} \times \vec{E} = -\frac{1}{c}\left(\partial\vec{B}/\partial t\right)$ and $\vec{\nabla} \times \vec{B} = \frac{\varepsilon}{c}\left(\partial\vec{E}/\partial t\right) + \frac{4\pi}{c}\vec{J}^{NL}$

The wave equation for THz generation is as follows.

$$\Rightarrow \vec{\nabla}.\left(\vec{\nabla}.\vec{E}_{THz}\right) - \nabla^2\vec{E}_{THz} = \frac{\omega^2}{c^2}\varepsilon\vec{E}_{THz} + \frac{4\pi i\omega}{c^2}\vec{J}^{NL} \qquad (1.10)$$

The symbol $\vec{E}_{THz}$ represents the electric field of the generated THz pulse.

Here, we disregard the higher order derivatives because of the rapid fluctuations in the THz field.

here, In this equation, $\varepsilon = 1 - \left[\omega_P^2/\{\omega^2 + i\omega\gamma_{en}\}\right]$ represents electrical permittivity of collisional plasma.

To solve equation (10), we use nonlinear oscillatory current density value from equation (9) and ε value and get the normalized amplitude of THz field. Here we consider electric field component towards radial direction.

$$\frac{E_{THz}}{E} = \frac{i\omega_P^2}{\varepsilon\,\omega}\frac{e}{2r_0}\left\{\frac{\omega^2 + i\omega\gamma_{en} - \omega_P^2 + \omega_P^2(e^{k_z z})}{(-i\omega + \gamma_{en})(\omega^2 + i\omega\gamma_{en} - \omega_P^2)}\right\}\frac{E_0 H_s\left(\frac{\sqrt{2}r}{r_0}\right)e^{-\left(r^2/{r_0}^2\right)}}{2m\,(i\omega_1 - \gamma_{en})(i\omega_2 + \gamma_{en})}$$

$$\left[\hat{r}\left\{s(4\sqrt{2})H_{s-1}\left(\frac{\sqrt{2}r}{r_0}\right) + (2b)H_s\left(\frac{\sqrt{2}r}{r_0}\right) - \left(\frac{4r}{r_0}\right)H_s\left(\frac{\sqrt{2}r}{r_0}\right)\right\}\right] \qquad (1.11)$$

Here, $\frac{E_{THz}}{E}$ represents the ratio of generated THz electric field to the applied laser electric field. This ratio referred to as THz conversion efficiency.

1.9 Thesis outline

This study seeks to examine the interaction between ultra-short laser pulses and under-dense plasma to facilitate energy-efficient THz generation. Analytical research is an essential component of the entire study. The structure of the thesis project is as follows.

Chapter 2 presents the comparison of intensity profiles of various Gaussian laser pulses and their comparative study for use in laser plasma interactions. This study is specifically useful for the researchers to select suitable pulse profile for particular laser plasma interactions.

Chapter 3 presents the results of the interaction between two radially polarised HchG laser pulses that are co-propagating in the z direction and interacting with slanting density plasma modulation. This entails doing a thorough analysis of the non-homogeneous under dense plasma to achieve effective creation of terahertz (THz) waves. The findings of this work were published in the paper, titled "Efficient THz generation by Hermite-cosh-Gaussian lasers in plasma with slanting density modulation" was published in the Journal of Optics [52] on October 18, 2023.

Chapter 4 This study employs a pair of p-polarised chirped laser beams that are directed towards a hot collisional plasma with a slanting up density profile. The paper, titled "Resonant Terahertz radiation by p-polarised chirped laser in hot plasma with slanting density modulation" was published in the Journal of Optics [53] on December 23, 2023.

Chapter 5 investigates the propagation of two linearly polarised Hermite-cosh-Gaussian beams in the z direction. These laser beams exhibit a positive chirp. The laser beams travelled through a under-dense, collision-free plasma while encountering a static magnetic field orthogonal to their propagation path. This research paper, titled "Enhanced THz generation by Hermite-cosh-Gaussian chirped laser in static magnetized plasma" is published in the journal Applied Physics B [54] on June 28, 2024.

Chapter 6 provides a comprehensive study for THz generation by using Gaussian pulse profile in the plasma with slanting density profile. The research outcomes based on this study titled “Enhancing terahertz radiation in slanting density plasma using Gaussian laser beams” is published in the journal of optics on December 29, 2024 .

Chapter 7 provides a concise overview and final analysis of the research conducted for this thesis. In addition, this work examines the potential consequences that might be inferred from the findings and suggests areas for future research on the topic.

CHAPTER- 2

Intensity profile of various gaussian laser pulses and their applications

2.1 Introduction

Laser is considered as one of the revolutionary inventions of 20th century. The theoretical concept of laser was given by Albert Einstein in 1916. A photon can stimulate other atom to emit identical photon is the key theory suggested by Einstein [55]. It was called negative absorption that time. Later this concept was termed as stimulated emission. After further experiments made by various scientists it was found that gas discharge can amplify light under specific suitable conditions. This concept of amplification of light was applied to microwaves also. Different type of MASERS was invented using solid and gaseous mediums. Ali Javan invented a gaseous laser using electric discharge in He-Ne gas [56]. Maiman had invented a solid-state laser using ruby material [57], [58]. John von Neumann proposed the idea of semiconductor diode lasers. Kumar Patel had investigated Carbon di oxide laser which is a high-power continuous power supply laser source of infrared region [59]. J. Hetch has explained the history of laser sources briefly [60]. Now a days pulsed operation of laser is more effectively used rather than continuous power supply lasers. With the help of Q-switching techniques, a continuous source of light can be converted into short pulse laser of very high intensity [61]. Mode locking technique is also an effective method to produce ultra-short laser pulse (femtosecond) of petawatt intensity [62]. Gaussian and super- Gaussian laser profiles are investigated by Varaki et al. [63].

Gaussian laser profiles interaction with plasma generates important practical applications. Laser-plasma interaction is a complex and fascinating field of research in which a high-intensity laser beam interacts with a plasma, leading to numerous physical phenomena and potential applications. When considering various Gaussian profiles for the laser beam, the interaction with the plasma can exhibit different characteristics and outcomes. There are some aspects of laser-plasma interaction with various Gaussian profiles:

A Gaussian laser beam has a peak intensity at the center, which can be significantly higher than the intensity at the edges. When such a beam interacts with a plasma, the

high-intensity region at the center can cause significant ionization and heating of the plasma, leading to the creation of a plasma channel or filament. This self-guiding effect can enhance the propagation of the laser beam through the plasma, enabling it to travel longer distances with minimal diffraction. High-intensity Gaussian beams can undergo self-focusing on a plasma due to the plasma's nonlinear refractive index. As the laser beam intensity increases, it modifies the plasma's refractive index, creating a feedback mechanism that focuses the beam further. This self-focusing effect can lead to the formation of a plasma filament, which is a highly localized and intense region of the laser beam within the plasma. Laser Fusion: Self-focusing plays a crucial role in laser-driven inertial confinement fusion experiments, where intense lasers are used to compress and heat plasma to induce nuclear fusion reactions [64], [65], [66], [67], [68], [69], [70]. The self-focusing process can accelerate charged particles to high energies, making it relevant for particle acceleration research. Understanding self-focusing on laser plasma interactions helps researchers explore the behavior of matter under extreme conditions, leading to insights into astrophysical phenomena like supernovae and black holes. The self-focusing effect can be harnessed to create plasma-based waveguides for guiding and controlling laser beams.

In the context of laser-plasma interaction, high harmonics refer to the generation of higher-frequency light than the incident laser beam. A Gaussian laser beam's intensity distribution affects the efficiency and directionality of high harmonic generation. The high-intensity region at the center of the Gaussian beam can lead to enhanced harmonic generation compared to the lower-intensity regions. when a Gaussian profile laser beam undergoes Second Harmonic Generation, the resulting second harmonic beam will also have a Gaussian profile, maintaining the spatial characteristics of the fundamental beam but with a different frequency [71], [72], [73], [74], [75], [76]. Nonlinear processes, such as parametric instabilities, THz generation and stimulated Raman scattering, can occur during laser-plasma interaction. The Gaussian intensity distribution affects the growth and development of these nonlinear processes, which can impact the overall interaction dynamics [76], [77], [78].

Laser-plasma interaction can lead to the acceleration of electrons to elevated energy, resulting in a plasma-based electron accelerator. The interaction dynamics depend on the laser intensity, pulse duration, and profile. A Gaussian beam with high peak

intensity can efficiently drive electron acceleration in the central region of the beam. The mechanism of electron acceleration during laser plasma interaction is highly complex and requires sophisticated simulations and experimental setups to optimize and control the acceleration process effectively. Research in this area is rapidly advancing, with potential applications in next-generation particle accelerators, medical imaging, and industrial applications. Additionally, it provides insights into high-energy astrophysical phenomena and helps understand the behavior of matter under extreme conditions. In laser Wakefield acceleration, a laser pulse generates a plasma Wakefield that can accelerate charged particles, such as electrons. The laser beam's intensity profile affects the plasma Wakefield structure and the consequent particle acceleration. A Gaussian beam can lead to more controlled and stable Wakefield. Wakefield generation is a powerful technique for accelerating particles to high energies in a relatively compact space, compared to traditional accelerator technologies. It has significant implications for various applications, including generating intense X-rays for imaging and material research, producing compact particle accelerators for medical and industrial purposes, and advancing the field of high-energy physics [63], [79], [80], [81], [82]. Application of various laser pulses are analyzed by prominent scientists and scholars [83], [84], [85].

Laser-plasma interaction is a highly nonlinear and dynamic phenomenon, with consequences contingent upon several parameters, including laser power, plasma density, pulse duration, and the precise Gaussian profile employed. Experimental and computational investigations are frequently utilised to examine the complexities of these interactions and enhance them for particular applications, including laser-driven fusion, particle acceleration, and plasma-based light sources.

In this paper I have studied mathematical expression for Gaussian, Hermite Gaussian, Hermite-cosh-Gaussian laser pulse profiles. I have plotted cross- sectional view of laser pulse electric field and compare their advantages over each other in various applications.

2.2Various Gaussian Laser Profiles and applications

2.2.1 Gaussian pulse

It is a single-cycle pulse. Transverse variation in laser electric field is represented by the subsequent equation.

$$E = E_0 e^{-r^2/r_0^2}$$

Where, E_0 is the peak amplitude of the pulse, r is transverse position of particle, r_0 is minimum spot size or beam waist. Gaussian pulses have useful properties that make them important in a variety of applications. Some of these properties are:

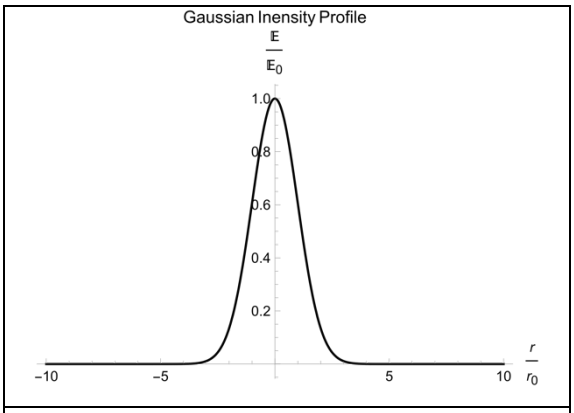

Fig.2.1 Gaussian laser intensity profile distribution

Gaussian Envelope: Gaussian pulses have a Gaussian-shaped envelope, which is a bell-shaped curve that is symmetric about its centre. This shape makes Gaussian pulses like natural light pulses, which is useful in few applications.

Dispersion Properties: Gaussian pulses have good dispersion properties, which means that they can maintain their shape over longer distances. This property is important in optical communication systems where pulses are transmitted over long distances.
Easily Modulated: Gaussian pulses are easily modulated to carry information. By changing the amplitude or phase of the pulse, information can be encoded onto the pulse.

Optical Fourier Transform: Gaussian pulses have a Fourier transform that is also a Gaussian function, which is useful for optical Fourier transform applications.

Self-Focusing: Gaussian pulses can self-focus in media, which means that the pulse can become narrower as it propagates. This property is useful in laser applications.

2.2.2 q-Gaussian pulse

Q-Gaussian pulses are a class of non-Gaussian optical pulses with specific properties. They are based on the Tsall is q-exponential function, which generalizes the ordinary exponential function.

$$E = E_0 e^{-\left(\frac{r}{r_0}\right)^q},$$

Q-Gaussian pulses are a class of non-Gaussian pulses that have a number of interesting properties. Some of these properties are:

Non-Gaussian Shape: Q-Gaussian pulses have a non-Gaussian shape that is described by a q-exponential function, which is a generalization of the usual exponential function. The q-exponential function is characterized by a parameter q, which determines the degree of non-Gaussian.

Long Tailed Distribution: Q-Gaussian pulses have a long-tailed distribution, which means that the probability of observing large amplitude fluctuations is much higher than for a Gaussian pulse.

Self-Similar Properties: Q-Gaussian pulses are self-similar, which means that the pulse shape remains the same under rescaling. This property is useful in applications like fractal analysis and turbulence etc.

Robustness to Noise: Q-Gaussian pulses are robust to noise, which means that they can maintain their shape and properties in the presence of noise or other disturbances.

Applications: Q-Gaussian pulses have several potential applications, such as in information theory, signal processing, and statistical physics.

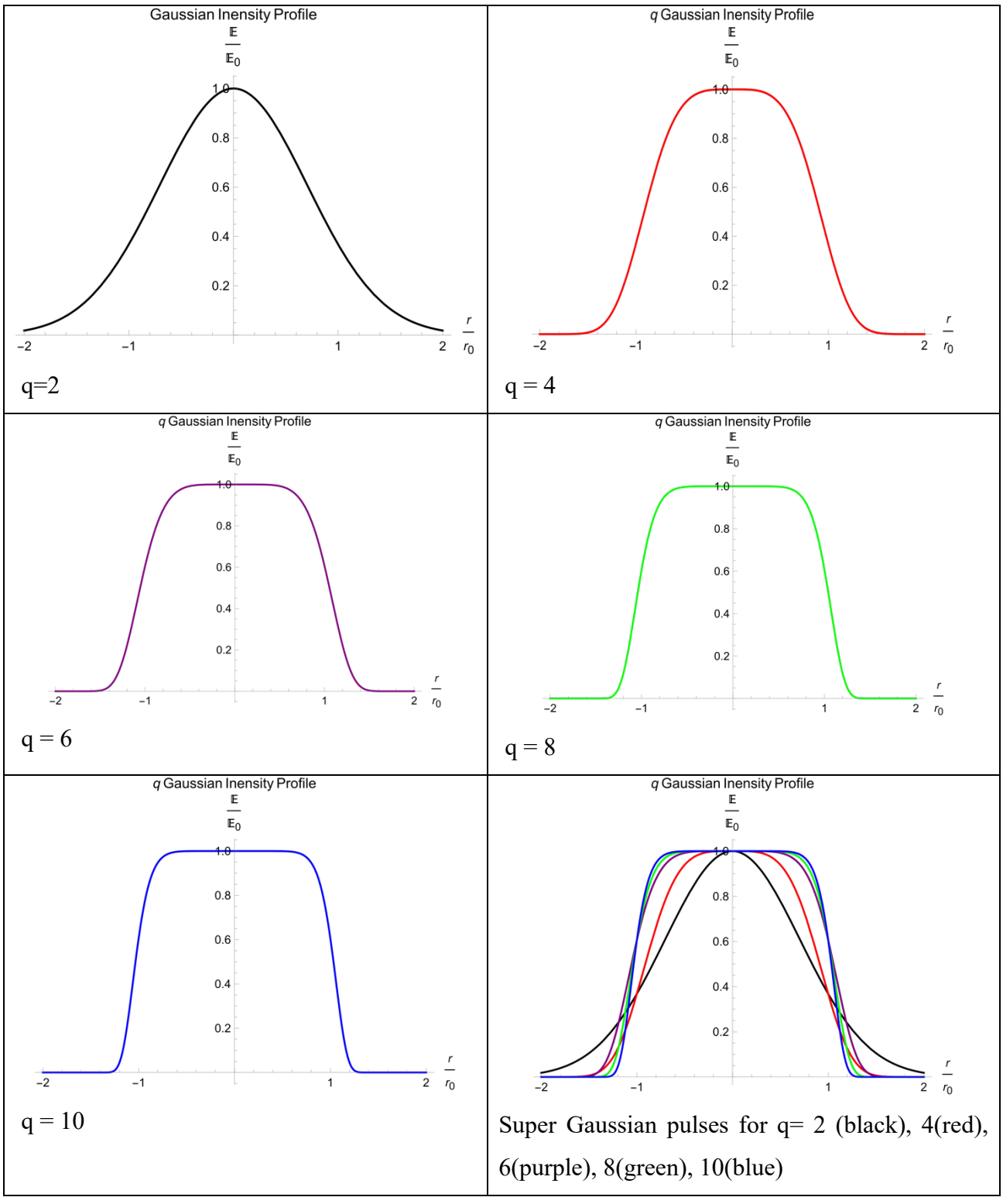

Fig. 2.2 q-Gaussian laser profile intensity distribution for q=2(black), 4(red), 6(purple), 8(green), 10(blue)

q-Gaussian pulses have advantages over Gaussian pulses in certain applications:

Non-Gaussian Shape: Q-Gaussian pulses have a non-Gaussian shape that is characterized by a q-exponential function, which is a generalization of the usual exponential function. This non-Gaussian shape can provide better control over the pulse's properties and behaviour.

Long-Tailed Distribution: Q-Gaussian pulses have a long-tailed distribution, which means that they have a higher probability of having large amplitude fluctuations than Gaussian pulses. This property can make Q-Gaussian pulses more robust to noise and other disturbances.

Self-Similar Properties: Q-Gaussian pulses are self-similar, which means that they maintain their shape and properties under rescaling. This property is useful in several applications, such as fractal analysis and turbulence.

Statistical Physics Applications: Q-Gaussian pulses have a number of potential applications in statistical physics, such as modelling complex systems with long-range interactions and studying anomalous diffusion processes.

However, Gaussian pulses also have advantages over Q-Gaussian pulses in certain applications, such as optical communication systems, where the Gaussian shape provides good dispersion properties and low distortion over long distances. The choice between Gaussian and Q-Gaussian pulses depends on the specific application and the desired properties of the pulse.

2.2.3 Hermite-Gaussian pulse

A Hermite-Gaussian pulse is a type of optical pulse that has a specific shape determined by the Hermite polynomials and a Gaussian envelope.

Hermite-Gaussian pulses are extensively utilised in laser physics and optical communication systems.

The Hermite polynomials are a set of orthogonal polynomials that have specific shapes and are used to describe the modes of a laser cavity. The Gaussian envelope, on the other hand, describes the shape of the pulse in the time domain.

The Hermite-Gaussian pulse can be quantitatively represented by the subsequent equation:

$$E = H_n(r/r_0)\, E_0 e^{-r^2/r_0^2}$$

$H_n(r)$ is Hermite polynomial which is a function of n and r.

$$H_0(r) = 1 \qquad H_1(r) = 2r$$

$$H_2(r) = 4r^2 - 2 \qquad H_3(r) = 8r^3 - 12r$$

Hermite-Gaussian pulses have several useful properties, including their ability to propagate over long distances without significant dispersion and their ability to be modulated easily to carry information. They are often used in fibre optic communication systems and in ultrafast laser experiments.

Hermite-Gaussian (HG) pulses are a class of optical pulses with specific properties:

Orthogonality: HG pulses are orthogonal to each other, which means that they can be used as a basis for a complete set of functions to represent any optical pulse. This property allows for greater control over the pulse's shape and behaviour, making HG pulses useful in applications such as pulse shaping and optical communication systems.

Gaussian Envelope: HG pulses have a Gaussian envelope, which provides good dispersion properties and low distortion over long distances in optical communication systems. This property is important for maintaining pulse shape and quality over longer distances.

Well-Behaved: HG pulses have a smooth, well-behaved shape that is easy to model and manipulate. They are commonly used in ultrafast laser experiments and in applications such as laser spectroscopy.

High Intensity: HG pulses can have high peak intensities, which make them useful in applications such as nonlinear optics and high-intensity laser experiments.

Order: HG pulses are characterized by an integer order, which determines the number of oscillations in the pulse. Higher order HG pulses have more oscillations and a narrower width than lower order HG pulses.

In general, HG pulses are a versatile and well-behaved class of optical pulses that can be used in a variety of applications where control over the pulse's shape and behaviour is important.

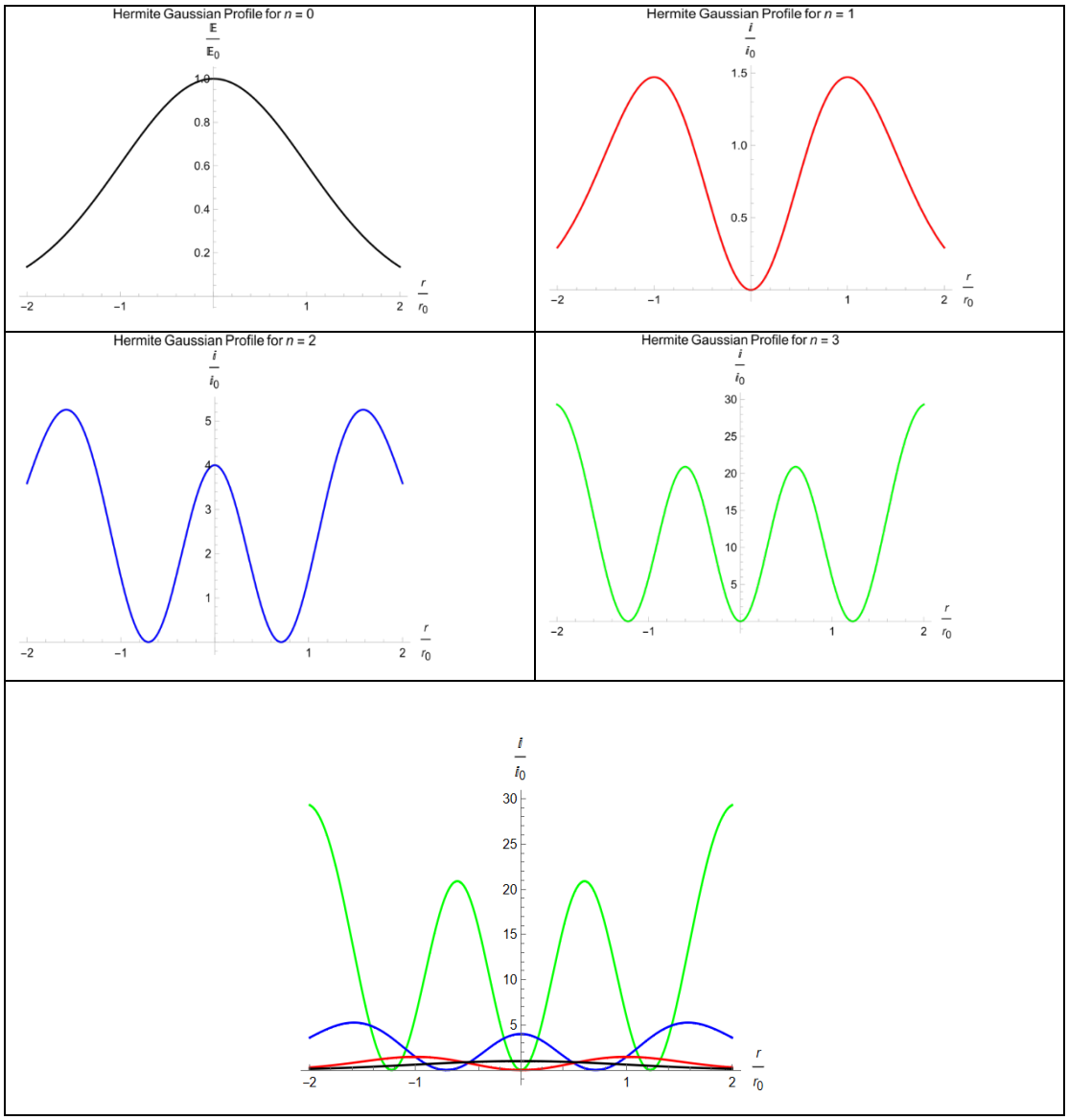

Fig. 2.3 Hermite-Gaussian laser profile intensity distribution for n = 0(black), 1(red), 2(blue), 3(green)

Hermite-Gaussian (HG) pulses have advantages over Q-Gaussian pulses in certain applications:

Orthogonality: HG pulses are orthogonal to each other, which means that they can be used as a basis for a complete set of functions to represent any optical pulse. This property allows for greater control over the pulse's shape and behaviour, making HG pulses useful in applications such as pulse shaping and optical communication systems.

Gaussian Envelope: HG pulses have a Gaussian envelope, which provides good dispersion properties and low distortion over long distances in optical communication systems. This property is important for maintaining pulse shape and quality over longer distances.

Well-Studied: HG pulses are well-studied and understood, with a large body of literature on their properties and applications. This makes it easier to design and optimize optical systems using HG pulses.

Ultrafast Laser Experiments: HG pulses are commonly used in ultrafast laser experiments for generating high-intensity pulses. Their Gaussian envelope allows for easy control over the laser's intensity and pulse shape.

However, Q-Gaussian pulses have advantages over HG pulses in certain applications, such as modelling complex systems with long-range interactions and studying anomalous diffusion processes in statistical physics.

The choice between HG and Q-Gaussian pulses depends on the specific application and the desired properties of the pulse. In general, HG pulses are a good choice for applications where orthogonality and a Gaussian envelope are important, while Q-Gaussian pulses may be better suited for applications where non-Gaussian behaviour and long-tailed distributions are important.

2.2.4 Hermite-cosh-Gaussian Pulse

A Hermite-cosh-Gaussian (HchG) pulse is a type of optical pulse that is like a Hermite-Gaussian pulse but has a hyperbolic cosine (cosh) envelope instead of a Gaussian envelope.

The mathematical equation for an HCG pulse can be written as:

$$E = E_0 \, H_n(r/r_0) \, \mathrm{Cosh}\,(r/r_0) \; e^{-r^2/r_0^2}$$

HchG pulses have several useful properties, including their ability to maintain their shape over long propagation distances and their suitability for use in high-speed optical communication systems. They are also used in ultrafast laser experiments for generating high-intensity pulses. Hermite-cosh-Gaussian (HchG) pulses are a special type of Hermite-Gaussian pulse that has a hyperbolic cosine (cosh) envelope.

Properties of HchG pulses are:

Hyperbolic Cosine Envelope: The hyperbolic cosine envelope of HchG pulses gives them a unique shape that is different from the Gaussian envelope of Hermite-Gaussian pulses. This shape allows HchG pulses to maintain their shape over longer distances.

Orthogonality: Like other Hermite-Gaussian pulses, HchG pulses are orthogonal to each other. This property allows them to be used as a basis for a complete set of functions to represent any optical pulse.

Higher-Order Hermite Polynomials: HchG pulses are generated using higher-order Hermite polynomials, which allows for greater control over the pulse shape. The order of the polynomial determines the number of nodes in the pulse, which affects the pulse's bandwidth and other properties.

Dispersion Management: HchG pulses can be used to manage dispersion in optical communication systems. Dispersion is the effect of different wavelengths of light traveling at different speeds in a medium, which can cause distortion of optical pulses. HchG pulses can be used to compensate for dispersion and maintain pulse shape over longer distances.

Ultrafast Laser Experiments: HchG pulses are used in ultrafast laser experiments for generating high-intensity pulses. The hyperbolic cosine envelope allows for greater control over the pulse shape, which is important for controlling the laser's intensity and achieving specific effects.

Overall, HchG pulses have unique properties that make them useful in a variety of applications, including optical communication systems, pulse shaping, and ultrafast laser experiments. The hyperbolic cosine envelope of HchG pulses gives them a

different shape than other Hermite-Gaussian pulses, allowing for greater control over the pulse's properties.

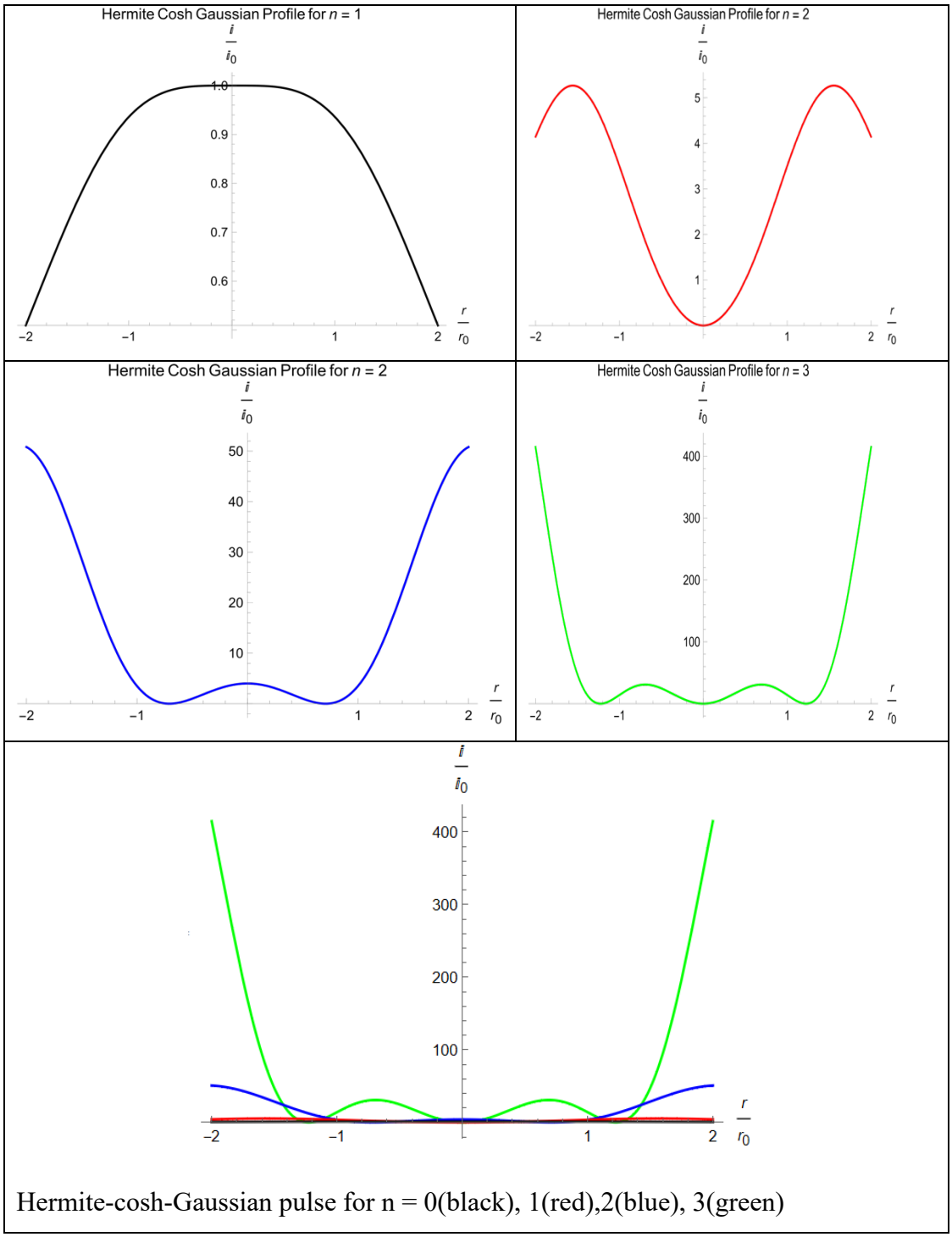

Fig. 2.4. Hermite-cosh-Gaussian laser profile intensity distribution for n = 0 (black), 1(red), 2(blue), 3(green)

Hermite-cosh-Gaussian (HchG) pulses have advantages over Hermite-Gaussian (HG) pulses in certain applications:

Zero-Crossings: HchG pulses have zero-crossings, which can be useful in applications such as pulse compression and mode-locking. The zero-crossings provide a mechanism for controlling the pulse's temporal and spectral characteristics.

Cosh Envelope: HchG pulses have a hyperbolic-cosine (cosh) envelope, which provides a balance between the spatial and temporal widths of the pulse. This property can be useful in applications such as microscopy, where a balance between spatial and temporal resolution is important.

Improved Focusing: HchG pulses can be focused to smaller spot sizes than HG pulses of the same order, which can be useful in applications such as laser micro-machining and material processing.

Higher Intensity: HchG pulses can have higher peak intensities than HG pulses of the same order, which can be useful in applications such as nonlinear optics and high-intensity laser experiments.

However, HG pulses also have advantages over HchG pulses in certain applications, such as ultrafast laser experiments and optical communication systems, where a Gaussian envelope provides good dispersion properties and low distortion over long distances.

The choice between HchG and HG pulses depends on the specific application and the desired properties of the pulse. In general, HchG pulses may be a good choice for applications where zero-crossings, a cosh envelope, improved focusing, and higher peak intensities are important, while HG pulses may be a better choice for applications where a Gaussian envelope and orthogonality are important.

2.3 Conclusion

The choice between Gaussian and Q-Gaussian pulses depends on the specific application and the desired properties of the pulse. Here are some general guidelines:

Gaussian pulses are a good choice for applications where a smooth, bell-shaped envelope is desired. They are commonly used in optical communication systems and

laser spectroscopy, where the Gaussian envelope provides good dispersion properties and low distortion over long distances.

Q-Gaussian pulses are a good choice for applications where a non-Gaussian shape is desired. They have a long-tailed distribution, which makes them more robust to noise and other disturbances. They are commonly used in statistical physics applications and in modelling complex systems with long-range interactions.

In applications where the pulse shape needs to be controlled and manipulated, such as pulse shaping and ultrafast laser experiments, Hermite-Gaussian (HG) pulses are a good choice. They are orthogonal to each other, which makes them a complete set of functions to represent any optical pulse.

Hermite-cosh-Gaussian (HchG) pulses are a good choice for applications where a balance between spatial and temporal widths is desired, such as microscopy. They also have zero-crossings, which can be useful in applications such as pulse compression and mode-locking.

In general, the choice between Gaussian, Q-Gaussian, HG, and HchG pulses depends on the specific requirements of the application, such as the desired pulse shape, width, intensity, and dispersion properties.

CHAPTER- 3

Hermite-cosh-Gaussian lasers Interaction with plasma of slanting density modulation for Efficient THz generation

3.1 Introduction

The term "terahertz region" refers to the portion of the electromagnetic spectrum that lies roughly between 100 GHz and 10^4 GHz and includes the high frequency microwave band and the long wavelength infrared region. This area enables the integration of optics and electronics, which broadens the scope of the optoelectronics stream in the physical, chemical, biological, and applied sciences. These waves are nonionizing in nature and undetectable to naked human eyes [1]. Explosive detection, remote sensing, defense, material characterization, high-field condensed matter research, non-destructive assessment, biological and chemical imaging, and short-range wireless sensing and communication and ultrafast magnetic switching are some of the applications of these terahertz waves (also known as T-waves or T-light) [2], [3], [4], [5], [6], [7], [86]. For applications like microscopy where a balance between spatial and temporal widths is sought, Hermite-cosh-Gaussian (HchG) pulses are a promising option. Additionally, they have zero-crossings, which are advantageous in processes like pulse compression and mode-locking [87].

Due to the wide variety of applications, scientists have shown a major interest in the development of THz field generation, detection, and application throughout the past few decades. To build adaptable broadband THz sources, researchers highlight their enormous contribution to laser plasma interaction approaches from both a theoretical [12], [13], [14], [15], [16], [17], [18], [19], [66], [73], [77]and a practical [23], [24], [25], [26], [27] perspective. Kant *et al.* [72] theoretically analysed the cosh-Gaussian laser in wiggler-magnetized plasma and looked at how the decentered parameter and incoming laser intensity affected the production of second harmonics. Third harmonic generation using a HchG laser beam in a wiggler magnetic field was studied by Sharma *et al.* [88]. They concluded that the laser pulse $m = 2$ mode index parameter boosts the efficiency of third harmonic generation. The HchG laser beam with exponential plasma density Ramp profile in self-focusing action is theoretically studied by Thakur *et al.* [67]. This demonstrates that the plasma density ramp and chirp parameter have a key

impact in the effective self-focusing increase laser intensity. The HchG Laser pulse is investigated by Thakur *et al.* [75] for self-focusing in collision-less cold quantum plasma. They analyse the self-focusing effect with and without an exponential plasma density ramp profile.

In the presence of magneto plasma, Kant *et al.* investigated the relativistic self-focusing with a HchG laser pulse in tangential exponential plasma density. For mode index values $0{,}1\ and\ 2$ they exhibit a robust self-focusing effect along with a rise in plasma density and the magnetic [89] a radially polarized HchG laser, they concluded that the laser intensity gradient and the electron collisional effect have an impact on the terahertz amplitude.

The chirp laser effect on transversely magnetized plasma with an exponential ramp shape was studied by Kant *et al.* [90]. They concluded that an increase in positive chirp and an external magnetic field leads to an increase in the second harmonic generation's conversion efficiency. The HchG laser pulses in ripple density plasma in the presence of an external DC magnetic field was theoretically studied by Malik *et al.* [91]. According to their research, the magnitude of the terahertz field rises with the magnetic field and falls with an increase in electron collusion.

The simulation impact of Gaussian, Hermit-Gaussian, and cosh-Gaussian Laser pulse influence on the irradiance profile of composite beam profile and far field power concentration is studied by Qian-jin *et al.* [92]. With Chirp laser pulses, Gurjar *et al.* [93] investigated the oblique spatial density ripple. They demonstrate that, at a specific slanting angle, there is an amplification of the Terahertz field. The combination of two dark hollow intense laser beams with collisional plasma and a nonlinear ponderomotive force produces terahertz radiation. Bakhtiari *et al.* [29] looked at how laser and plasma characteristics affected efficient terahertz generation. According to Mori *et al.* [42], a linearly polarized terahertz pulse with a five times higher terahertz yield is produced when two noncollinear laser pulses pass through an Argon clustered plasma. In the presence of a stationary magnetic field, collisional plasma absorbs a HchG laser beam, according to a theoretical analysis by Verma *et al.* [94] According to research by Kad *et al.* [95], the laser beam's passage through the plasma excites the plasma wave, and the nonlinear coupling of the Hermite-Gaussian beam and plasma wave results in the production of THz radiation. The collisional nanocluster plasma was investigated by

Kumar *et al.* [96] using two Hermite-cosh-Gaussian laser beams. The researchers investigated the thermal impact resulting from the propagation of plasma waves. In their research, Gupta *et al.* [97] investigate the interaction between Bessel-Gaussian laser beams and a plasma medium under the influence of an axial temperature ramp. The researchers investigate the phenomenon of self-action effects in the context of laser plasma interaction. In their research, Gupta *et al.* [98] investigate the characteristics of the elliptical q-Gaussian laser beam within a plasma environment featuring an axial density ramp. The researchers investigate the phenomenon of stimulated Raman scattering using the W.K.B. approximation technique. Nature of laser plasma interaction is nonlinear in nature. It is highly affected by various properties of laser and plasma like asymmetric chirped laser pulse, plasma density profile, laser intensity, Hermite polynomial mode index etc.

In the current study, two radially polarized HchG lasers pulses are co-propagating in the z direction and interacting with slanting density plasma modulation at frequencies and wave numbers of $\omega_1, \omega_2 \; and \; \vec{k}_1 \, , \vec{k}_2$ respectively. By solving equation of motion, equation of continuity, Poisson equation, we obtain nonlinear current density. This nonlinear current density is responsible for THz field generation. In this study we include the effect of electron collision and neglect the plasma electron temperature effect.

3.2 Analytical study of THz generation

Two radially polarized spatial HchG laser pulses are propagating in z direction and interact with slanting density plasma modulation having density profile $n = n_0 e^{k_z z}$ (where n_0 is plasma density at $z = 0$ and k_z is wave number of plasma density). Electric and magnetic fields of laser pulses are given by these equations.

$$\overrightarrow{\mathrm{E_J}}(\mathrm{r,z}) = \hat{\mathrm{r}}\mathrm{E_0}\mathrm{H_s}\left(\frac{\sqrt{2}\mathrm{r}}{\mathrm{r_0}}\right)\cosh\left(\frac{\mathrm{br}}{\mathrm{r_0}}\right)\mathrm{e}^{-\left(\frac{\mathrm{r}^2}{\mathrm{r_0}^2}\right)}\mathrm{e}^{\mathrm{i(k_J z-\omega_J t)}} \tag{3.1}$$

$$\overrightarrow{\mathrm{B_J}}(\mathrm{r,z}) = \frac{\left\{\vec{\mathrm{k}}_\mathrm{J}\times\overrightarrow{\mathrm{E}_J}(\mathrm{r,z})\right\}}{\omega_\mathrm{J}} \quad \text{where } J = 1,2 \tag{3.2}$$

here, $r = r(x, y) = \sqrt{x^2 + y^2}$ is radius of Gaussian pulse, E_0 is amplitude of laser pulse, r_0 is pulse waist, b is decentred parameter of cosh profile, s is the mode index of Hermite polynomial H_s.

In initial stage, electrons can be considered at rest so electrons will not experience any magnetic force. As laser pulses propagate in the plasma, it gives oscillatory velocity to plasma electron.

By using the Equation of motion $m d\vec{V}_J/dt = -e\,\vec{E_J} - m\gamma_{en}\vec{V_J}$ where γ_{en}, m and e are collision frequency, rest mass and charge of plasma electron respectively. We get plasma electron velocity such as

$$\vec{V_J} = \frac{e\,\vec{E_J}}{m(i\omega_J - \gamma_{en})} \tag{3.3}$$

This oscillatory velocity gives rise to nonlinear ponderomotive force$\left(\overrightarrow{F_P}^{NL}\right)$. This force is defined as

$$\overrightarrow{F_P}^{NL} = -\frac{m}{2}\vec{\nabla}\left(\overrightarrow{V_1}.\overrightarrow{V_2}^{*}\right)$$

so, we get

$$\Rightarrow \overrightarrow{F_P}^{NL} = \overrightarrow{F_{or}}^{NL} e^{i((k_1-k_2)z-(\omega_1-\omega_2)t)} = \overrightarrow{F_{or}}^{NL} e^{i(k'z-\omega' t)} \tag{3.4}$$

where, $\Delta = E_0{}^2 e^2 H_s\left(\sqrt{2}r/r_0\right)\cosh^2\left(br/r_0\right) e^{-\left(2r^2/r_0{}^2\right)} e^{ik'z-\omega' t)} \Big/ [2m\,(i\omega_1 - \gamma_{en})(i\omega_2 + \gamma_{en})]$, $k' = (k_1 - k_2)$, $\omega' = (\omega_1 - \omega_2)$, and

$$\overrightarrow{F_{or}}^{NL} = \Delta\left[\hat{r}\left\{s\left(4\sqrt{2}r/r_0\right)H_{s-1}\left(\sqrt{2}r/r_0\right) + \left(2b/r_0\right)H_s\left(\sqrt{2}r/r_0\right)\tanh\left(br/r_0\right) - \left(4r/r_0{}^2\right)H_s\left(\sqrt{2}r/r_0\right)\right\} + \left\{\hat{z}ik' H_s\left(\sqrt{2}r/r_0\right)\right\}\right]$$

By solving the equation of motion $\partial\vec{V}_{\omega'}^{NL}/\partial t = \left(\vec{F}_P^{NL}/m\right) - \nu_{en}\vec{V}_{\omega'}^{NL}$ and equation of continuity $\partial n_{\omega'}^{NL}/\partial t + \vec{\nabla}.n\vec{V}_{\omega'}^{NL} = 0$, For slanting density profile $n = n_0 e^{k_z z}$, we get nonlinear oscillatory velocity and nonlinear density perturbation of plasma electron as per given equation.

$$\Rightarrow \vec{V}_{\omega'}^{NL} = \frac{i\omega'\vec{F}_P^{NL}}{m\left(\omega'^2 + i\omega'\gamma_{en}\right)} \tag{3.5}$$

$$\Rightarrow n_{\omega'}^{NL} = \frac{n_0\vec{\nabla}.(e^{k_z z})\vec{F}_P^{NL}}{m\left(\omega'^2 + i\omega'\gamma_{en}\right)} \tag{3.6}$$

In this derivation we consider n is constant with time, and is a function of z only so

$\partial(\mathrm{n})/_{\partial \mathrm{t}} = 0.$

This nonlinear density perturbation $n_{\omega'}^{NL}$ give rise to self-consistent space charge potential ϕ and field, because of separation of electrons from ions. This gives rise to linear density perturbation as $n_{\omega'}^{L} = -\chi_P \vec{\nabla}.(\vec{\nabla}\phi)/_{4\pi e}$ where, $\chi_P = -\omega_P^2/_{\left(\omega'^2 + i\omega'\gamma_{en} - k'^2 V_{th}^2\right)}$ is electric susceptibility of collisional plasma.

Using Poisson's equation $\nabla^2\phi = 4\pi\left(n_{\omega'}^{L} + n_{\omega'}^{NL}\right)e$, we get linear force $\vec{F}_P^L$ attributable to the space charge field affecting electrons, such as

Linear force $\vec{F}_P^L = \mathrm{e}\vec{\nabla}\phi = \frac{\omega_P^2\, e^{k_z z}\, \vec{F}_P^{NL}}{(1+\chi_P)\left(\omega'^2 + i\omega'\gamma_{en}\right)}$ (3.7)

as, $\omega_P = \sqrt{\left(4\pi n_0 e^2/_m\right)}$ is plasma frequency.

By solving the equation of motion $\partial\vec{V}^{NL}/_{\partial t} = \left(\vec{F}_P^{NL} + \vec{F}_P^{L}\right)/_m - \gamma_{en}\vec{V}^{NL}$, The nonlinear oscillatory velocity of electrons caused by both linear and nonlinear ponderomotive forces can be calculated as

$$\Rightarrow \vec{V}^{NL} = \frac{1}{m}\left\{\frac{\omega'^2 + i\omega'\gamma_{en} - \omega_P^2 + \omega_P^2\,(e^{k_z z})}{(-i\omega' + \gamma_{en})\left(\omega'^2 + i\omega'\gamma_{en} - \omega_P^2\right)}\right\}\vec{F}_P^{NL} \quad (3.8)$$

Nonlinear oscillatory current density is

$$\vec{J}^{NL} = -\frac{1}{2}n' e\vec{V}^{NL} = -\frac{n_0 e}{2m}\left\{\frac{\omega^2 + i\omega\gamma_{en} - \omega_P^2 + \omega_P^2(e^{k_z z})}{(-i\omega + \gamma_{en})\left(\omega'^2 + i\omega\gamma_{en} - \omega_P^2\right)}\right\}\overrightarrow{F_{or}}^{NL} e^{i(kz-\omega t)} \quad (3.9)$$

where, $n' = n_0 e^{k_r z}$ is density perturbation which is much greater than the n_0 and $(k_1 - k_2) = k \approx k',\ (\omega_1 - \omega_2) = \omega \approx \omega'$.

k and ω are the propagation constant and frequency of generated THz field respectively. This $\vec{J}^{NL}$ gives rise to THz field generation.

By solving Maxwell's equations $\vec{\nabla}\times\vec{E} = -\frac{1}{c}\left(\partial\vec{B}/_{\partial t}\right)$ and $\vec{\nabla}\times\vec{B} = \frac{\varepsilon}{c}\left(\partial\vec{E}/_{\partial t}\right) + \frac{4\pi}{c}\vec{J}^{NL}$

we get the following wave equation for THz generation.

$$\Rightarrow \vec{\nabla}.\left(\vec{\nabla}.\vec{E}_{THz}\right) - \nabla^2\vec{E}_{THz} = \frac{\omega^2}{c^2}\varepsilon\vec{E}_{THz} + \frac{4\pi i\omega}{c^2}\vec{J}^{NL} \quad (3.10)$$

where $\vec{E}_{THz}$ is electric field of generated THz pulse.

Here we neglect the higher order derivatives, due to fast variation of THz field.

here, $\varepsilon = 1 - \left[\omega_P^2 \Big/ \{\omega^2 + i\omega\gamma_{en}\}\right]$ is electrical permittivity electron collisional plasma.

To solve equation (10), we use nonlinear oscillatory current density value from equation (9) and ε value and Obtain the terahertz field's normalised amplitude. We investigate the radial component of the electric field.

$$\frac{E_{THz}}{E} = \frac{i\omega_P^2}{\varepsilon\,\omega}\frac{e}{2r_0}\left\{\frac{\omega^2+i\omega\gamma_{en}-\omega_P^2+\omega_P^2(e^{k_z z})}{(-i\omega+\gamma_{en})(\omega^2+i\omega\gamma_{en}-\omega_P^2)}\right\}\frac{E_0 H_s\left(\frac{\sqrt{2}r}{r_0}\right)\cosh\left(\frac{br}{r_0}\right)e^{-\left(r^2/{r_0}^2\right)}}{2m\,(i\omega_1-\gamma_{en})(i\omega_2+\gamma_{en})}$$

$$\left[\hat{r}\left\{s\left(4\sqrt{2}\right)H_{s-1}\left(\frac{\sqrt{2}r}{r_0}\right)+(2b)H_s\left(\frac{\sqrt{2}r}{r_0}\right)\tanh\left(\frac{br}{r_0}\right)-\left(\frac{4r}{r_0}\right)H_s\left(\frac{\sqrt{2}r}{r_0}\right)\right\}\right] \qquad (3.11)$$

Here, $\frac{E_{THz}}{E}$ is the ratio of generated THz electric field to the applied laser electric field. This ratio is also known as THz conversion efficiency.

3.3 Result and discussion

In the current study, I have studied the phenomenon of generation of THz by interaction of HchG laser pulses in under dense plasma. For this investigation, plasma density is $9.74 \times 10^{22}\ m^{-3}$ and Corresponding plasma frequency is 1.76×10^{13} Hz. Laser frequencies (CO_2 laser) are taken as $\omega_1 = 1.973 \times 10^{14}\text{rad/s}$ and $\omega_2 = 1.783 \times 10^{14}$ rad/s where $\omega_1, \omega_2 > \omega_P$. Corresponding wavelength of laser pulses are $\lambda_1 = 9.57\mu m, \lambda_2 = 10.57\ \mu m$. Gaussian laser beam waist is taken as $r_0 = 5 \times 10^{-5}$ m and amplitude of laser field is $E_0 = 1 \times 10^{10}\ V/\text{m}$.

3.3.1 Effect of laser frequency

Variation of normalized THz wave amplitude is calculated at different normalized laser frequencies and a curve is plotted for different values of $s = 0, 1, 2$ and $b = 0, 1, 2, 3, 4, 5$ for collisional frequency $\gamma_{en} = 0.1\ \omega_P$. The comparative graphs are shown in Fig. 1(a), Fig. 1(b), and Fig. 1(c).

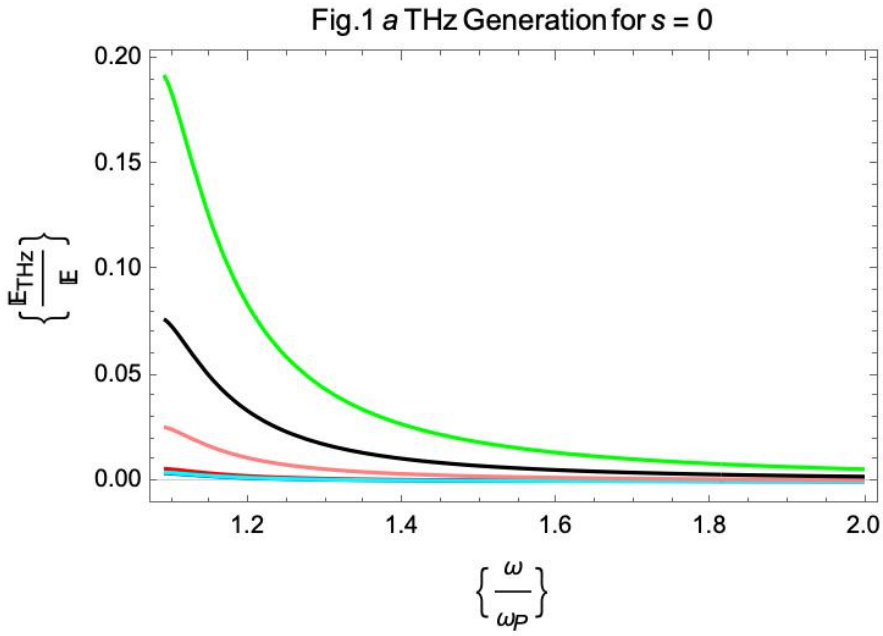

Fig. 3.1(a): Contrast of normalized THz amplitude with normalized THz frequency. For $s = 0, r = 0.6\, r_0$, b = 0 (red), 1 (blue), 2 (cyan), 3 (pink), 4 (black), 5 (green).

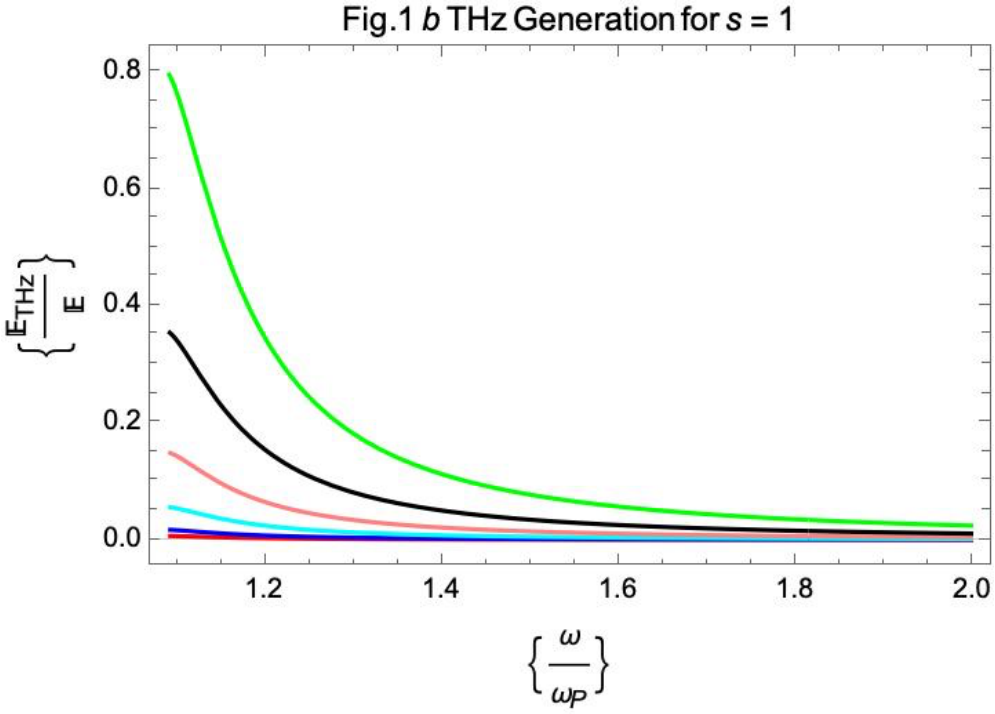

Fig. 3.1(b): Contrast of normalized THz amplitude with normalized THz frequency. For $s = 1, r = 0.6\, r_0$, , b = 0 (red), 1 (blue), 2 (cyan), 3 (pink), 4 (black), 5 (green).

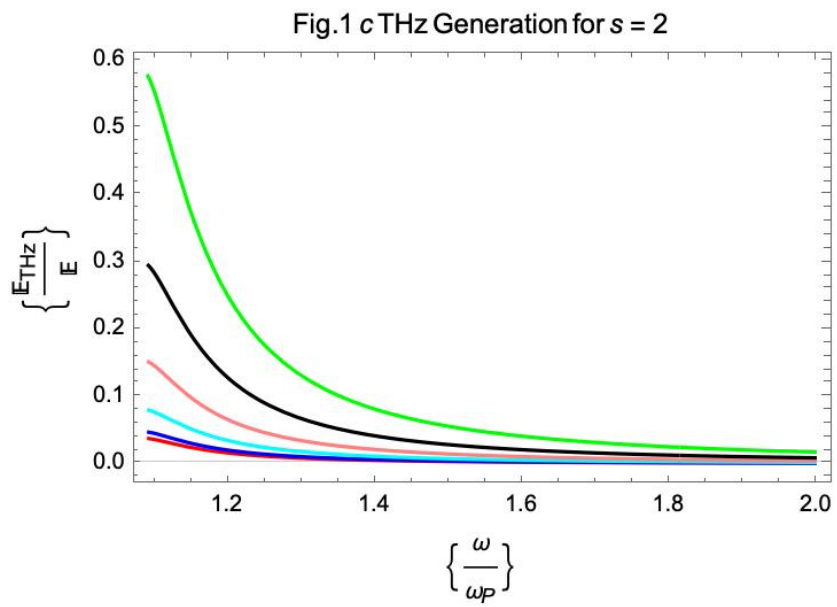

Fig. 3.1(c): Contrast of normalized THz amplitude with normalized THz frequency. For $s = 2, r = 0.6\, r_0$, , b = 0 (red), 1 (blue), 2 (cyan), 3 (pink), 4 (black), 5 (green).

For Hermite polynomial mode index($s = 0,1,2$). THz amplitude increases with increase in decentred parameter($b = 0,1,2,3,4,5$). For a particular value of decentred parameter, normalised THz amplitude is maximum for Hermite polynomial mode index $s = 1$ as compared to $s = 0$ and $s = 2$. At resonance, the generated THz amplitude is maximum, and with further increase in ω/ω_P beyond 1, THz amplitude decreases. For ω/ω_P beyond 1.6, THz amplitude reduces to nearly zero. There is no role of decentred parameter and Hermite polynomial mode index on THz generation at higher frequencies.

3.3.2 Effect of collision frequency (γ_{en})

Variation of normalized THz wave amplitude is calculated at different normalized collisional frequencies and a curve is plotted for different values of $s = 0, 1, 2$ and $b = 0, 1, 2, 3, 4, 5$ for $\omega = 1.9 \times 10^{13}$ Hz. The comparative graphs are shown in Fig. 2(a), Fig. 2(b), and Fig. 2(c).

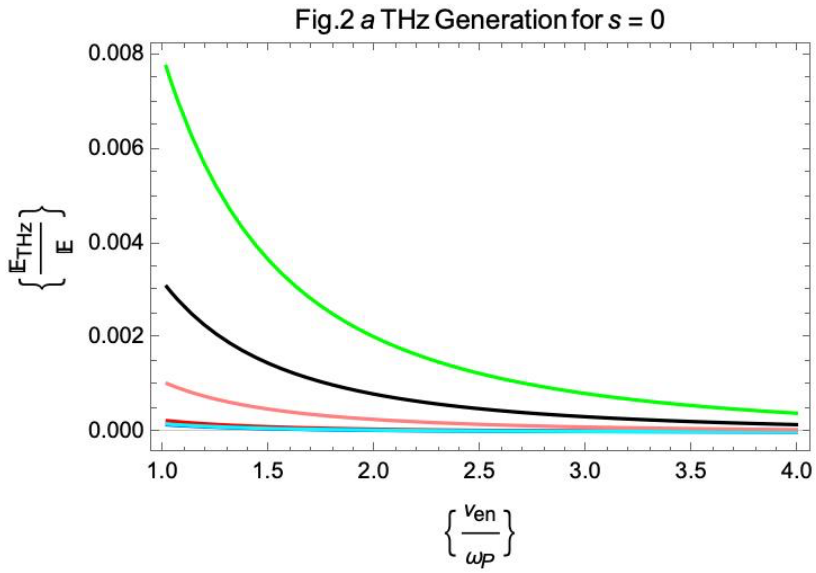

Fig. 3.2(a): Contrast of normalized THz amplitude with normalized collisional frequency. For $s = 0, r = 0.6\, r_0, , b = 0$ (red), 1 (blue), 2 (cyan), 3 (pink), 4 (black), 5 (green).

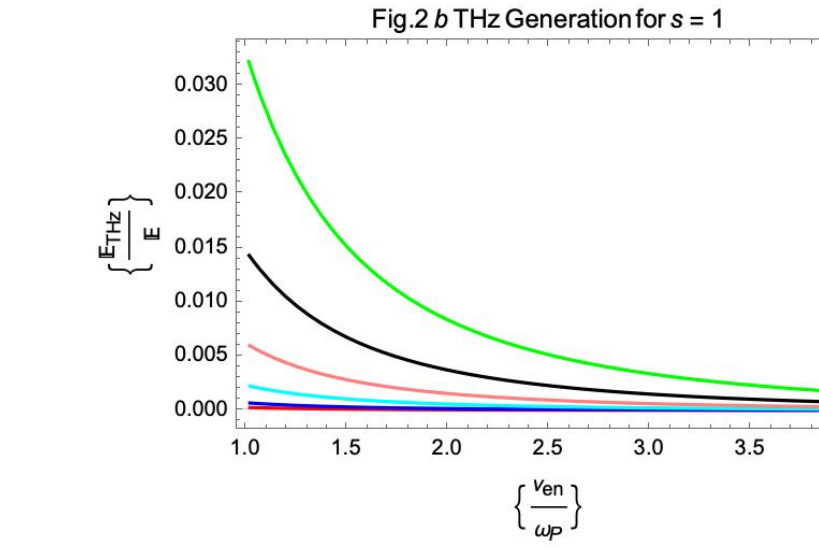

Fig. 3.2(b): Contrast of normalized THz amplitude with normalized collisional frequency. For $s = 1, r = 0.6\, r_0, , b = 0$ (red), 1 (blue), 2 (cyan), 3 (pink), 4 (black), 5 (green).

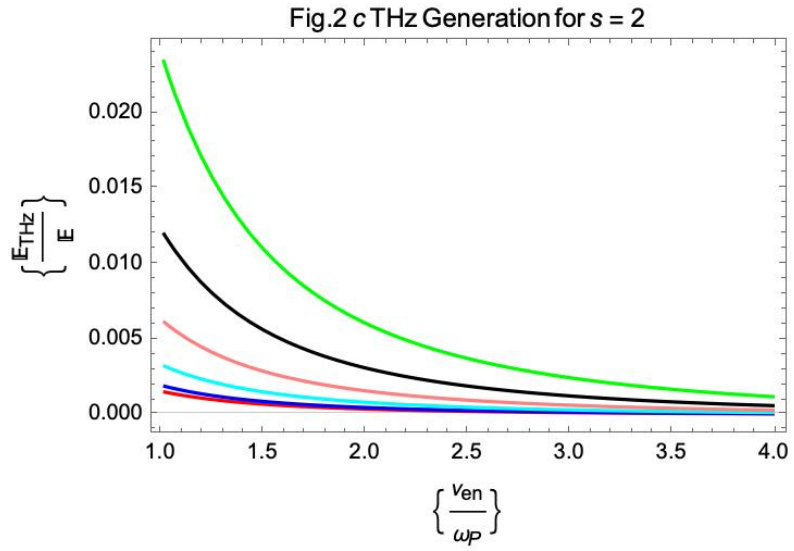

Fig. 3.2(c): Contrast of normalized THz amplitude with normalized collisional frequency. For $s = 2, r = 0.6\, r_0, , b = 0$ (red), 1 (blue), 2 (cyan), 3 (pink), 4 (black), 5 (green).

For Hermite polynomial mode index($s = 0,1,2$). THz amplitude increases with increase in decentred parameter($b = 0,1,2,3,4,5$). For a particular value of decentred parameter, normalised THz amplitude is maximum for Hermite polynomial mode index $s = 1$ as compared to $s = 0$ and $s = 2$. At resonance, the generated THz amplitude is maximum, and with further increase in ($\gamma_{en}/\ \omega_P$ beyond 1, THz amplitude decreases. For $\gamma_{en}/\ \omega_P$ beyond 4, THz amplitude reduces to nearly zero. There is no role of decentred parameter and Hermite polynomial mode index on THz generation at higher frequencies.

The outcomes of this investigation align with the findings reported by Choudhary et al. [23]. The researchers have arrived at the conclusion that employing the Hermite-cosh-Gaussian beam is a viable approach for the production of terahertz (THz) radiation. During the course of our investigation, we utilised a Hermite-cosh-Gaussian beam as a modality for the production of terahertz (THz) waves in slanting density plasma profile.

3.4 Conclusion

In this study, two HchG laser pulses are investigated which are co-propagating through a under dense plasma in an ascending density profile. THz radiation is effectively

produced by the nonlinear effects of laser plasma interaction. Analytical research is done on the relationship between THz conversion efficiency and plasma frequency as well as several laser characteristics as the Hermite polynomial mode index (s), decentered parameter (b), and collisional frequency. The findings demonstrate that the THz conversion efficiency diminishes as we go away from resonance and nearly disappears for normalized THz frequency and normalized collisional frequency for values > 1.6 and > 4 respectively. With increasing Hermite polynomial mode index values $(s = 0, 1, 2)$, THz conversion efficiency rises. By varying the values of the decentred parameter and the Hermite polynomial mode index values, the recommended method is particularly beneficial for creating high intensity, tuneable, energy-efficient THz radiation sources.

CHAPTER- 4

Interaction of p-polarised chirped laser in hot plasma with slanting density modulation

4.1 Introduction

The terahertz (THz) frequency range is situated between the infrared and microwave regions, namely between the frequency range of 10^{11} to 10^{13} Hz. The THz gap exhibits significant promise in various domains such as THz spectroscopy, topography, communication, food production and quality control, hence offering substantial chances for scholars and scientists [99], [100], [101], [102]. Over the past three decades, there has been a significant increase in the development of systems for generating THz radiation [97], [98], [103], [104], [105], [106], [107], [108], [109], [110], [111].

Forlov *et al.* [112] conducted a theoretical investigation on the effects of p-polarized radiation on semi-bounded plasma. Strong THz amplification is observed when an ultra-short laser pulse is incident at or near the critical angle. The study conducted by Xie *et al*. [113] focuses on investigating the creation of THz waves by the utilization of laser-induced air plasma. The findings demonstrate that efficient THz radiation production occurs when the incident laser possesses the same polarization state. The chirped laser pulse with a hot inhomogeneous ripple density plasma was investigated by Hashemzadeh [114]. The individual conducts research on the impact of frequency chirp, laser intensity, electron temperature, and electron density inhomogeneity on THz wave production. The investigation conducted by Li *et al.* [115] examines the interaction between laser and solid materials using chirped laser pulses at relativistic intensity. This study investigates the generation of transit current through the nonlinear interaction between laser and plasma, specifically focusing on the copper foil material. The study conducted by Huang *et al.* [116] investigated the concurrent emission of THz and X-rays resulting from the interaction between an intense, brief laser pulse and a thin, unconfined water flow in air. They demonstrate the progression of material alteration. In their study, Liao *et al.* [117] provide a comprehensive analysis of the diverse techniques employed for the generation of THz radiation. These approaches encompass the utilisation of plasma waves, electron transport, and emission as means

of THz generation. The study conducted by Zheng *et al.* [118] examined the utilisation of particle-in-simulations to investigate the creation of THz waves by laser interactions at the interface between a vacuum and plasma. The energy of induced THz waves is typically on the order of a few megawatts. The study conducted by Amouamouha *et al.* [119] focuses on the creation of THz radiation through the interaction of a super Gaussian laser beam with a plasma characterised by ripple density. The researchers employed the paraxial approximation approach in their investigation. The researchers tuned various laser plasma settings in order to achieve a THz efficiency of 6.5%. Hamsters [120] have the capability to generate sub-picosecond THz radiation by the use of laser-produced plasma. The author demonstrates that the creation of THz radiation is more pronounced when solid targets are employed as opposed to gas targets. In their study, Thakur *et al.*[121] investigate the phenomenon of second harmonic production induced by a chirped laser pulse in a plasma density ramp accompanied by a transverse magnetic field. In their research, Hashemzadeh [122] investigated the creation of THz radiation using Hermite-cosh-Gaussian and hollow Gaussian laser beams in a magnetised plasma with spatial variations. The researcher investigates the impact of a decentred parameter and an external magnetic field on the efficiency of THz generation. The study conducted by Jahangiri *et al.* [123] focuses on the development of powerful THz radiation within the range of 10-70 millijoules (mJ) from plasma formed by argon clusters. In this research, Sharma *et al.* [124] investigate the characteristics of the cosh-Gaussian laser beam within a wiggler magnetised plasma environment, with a specific focus on its potential for generating second harmonics. The results of argon gas are compared with those of argon clusters. The study conducted by Bakhtiari *et al.* [125] focuses on the creation of THz radiation by the utilisation of two Gaussian laser array beams. The researchers investigate the laser and array structure factors in order to optimise the creation of THz radiation for enhanced efficiency. In their study, Gurjar *et al.* [93] investigate the creation of THz waves in a spatially slanted density plasma profile through the beating of a chirped laser pulse. The maximum amplitude of THz waves occurs when the phase matching resonance condition is satisfied, namely at a specific slanting angle of plasma density. Thakur *et al.* [126]conducted a study on the phenomenon of self-focusing shown by Hermite-

cosh-Gaussian laser pulses in a collision less cold plasma characterised by an exponential density profile.

The work conducted by Mou *et al.* [127] investigates the impact of laser chirp on the polarisation of THz radiation. The findings demonstrate that positive and negative chirp have contrasting impacts on the polarisation state and phase difference of THz waves. The numerical investigation conducted by Nguyen *et al.* [128] examines the impact of chirp and time delay on the efficacy of THz generation. The researchers employ three-dimensional simulation techniques to achieve a conversion efficiency of 10^{-4} for THz radiation. Zhang *et al.* [129] employ the photocurrent model to theoretically investigate the creation of THz radiation through the interaction of a monochromatic chirped laser pulse with a gas plasma. The chirped and chirp-free laser pulses are compared in terms of their THz yield. In their research, Xing *et al.* [130] investigate the THz emission resulting from laser chirping in an air plasma. They employ the linear dipole array approach to analyse this phenomenon. In their study, Ghayemmoniri *et al.* [131] investigate the creation of THz pulses through the interaction of two chirped laser pulses with a carbon nanotube array in the presence of an external tapered magnetic field. The findings demonstrate that a tapered magnetic field has the ability to modulate the THz field.

Scientists and academics employ various laser and plasma characteristics to investigate distinct mechanisms, including self-focusing, Wakefield acceleration, harmonic creation, and THz generation [83], [132], [133], [134], [135], [136], [137], [138].

In the present investigation, a pair of p-polarized chirped laser beams are directed towards a hot collisional plasma characterised by a slanting up density profile. The phenomenon of laser-plasma interaction leads to the production of high-intensity THz waves. The optimisation of laser and plasma characteristics enables the attainment of an efficient source of THz radiation. Section II of this work involves the analytical derivation of the ponderomotive force, equation of motion, nonlinear plasma current density, and the subsequent generation of THz fields. In this study, Section III investigates the correlation between the normalised THz electric field and various parameters, such as the normalised THz frequency, normalised slanting up density modulation, incidence angle, normalised collisional frequency, and chirp parameter. In

the fourth section, the Conclusions are presented. The document is concluded by incorporating references.

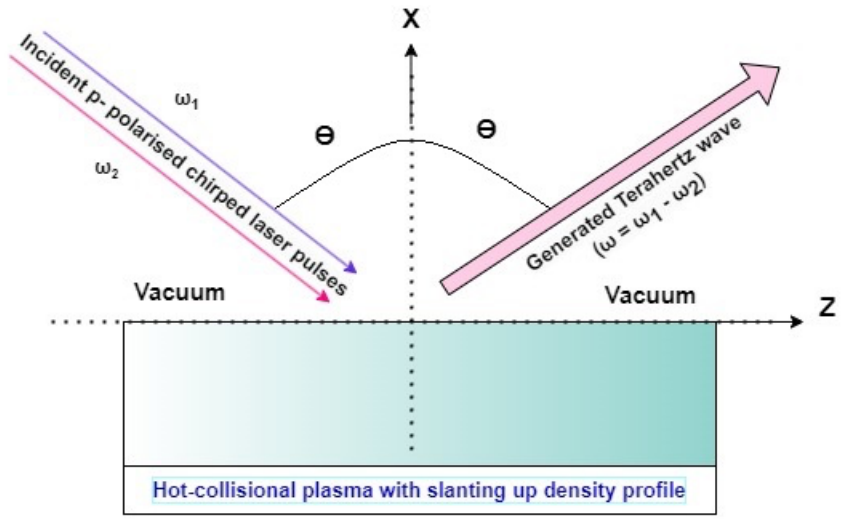

4.2 Analytical study of THz generation

Two p-polarised laser beams are propagating in x-z plane and interact with hot slanting up density plasma modulation having density profile $n = n_0 e^{k_z z}$ (where n_0 is plasma density at $z = 0$ and k_z is wave number of plasma density). Electric and magnetic fields of laser pulses are given by these equations. Electric field of two p-polarized laser beams are

$$\overrightarrow{E_J} = (\hat{z}\cos\theta - \hat{x}\sin\theta)\, E_{0J} e^{-i(\omega_J t - k_J(z\sin\theta + x\cos\theta))}, \text{ where J=1,2} \quad (4.1)$$

In this context, E_{0J} represents the amplitude of the laser beam, θ denotes the angle of incidence, ω_J signifies the angular frequency and k_J represents the propagation constant of incidental laser beam.

Corresponding magnetic field of laser beam are

$$\overrightarrow{B_j}(r,z) = \frac{\left(\vec{k}_j \times \overrightarrow{E_j}(r,z)\right)}{\omega_j}, \text{ where J = 1,2} \quad (4.2)$$

Incident laser beam is positively chirped and chirp is represented as

$$\omega_1 = \omega_0 + b\omega_0^2 \left(t - \frac{(z\sin\theta + x\cos\theta)}{c}\right),$$

where, ω_0 indicates the incident laser beam frequency when chirp is absent, b is the chirp parameter, and c is the vacuum light velocity. We choose ω_2 such as $\omega_1 - \omega_2 = \omega$ lies in THz range.

$$\text{So, } \omega_2 = \omega_1 - \omega = \left\{\omega_0 + b\omega_0^2\left(t - \frac{(z\sin\theta + x\cos\theta)}{c}\right)\right\} - \omega \qquad (4.3)$$

During the initial stage, it can be assumed that electrons are in a state of rest, resulting in the absence of any magnetic force acting upon them. The oscillatory velocity of a plasma electron can be determined by using the equation of motion $m\left(d\overrightarrow{V_J}/dt\right) = -e\,\overrightarrow{E_J} - m\overrightarrow{V_J}\nu_{en}$

Where, ν_{en} is collision frequency of collisional plasma.

By solving this equation, we get

$$\overrightarrow{V_1} = \frac{e\,\overrightarrow{E_1}}{im\omega_0\left\{1+b\omega_0\left(2t-\frac{(z\sin\theta + x\cos\theta)}{c}\right)\right\}-m\nu_{en}} \qquad (4.4)$$

$$\overrightarrow{V_2} = \frac{e\,\overrightarrow{E_2}}{im\omega_0\left\{1+b\omega_0\left(2t-\frac{(z\sin\theta + x\cos\theta)}{c}\right)-\frac{\omega}{\omega_0}\right\}-m\nu_{en}} \qquad (4.5)$$

Here, e, m, ν is charge, rest mass and collisional frequency of the plasma electron respectively.

This oscillatory velocity of plasma electron give rise to nonlinear ponderomotive force.

Nonlinear ponderomotive force is

$$\overrightarrow{F_P}^{NL} = -\frac{e}{2c}\left(\overrightarrow{V_1}\times\overrightarrow{B_2}^{*} + \overrightarrow{V_2}^{*}\times\overrightarrow{B_1}\right) - \frac{m}{2}\vec{\nabla}\left(\overrightarrow{V_1}\,\overrightarrow{V_2}^{*}\right) \qquad (4.6)$$

Here, * represents the complex conjugate.

Solving this equation by putting values of $\overrightarrow{V_1}, \overrightarrow{V_2}^{*}, \overrightarrow{B_1}, and\ \overrightarrow{B_2}^{*}$ and neglecting the higher order derivatives of second term, we get

$$\overrightarrow{F_P}^{NL} =$$

$$(\hat{x}\cos\theta + \hat{z}\sin\theta)\,\frac{e^2\,E_1E_2^{*}}{2im\omega_0 c}\left(\frac{2\frac{\nu}{i\omega_0} - \frac{\omega}{\omega_0}}{\left\{1+b\omega_0\left(2t-\frac{(z\sin\theta + x\cos\theta)}{c}\right)-\frac{\nu_{en}}{i\omega_0}\right\}\left\{1+b\omega_0\left(2t-\frac{(z\sin\theta + x\cos\theta)}{c}\right)-\frac{\omega}{\omega_0}+\frac{\nu_{en}}{i\omega_0}\right\}}\right) \qquad (4.7)$$

By solving the equation of motion $\partial\vec{V}_\omega^{NL}/\partial t = \vec{F}_P^{NL}/m - \nu_{en}\vec{V}_\omega^{NL}$ and equation of continuity $\partial n_\omega^{NL}/\partial t + \vec{\nabla}.n\vec{V}_\omega^{NL} = 0$, For slanting up density profile $n = n_0e^{k_zz}$, we get nonlinear oscillatory velocity and nonlinear density perturbation of plasma electron as per given equation.

$$\vec{V}_\omega^{NL} = \frac{i\omega\vec{F}_P^{NL}}{m(\omega^2+i\omega\nu_{en})} \qquad (4.8)$$

$$n_{\omega}^{NL} = \frac{n_0 \vec{\nabla}.(e^{k_z z})\vec{F}_P^{NL}}{m(\omega^2 + i\omega\nu_{en})} \quad (4.9)$$

In this derivation we consider n is constant with time, and is a function of z only so $\partial(\mathrm{n})/\partial \mathrm{t} = 0$.

This nonlinear density perturbation n_{ω}^{NL} give rise to self-consistent space charge potential ϕ and field, because of separation of electrons from ions. This gives rise to linear density perturbation as $n_{\omega}^{L} = -\chi_P \vec{\nabla}.(\vec{\nabla}\phi)/4\pi e$ where, $\chi_P = -\omega_P^2/(\omega^2 + i\omega\nu_{en} - k^2 V_{th}^2)$ is electric susceptibility of collisional plasma.

Using Poisson's equation $\nabla^2\phi = 4\pi(n_{\omega}^{L} + n_{\omega}^{NL})e$, we get linear force $\vec{F}_P^{L}$ due to space charge field on electrons such as

Linear force $\vec{F}_P^{L} = \mathrm{e}\vec{\nabla}\phi = \frac{\omega_P^2 \, e^{k_z z} \, \vec{F}_P^{NL}}{(1+\chi_P)(\omega^2 + i\omega\gamma_{en})}$ (4.10)

as, $\omega_P = \sqrt{\left(4\pi n_0 e^2/m\right)}$ is plasma frequency.

By solving the equation of motion $\partial\vec{V}^{NL}/\partial t = \left(\vec{F}_P^{NL} + \vec{F}_P^{L}\right)/m - \nu_{en}\vec{V}^{NL}$, nonlinear oscillatory velocity of electrons because of the linear and nonlinear ponderomotive forces calculated as

$$\vec{V}_{\omega}^{NL} = \frac{1}{m}\left\{\frac{\omega^2 + i\omega\nu_{en} - \omega_P^2 + \omega_P^2(e^{k_z z})}{(-i\omega + \nu_{en})(\omega^2 + i\omega\nu_{en} - \omega_P^2)}\right\}\vec{F}_P^{NL} \quad (4.11)$$

Here, we consider $\omega_{1,}\omega_2 \gg \omega_P$

$\vec{J}^{NL} = -\frac{1}{2}ne\vec{V}^{NL}$, where $n = n_0 e^{k_z z}$ is density perturbation which is much greater than the n_0.

$$\Rightarrow \vec{J}^{NL} = -\frac{n_0 e}{2m}\left\{\frac{\omega^2 + i\omega\nu_{en} - \omega_P^2 + \omega_P^2(e^{k_z z})}{(-i\omega + \nu_{en})(\omega^2 + i\omega\nu_{en} - \omega_P^2)}\right\}\vec{F}_P^{NL} e^{i(kz - \omega t)} \quad (4.12)$$

Where $(k_1 - k_2) = k \; and \; (\omega_1 - \omega_2) = \omega$

This nonlinear current density is responsible for THz generation. By using III and IV Maxwell's equation, $\vec{\nabla} \times \vec{E} = -\frac{1}{c}\left(\partial\vec{B}/_{\partial t}\right)$ and $\vec{\nabla} \times \vec{B} = (\varepsilon/_c)\left(\partial\vec{E}/_{\partial t}\right) + \left(4\pi/_c\right)\vec{J}^{NL}$, we can calculate the THz wave generation equation.

Equation for THz generation is

$$\vec{\nabla}.\left(\vec{\nabla}\overrightarrow{E_{THz}}\right) - \nabla^2\overrightarrow{E_{THz}} = \frac{\omega^2}{c^2}\varepsilon\overrightarrow{E_{THz}} + \frac{4\pi i\omega}{c^2}\vec{J}^{NL} \tag{4.13}$$

In order to neglect higher order derivatives due to fast variation of THz field. So normalized THz amplitude is

$$\frac{E_{THz}}{E} = \left[\frac{\omega_p^2 eE}{\varepsilon\,\omega m\omega_0 c}\left\{\frac{\omega^2 + i\omega\nu_{en} - \omega_p^2 + \omega_p^2(e^{k_z z})}{(-i\omega + \nu_{en})(\omega^2 + i\omega\nu_{en} - \omega_p^2)}\right\} e^{i(kz-\omega t)}(\hat{x}\cos\theta + \hat{z}\sin\theta)\left(\frac{\frac{\omega}{\omega_0} - 2\frac{\nu_{en}}{i\omega_0}}{\left\{1 + b\omega_0\left(2t - \frac{(z\sin\theta + x\cos\theta)}{c}\right) - \frac{\nu_{en}}{i\omega_0}\right\}\left\{1 + b\omega_0\left(2t - \frac{(z\sin\theta + x\cos\theta)}{c}\right) - \frac{\omega}{\omega_0} + \frac{\nu_{en}}{i\omega_0}\right\}}\right)\right] \tag{4.14}$$

Here, we consider incidental beam have same electric field amplitude $E_{01} = E_{02} = E$ is the amplitude of incident laser beam.

4.3 Result and discussion

In this investigation of THz generation, two p-polarised laser beams are positively chirped and propagating in hot collisional under dense plasma. For this study we choose suitable laser parameter such as femtosecond Ti-Sapphire laser with wave length of 800 nm having angular frequency 2.35×10^{15} rad/sec, chirp parameter of 0.0011, propagation distance (z) = propagation distance (x) = 20 μm, time $t = 50\ fs$, incidence angle is $\pi/6$ radian and electric field amplitude of 1×10^{12} V/m. Plasma parameters are optimised as plasma density is $5\times10^{23}m^{-3}$. Here in present study, we choose $\omega = 1.025\ \omega_P$ where, $\omega_1, \omega_2 > \omega_P$ and $\nu_{en} = 0.1\ \omega_P$.

4.3.1 Effect of normalised THz frequency (ω/ω_P)

In this study variation of normalised THz amplitude is analysed with normalised THz frequency at $k_z = 0.9$ k for chirp parameter b = 0.0011(red), 0.0044(blue), 0.0066(green), 0.0099(black).

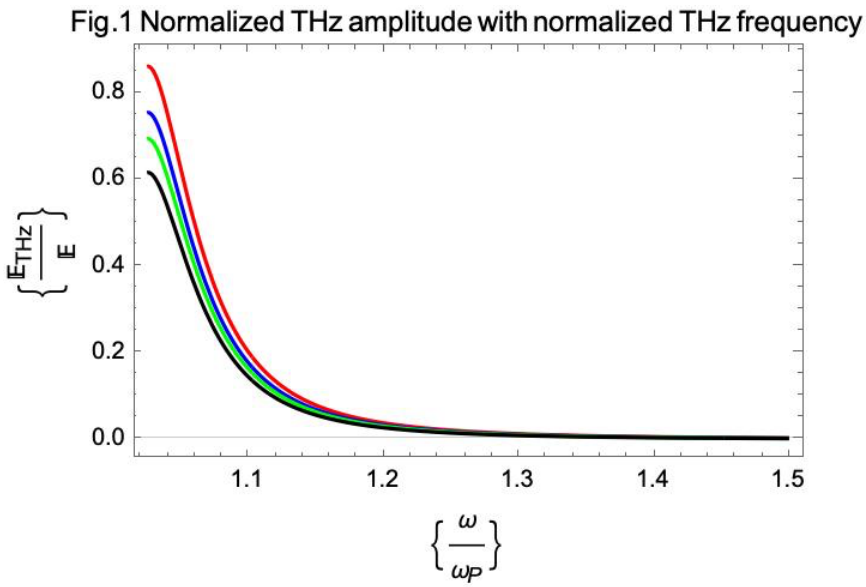

Fig. 4.1: Variation of normalized THz amplitude with normalized THz frequency for chirp parameter $\mathrm{b} = 0.0011(\mathrm{red}),\ 0.0044(\mathrm{blue}),\ 0.0066(\mathrm{green}),\ 0.0099(\mathrm{black})$. For $k_z = 0.9$ k. Other parameters are same as mentioned above.

For off-resonant condition, normalised THz amplitude decreases rapidly and approaches to zero for normalised THz frequency (ω/ω_P) greater than 1.2. Normalised THz amplitude approaches more than 0.8, as we decrease the chirp parameter from 0.0099 to 0.0011. The maximum normalised THz amplitude decreases from approximately 0.8 to 0.6. So, increase in chirp parameter decreases the THz conversion efficiency significantly.

4.3.2 Effect of normalised slanting up density modulation parameter (k_z/k)

This study aims to conduct a theoretical analysis of the relationship between the normalised amplitude of THz radiation and the wave propagation distance of THz waves. The analysis focuses on various values of the chirp parameter $\mathrm{b} = 0.0011(\mathrm{red}),\ 0.0044(\mathrm{blue}),\ 0.0066(\mathrm{green}),\ 0.0099(\mathrm{black})$.

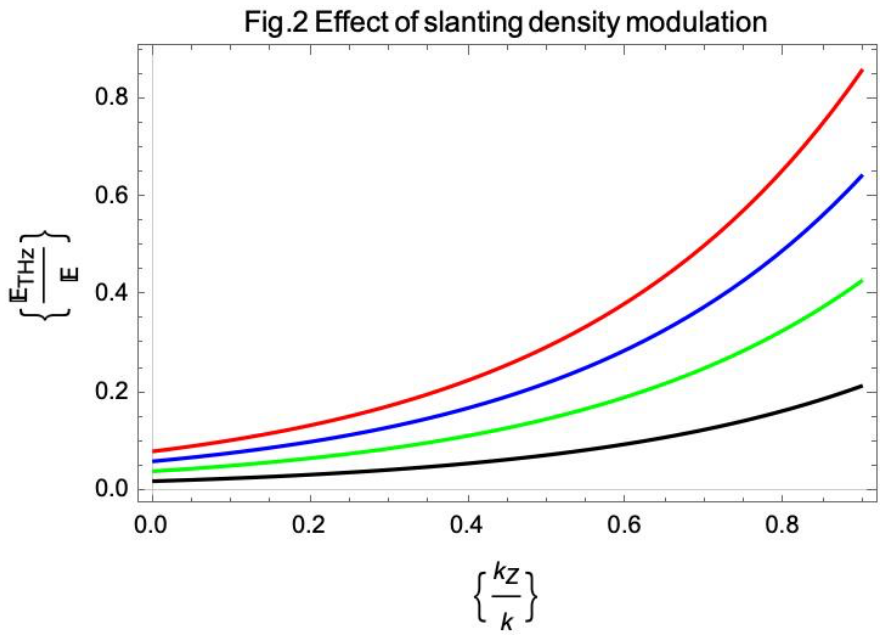

Fig. 4.2: Variation of normalized THz amplitude with normalized slanting up density parameter for chirp parameter b = 0.0011 (red), 0.0044 (blue), 0.0066 (green), 0.0099 (black). Other parameters are same as mentioned above.

This study shows that normalised THz amplitude increases with normalised slanting up density modulation parameter (k_z/k). With the increase in the chirp parameter from 0.0011 to 0.0099, the maximum value of normalised THz amplitude decreases from 0.8 to 0.2 approximately.

4.3.3 Effect of incidence angle (θ)

This study focus on examining the relationship between the normalised THz amplitude and the incident angle for chirp parameter b=0.0011. In Fig. (3), normalized THz amplitude is shown along vertical axis while, oblique angle (normalized by π/12) is represented along horizontal axis. This examination shows that normalised THz amplitude changes in oscillatory manner with incidence oblique angle and the peak of the curve (maximum THz amplitude) is obtained at normalized oblique value 3.

Corresponding oblique angle is 3* π/12 or 45^0 with selected parameters. It concludes that for effective THz generation, oblique angle also plays a crucial role, and this angle should be optimized to obtain energy efficient THz generation.

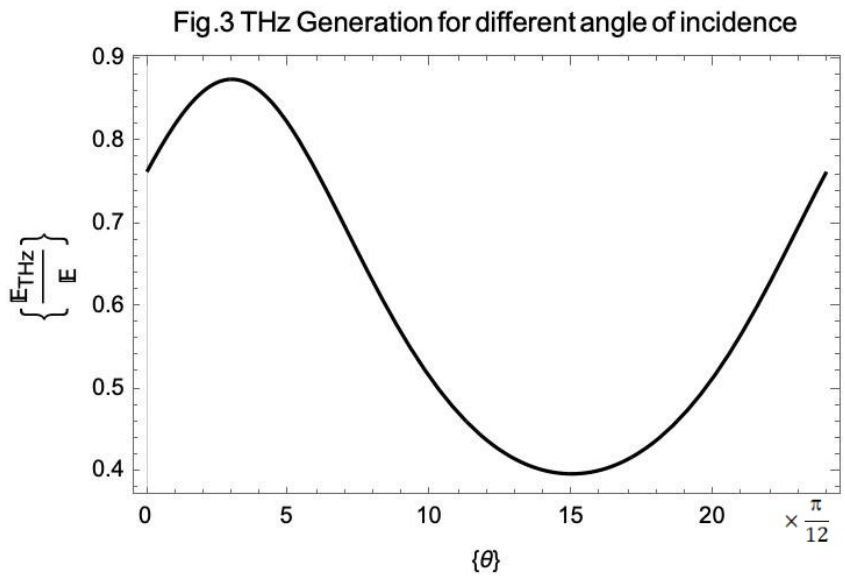

Fig. 4.3: Variation of normalized THz amplitude with normalized THz frequency for chirp parameter b $= 0.0011$ and $k_z = 0.9$ k. Other parameters are same as mentioned above.

Normalised THz amplitude has maximum value is 0.86 for incidence angle 45^0 and minimum value is 0.4 for incidence angle 225^0.

4.3.4 Effect of normalised collisional frequency ($^{\nu_{en}}/_{\omega_P}$)

This study focuses on examining the relationship between the normalised THz amplitude and the normalised collisional frequency for b=0.0011 and $\theta = \pi/6$.

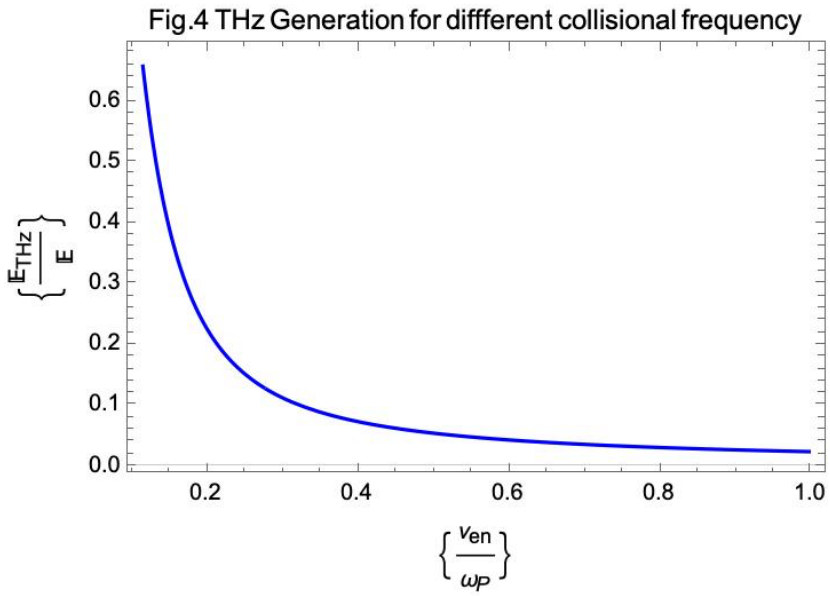

Fig. 4.4: Contrast of normalized THz amplitude with normalized collisional frequency for chirp parameter b=0.0011 and k_z=0.9 k, λ=800 nm, z = x = 20 μm, t=50 fs. Other parameters are same as mentioned above.

According to the findings of the investigation, the normalised THz amplitude experiences a precipitous drop as the normalised collisional frequency rises. Approximately 0.7 is the maximum value for the normalised THz amplitude. When the normalised collisional frequency is bigger than 0.8 value, the normalised THz amplitude gets closer and closer to zero. This indicates that an increase in collisional properties of plasma, there is corresponding decrease in generated THz amplitude.

This investigation's results are consistent with the findings documented by Hashemzadeh [114] The conclusion drawn by the researchers is that the utilisation of a p-polarised chirped laser beam proves to be an efficacious approach in the generation of THz radiation. During the course of our investigation, we utilised a chirped p-polarized beam within a hot collisional slanting up plasma profile as a method for producing THz waves.

4.4 Conclusion

This study examines the propagation of two p-polarised chirped laser beams in a hot collisional under dense plasma medium. An analytical solution is derived to determine the efficiency of THz generation, considering various characteristics such as the normalized THz frequency, incidence angle, collisional frequency, normalized transverse distance, and frequency chirp. The resulting solution is then analysed to optimize these parameters, aiming to achieve a tunable and energy-efficient THz source. The normalized THz amplitude exhibits significant values up to 0.8 for normalized THz frequency corresponding to chirp parameter b = 0.0011. The findings indicate that as the value of the chirp parameter increases from 0.0011 to 0.0099, there is a decrease in the normalized amplitude of the THz signal. The normalised THz amplitude changes in oscillating manner with change in incidence angle from zero to 2π and shows a maximum for incident oblique angle 45^0 and minima at 225^0. This study aims to contribute to the existing body of information about the determination of optimal incident oblique angle, chirp parameter, and collisional frequency for the purpose of achieving an energy-efficient THz source.

CHAPTER- 5

Hermite-cosh-Gaussian chirped laser in static magnetized plasma for enhanced THz generation

5.1 Introduction

Terahertz wave applications in the fields of chemical analysis, non-destructive testing, medical imaging and research is gaining attention of scholars and industries [86], [139], [140], [141]. A wide variety of fields such as nonlinear optics, harmonic generation, self-focusing, filamentation, electron acceleration, wake field generation, terahertz wave generation, etc. uses the laser plasma interaction process [12], [13], [14], [66], [73], [77]. Hermite-cosh-Gaussian beam is the member of Hermite sinusoidal Gaussian family. The Hermite-Cosh function is utilized to represent a laser beam profile that encompasses Hermite polynomials, Gaussian and hyperbolic cosine components, and Gaussian-like spatial variation. Lasers with higher-order transverse modes, characterized by more complex intensity distributions compared to the fundamental Gaussian mode. The Hermite-cosh-Gaussian function's paraxial wave solution is introduced by Casperson and Tovar [142]. Through the use of a paraxial wave solution, Belafhal et al. theoretically examined the wave propagation characteristics of the Hermite-cosh-Gaussian function in the ABCD system [143].

Scientists study the Hermite-cosh-Gaussian laser pulse in various laser plasma interaction phenomena. The Hermite-cosh-Gaussian laser beam in magneto-active plasma was studied by Patil et al. They investigated how the decentred parameter and the mode index affected self-focusing [144]. The self-focusing of a Hermite-cosh-Gaussian laser beam in ramp density and under density plasma profiles was investigated by Nanda et al [145], [146]. The Hermite-cosh-Gaussian laser beam in ripple density plasma was studied numerically by Kaur et al.[147]. In semiconductor plasma, Wani et al. [148]looked at the self-focusing of a Hermite-cosh-Gaussian beam. The third harmonics generation by Hermite-cosh-Gaussian beam in the presence of wiggler magnetic field was theoretically investigated by Sharma et al.[88]. The beat wave of Hermite-cosh-Gaussian laser beam absorption in collisional nano cluster plasma profile was studied by Ashish Verma and Asheel Kumar[149]. In this research, they looked at the Bernstein wave parameters. In collisional plasma, the second harmonics generation

of the Hermite Gaussian beam was explored by Jyoti Wadhwa and Arvinder Singh. The researchers conducted an investigation on the influence of mode indices on the generation of harmonics and the phenomenon of self-focusing[150]. In order to generate Terahertz waves, Hamster et al.[151] investigate the interaction between a short, powerful laser pulse and plasma. The researchers conducted an investigation on the nonlinear ponderomotive force effect in the production of Terahertz waves. In their study, Safari and Jazi investigated the properties of collisional plasma by employing laser beams with Gaussian and Hermite-cosh-Gaussian profiles. They came to the conclusion that plasma and laser parameters are crucial for Terahertz field amplitude [152]. The Terahertz wave generation with radially polarized Hermite-cosh-Gaussian laser beam in hot collisional plasma was studied by Chaudhary et al. [153]. In their theoretical inquiry, Malik et al.[91] looked at the creation of Terahertz waves using two Hermite-cosh-Gaussian laser beams in a periodically varying plasma density profile with an applied magnetic field. They investigated how Terahertz wave production was affected by the decentred parameter, Hermite function order, and applied magnetic field. Hashemzadeh looked into the production of Terahertz waves in magnetized plasma using laser beams that were Hermite-cosh-Gaussian and hollow Gaussian. The researchers reached the conclusion that the introduction of external magnetic fields results in a radial increase in the magnitude of the Terahertz field[154]. In collisional inhomogeneous plasma, Safari et al.[155] looked at the nonlinear processes of Hermite-cosh-Gaussian and Laguerre-Gaussian beam interaction. For the greatest electric field amplitude at Terahertz frequencies, they examined various laser parameters and density ripple. The Hermite-cosh-Gaussian laser pulse is investigated by Rajput et al.[156] in their work on electron acceleration in a vacuum. The researchers utilized laser pulses with both circular and linear polarization. The Terahertz production was investigated by Mehta et al.[46] by the utilization of a transverse external magnetic field in conjunction with under dense plasma and chirped laser pulses. The authors of the study illustrate the enhancement of the Terahertz electric field in the presence of a magnetic field, as well as the optimization of the chirp value. They also investigate the impact of chirped laser pulses on the ripple in density[47].

Wu et al.[157] studied the chirped laser pulse-induced Terahertz pulse production in a lithium niobate crystal at ambient temperature. They produce a 0.2 mJ Terahertz pulse

for their research. Jiang et al.[158] generated 0.3 mW Terahertz pulses while studying the GaP crystal using a negatively chirped femtosecond laser pulse. In order to generate Terahertz waves at beat frequency, Gurjar et al.[93] looked at the nonlinear interaction of chirped laser pulse interaction with slanting plasma modulation. They demonstrate that the generated Terahertz wave amplitude is strongly affected by the slanting plasma profile.

In the current study, two linearly polarized Hermite-cosh-Gaussian beams propagate in z direction. These laser beams are positively chirp. These laser beams propagated in under dense collision less plasma with transverse static magnetic field. The interaction between laser and plasma results in the generation of intense terahertz (THz) waves. Tunable efficient THz radiation source can be achieved by adjusting the laser and plasma parameters.

5.2 Analytical study of THz generation

Two waves, which are linearly polarized and have the Hermite-cosh-Gaussian profile, are propagating in the z direction. The direction of polarization of the electric field is aligned with the x-axis, and can be mathematically expressed by the following equation.

$$\overrightarrow{E_J} = \hat{x}E_0H_s\left(\frac{\sqrt{2}x}{w_0}\right)\cosh\left(\frac{ax}{w_0}\right)e^{-\left(x^2/w_0{}^2\right)}e^{i(k_Jz-\omega_Jt)};\ \text{Where, J=1,2}$$

Here, E_0 is the amplitude of laser pulse, w_0 is pulse waist, a is decentered parameter of cosh profile, s is the mode index of Hermite polynomial H_s.

A static external magnetic field is applied along the y-axis i.e., $B_s = B_0\hat{y}$. Incident laser beam is positively chirped and chirp is represented as $\omega_1 = \omega_0 + b\omega_0^2\left(t - \frac{z}{c}\right)$, where b is the chirp parameter, c is the light velocity, and ω_0 is the incident laser beam in the absence of chirp. We choose ω_2 such as $\omega_1 - \omega_2 = \omega$ lies in THz range.

Two linearly polarized Hermite-cosh-Gaussian laser beams are propagating in z direction. Electric field of two linearly polarized Hermite-cosh-Gaussian laser beams

$$\overrightarrow{E_1}(x,z) = \hat{x}E_0H_s\left(\frac{\sqrt{2}x}{w_0}\right)\cosh\left(\frac{ax}{w_0}\right)e^{-\left(x^2/w_0{}^2\right)}e^{i(k_1z-\omega_1t)} \quad (5.1)$$

$$\overrightarrow{E_2}(y,z) = \hat{x}E_0H_s\left(\frac{\sqrt{2}x}{w_0}\right)\cosh\left(\frac{ax}{w_0}\right)e^{-\left(x^2/w_0{}^2\right)}e^{i(k_2z-\omega_2t+\delta)} \quad (5.2)$$

Here, E_0 is amplitude of laser pulse, w_0 is beam waist, a is decentered parameter of cosh profile, s is the mode index of Hermite polynomial H_s ,

Corresponding magnetic field of laser beam are

$$\overrightarrow{B_J}(r,z) = \frac{\{\vec{k}_J \times \overrightarrow{E_J}(r,z)\}}{\omega_J} \quad \text{where } J = 1,2 \tag{5.3}$$

The positive frequency chirp is

$$\omega_1 = \omega_0 + b\omega_0^2\left(t - \frac{z}{c}\right), \tag{5.4}$$

$$\omega_2 = \omega_1 - \omega = \left\{\omega_0 + b\omega_0^2\left(t - \frac{z}{c}\right)\right\} - \omega \tag{5.5}$$

In the initial stage, electrons can be considered at rest so electrons will not experience any magnetic force. So, from equation of motion oscillatory velocity of plasma electron is

$$\Rightarrow \overrightarrow{V_1} = \frac{e\,\overrightarrow{E_1}}{im\omega_0\left\{1+b\omega_0\left(2t-\frac{z}{c}\right)\right\}-m\nu} = \frac{e\,\overrightarrow{E_1}}{im\omega_1'-m\nu} = \frac{e\,\overrightarrow{E_1}}{m(i\omega_1'-\nu)} \tag{5.6}$$

$$\Rightarrow \overrightarrow{V_2} = \frac{e\,\overrightarrow{E_2}}{im\omega_0\left\{1+b\omega_0\left(2t-\frac{z}{c}\right)-\frac{\omega}{\omega_0}\right\}-m\nu} = \frac{e\,\overrightarrow{E_2}}{im\omega_2'-m\nu} = \frac{e\,\overrightarrow{E_2}}{m(i\omega_2'-\nu)} \tag{5.7}$$

Here, $\omega_1' = \omega_0\left\{1 + b\omega_0\left(2t - \frac{z}{c}\right)\right\}$, $\omega_2' = \omega_0\left\{1 + b\omega_0\left(2t - \frac{z}{c}\right) - \frac{\omega}{\omega_0}\right\}$,

and e, m, ν is charge, rest mass and collisional frequency of the plasma electron respectively. This oscillatory velocity of plasma electron give rise to nonlinear ponderomotive force.

Nonlinear ponderomotive force is

$$\overrightarrow{F_P}^{NL} = -\frac{e}{2c}\left(\overrightarrow{V_1} \times \overrightarrow{B_2}^* + \overrightarrow{V_2}^* \times \overrightarrow{B_1}\right) - \frac{m}{2}\vec{\nabla}\left(\overrightarrow{V_1}\,\overrightarrow{V_2}^*\right) \tag{5.8}$$

Here, * represents the complex conjugate.

Solving this equation by putting values of $\overrightarrow{V_1}, \overrightarrow{V_2}^*, \overrightarrow{B_1}, and\ \overrightarrow{B_2}^*$, we get

$$\overrightarrow{F_P}^{NL} = -\hat{z}\,\frac{e^2 E_1 E_2^*}{2im\omega_0 c}\left(\frac{2\frac{\nu}{\omega_0} - \frac{\omega}{\omega_0}}{\left\{1+b\omega_0\left(2t-\frac{z}{c}\right)-\frac{\nu}{i\omega_0}\right\}\left\{1+b\omega_0\left(2t-\frac{z}{c}\right)-\frac{\omega}{\omega_0}+\frac{\nu}{i\omega_0}\right\}}\right) -$$

$$\hat{z}\,\frac{be^2 E_1 E_2^*}{m\omega_0 c}\left(\frac{\left\{1+b\omega_0\left(2t-\frac{z}{c}\right)-\frac{\omega}{2\omega_0}\right\}}{\left\{\left\{1+b\omega_0\left(2t-\frac{z}{c}\right)\right\}-\frac{\nu}{i\omega_0}\right\}^2\left\{1+b\omega_0\left(2t-\frac{z}{c}\right)-\frac{\omega}{\omega_0}+\frac{\nu}{i\omega_0}\right\}^2}\right) \tag{5.9}$$

Plasma electrons starts moving in circular path due to Lorentz force by external static magnetic field. Circular motion of plasma electron interacts with electric field of laser beam result into angular motion of plasma electron with cyclotron frequency ω_c.

By figuring out the equation of motion $\frac{\partial \vec{V}_{\omega'}^{NL}}{\partial t} = \frac{\vec{F}_P^{NL}}{m} - \nu_{en}\vec{V}_{\omega'}^{NL} - \frac{e}{mc}\{\vec{V}_{\omega'}^{NL} \times \vec{B}\}$ we get the oscillatory velocity of plasma electron such as

$$\overrightarrow{V_{\omega'}^{NL}} = \frac{\omega_c \hat{x} - i\omega\hat{z}}{m\,({\omega_c}^2 - \omega^2)} F_{Pz}^{NL}$$

Here, we consider $\omega_{1,}\omega_2 >> \omega_c, \omega_P$

Where ω_P is plasma frequency is such as ${\omega_P}^2 = \frac{4\pi ne^2}{m}$ and $\omega_c = {eB_0}/{mc}$ is cyclotron frequency. Nonlinear oscillatory current density can be calculated by solving this equation $\vec{J}^{NL} = -\frac{1}{2}ne\vec{V}^{NL}$,

$$\Rightarrow \vec{J}^{NL} = -\frac{{\omega_P}^2}{8\pi e}\frac{\omega_c\hat{x} - i\omega\hat{z}}{({\omega_c}^2 - \omega^2)} F_{Pz}^{NL} \tag{5.10}$$

The nonlinear current density facilitates THz production. By using III and IV Maxwell's equation, we can calculate the THz wave generation equation.

From Maxwell's equations $\vec{\nabla} \times \vec{E} = -\frac{1}{c}\frac{\partial \vec{B}}{\partial t}$

As $\vec{\nabla} \times \vec{B} = \frac{\varepsilon}{c}\frac{\partial \vec{E}}{\partial t} + \frac{4\pi}{c}\vec{J}^{NL}$

Equation for THz generation is

$$\Rightarrow \vec{\nabla}.\left(\overrightarrow{\nabla E_{THz}}\right) - \nabla^2\overrightarrow{E_{THz}} = \frac{\omega^2}{c^2}\varepsilon\overrightarrow{E_{THz}} + \frac{4\pi i\omega}{c^2}\vec{J}^{NL} \tag{5.11}$$

In order to neglect higher order derivatives due to fast variation of THz field So

$$E_{THz} = \frac{{\omega_P}^2}{2e\varepsilon\,\omega\sqrt{{\omega_c}^2 - \omega^2}}\left\{-\frac{e^2\,E_1E_2^*}{2im\omega_0 c}\left(\frac{2\frac{\nu}{\omega_0} - \frac{\omega}{\omega_0}}{\left\{1+b\omega_0\left(2t-\frac{z}{c}\right)-\frac{\nu}{i\omega_0}\right\}\left\{1+b\omega_0\left(2t-\frac{z}{c}\right)-\frac{\omega}{\omega_0}+\frac{\nu}{i\omega_0}\right\}}\right) - \right.$$

$$\left.\frac{be^2\,E_1E_2^*}{m\omega_0 c}\left(\frac{\left\{1+b\omega_0\left(2t-\frac{z}{c}\right)-\frac{\omega}{2\omega_0}\right\}}{\left\{\left\{1+b\omega_0\left(2t-\frac{z}{c}\right)\right\}-\frac{\nu}{i\omega_0}\right\}^2\left\{1+b\omega_0\left(2t-\frac{z}{c}\right)-\frac{\omega}{\omega_0}+\frac{\nu}{i\omega_0}\right\}^2}\right)\right\}$$

$$\frac{E_{THz}}{E_0} =$$

$$\frac{e{\omega_P}^2}{2\varepsilon\,\omega\sqrt{{\omega_c}^2-\omega^2}}\frac{\left\{H_s\left(\frac{\sqrt{2}x}{w_0}\right)\cosh\left(\frac{ax}{w_0}\right)\right\}^2 e^{-\left(2x^2/{w_0}^2\right)}E_0}{m\omega_0 c\left\{1+b\omega_0\left(2t-\frac{z}{c}\right)\right\}\left\{1+b\omega_0\left(2t-\frac{z}{c}\right)-\frac{\omega}{\omega_0}\right\}}\sqrt{b^2\left(\frac{\left\{1+b\omega_0\left(2t-\frac{z}{c}\right)-\frac{\omega}{2\omega_0}\right\}}{\left\{1+b\omega_0\left(2t-\frac{z}{c}\right)\right\}\left\{1+b\omega_0\left(2t-\frac{z}{c}\right)-\frac{\omega}{\omega_0}\right\}}\right)^2 - \frac{1}{4}\left[\frac{\omega}{\omega_0}\right]^2} \tag{5.12}$$

5.3 Result and discussion

In this investigation of THz generation, two Hermite-cosh Gaussian polarised laser beams are positively chirped and propagating in cold collision less under dense plasma.

For this study we choose suitable laser parameter such as femtosecond Ti:Sapphire laser with wave length of 800nm having angular frequency 2.35×10^{15} rad/sec , chirp parameter is 0.0099, beam waist of 5×10^{-5}m and electric field amplitude is 5×10^{9} V/m.. Plasma parameters are optimised as plasma density is $9.74\times10^{22}m^{-3}$, whose corresponding plasma frequency ω_P is $1.76\times10^{13}\ Hz$. Here in present study, we choose $\omega = 1.07\ \omega_P$ where $\omega_1, \omega_2 > \omega_P$ and applied external static magnetic field is 10 Tesla.

5.3.1 Effect of normalised transverse distance (x/w_0) and decentred parameter (b)

Variation of normalized THz wave amplitude is calculated at different normalized transverse distance and different decentred values a=0,1,2,3. A three-dimensional curve is plotted for different values of Hermite polynomial mode index values s=0,1,2 at $E_0 = 5\times10^{9}$ V/m and external static magnetic field is 10 T.

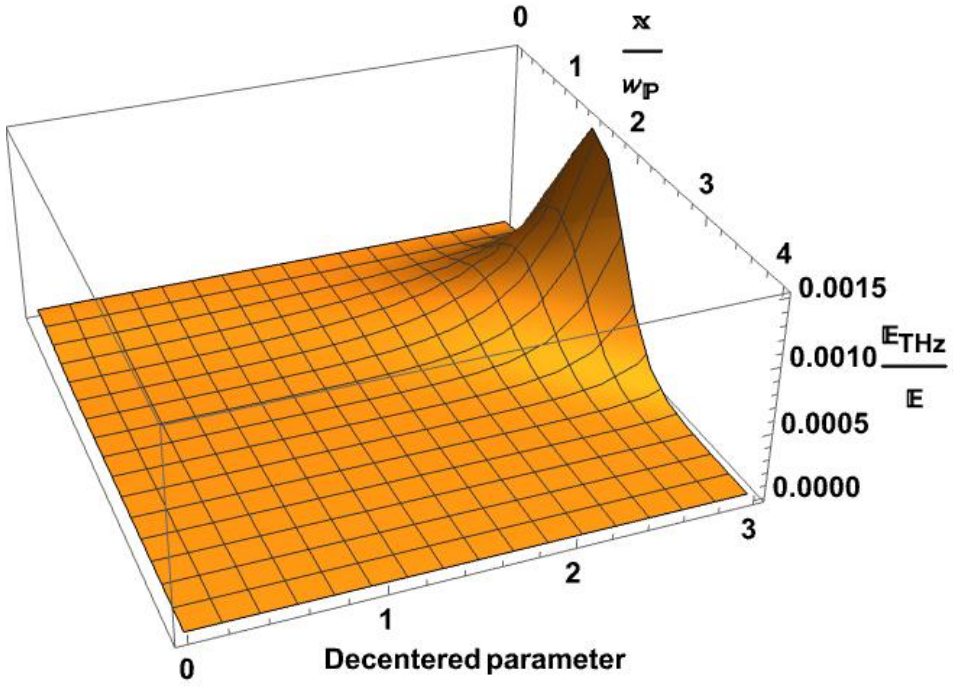

(a)

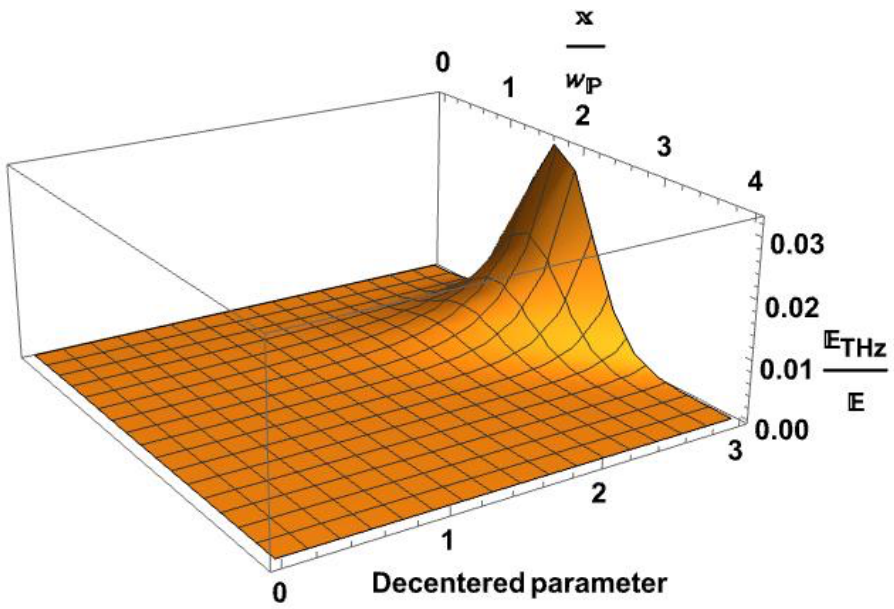

(b)

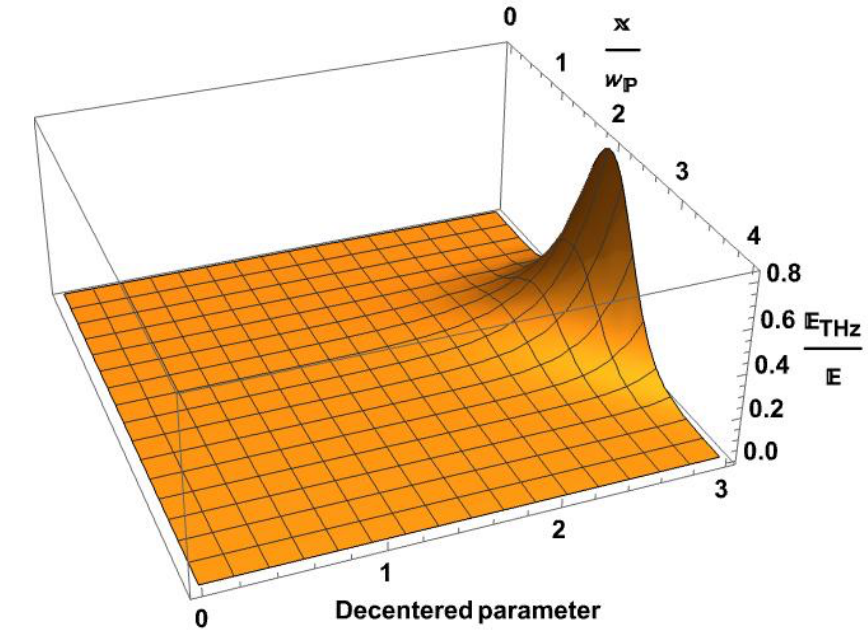

(c)

Fig. 5.1: Variation of normalized THz amplitude with normalized transverse distance and decentered parameter. (a) s = 0, (b) s=1, (c) s= 2.

When the Hermite polynomial mode index value is varied between s=0, 1, and 2, the normalized transverse distance and normalized THz amplitude exhibit a shift towards higher values, specifically from 1.4 to 1.9 and from 0.0015 to 0.8, respectively. The findings of this study indicate a significant rise in normalised Terahertz (THz) amplitude when the parameter an exceeds a value of 2.

5.3.2 Effect of normalised THz frequency ($^{\omega}/_{\omega_P}$)

This study aims to conduct a theoretical analysis of the relationship between the normalised frequency of THz waves and the normalised amplitude of THz radiation. The analysis focuses on various values of the Hermite polynomial mode index, specifically s=0,1,2.

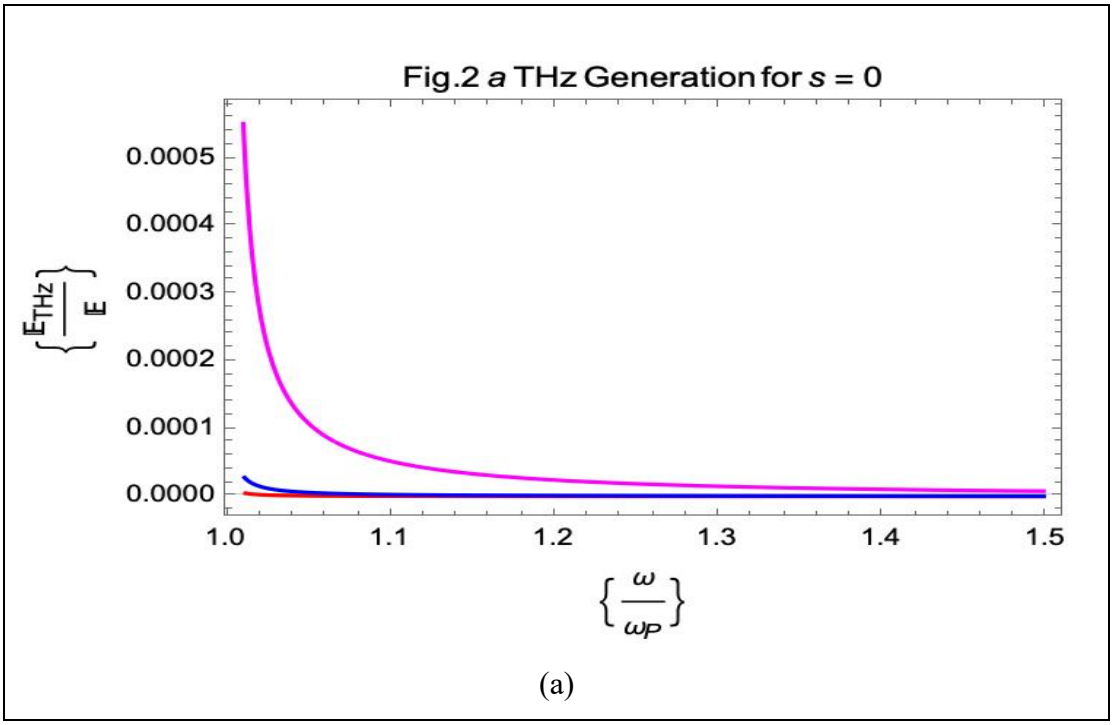

(a)

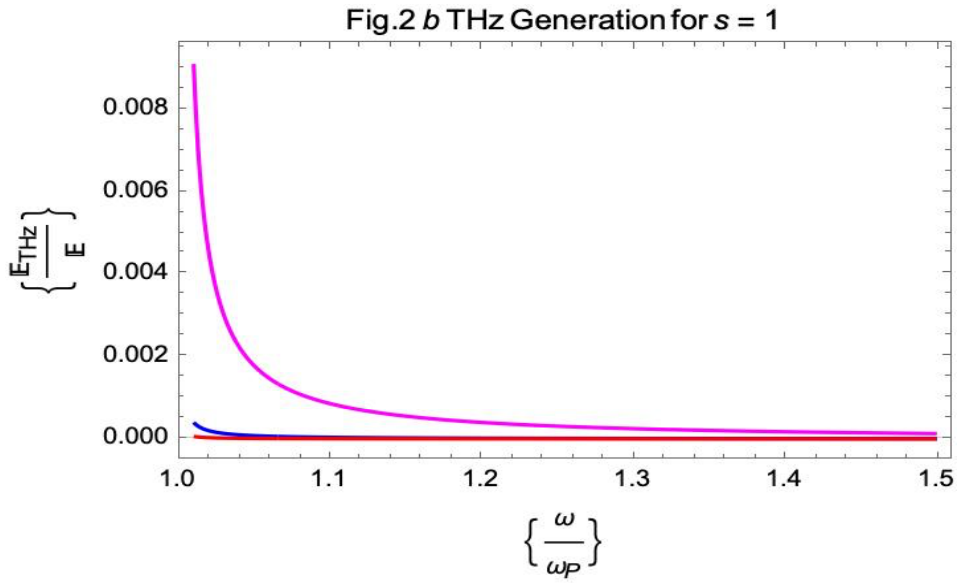

(b)

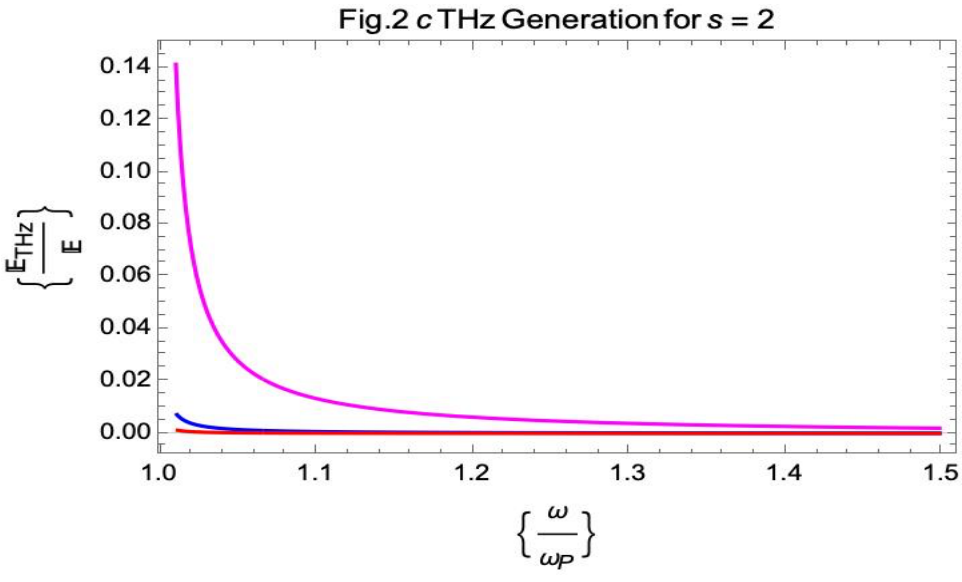

(c)

Fig. 5.2: Variation of normalized THz amplitude with normalized THz frequency with mode index (a) s= 0, (b) s = 1, (c) s = 2 are shown. For decentered parameter a = 0 (red), b = 1 (blue) and b = 2 (magenta) for chirp parameter b = .0099. Other parameters are same as mentioned above.

The normalized terahertz amplitude with the Hermite polynomial mode with index s=0,1,2 rises when the chirp parameter b is set to 0.0099 and a static magnetic field of 10T is applied. In the case of larger values of normalised THz frequency, it can be observed that the normalised THz amplitude experiences a rapid decline and eventually approaches zero when the frequency exceeds 1.2 times the normalised plasma frequency ($\omega > 1.2\ \omega_P$). There is a lack of substantial impact observed when considering the decentred parameter and chirp parameter beyond the specified threshold.

5.3.3 Effect of chirp parameter (b)

This study focuses on examining the relationship between the normalised THz amplitude and the normalised THz frequency. The examination explores various values of the Hermite polynomial mode index (s=0,1,2) and the decentred parameter value (a=2) under varied chirp levels b= 0.0011, 0.0044, 0.0066 and 0.0099.

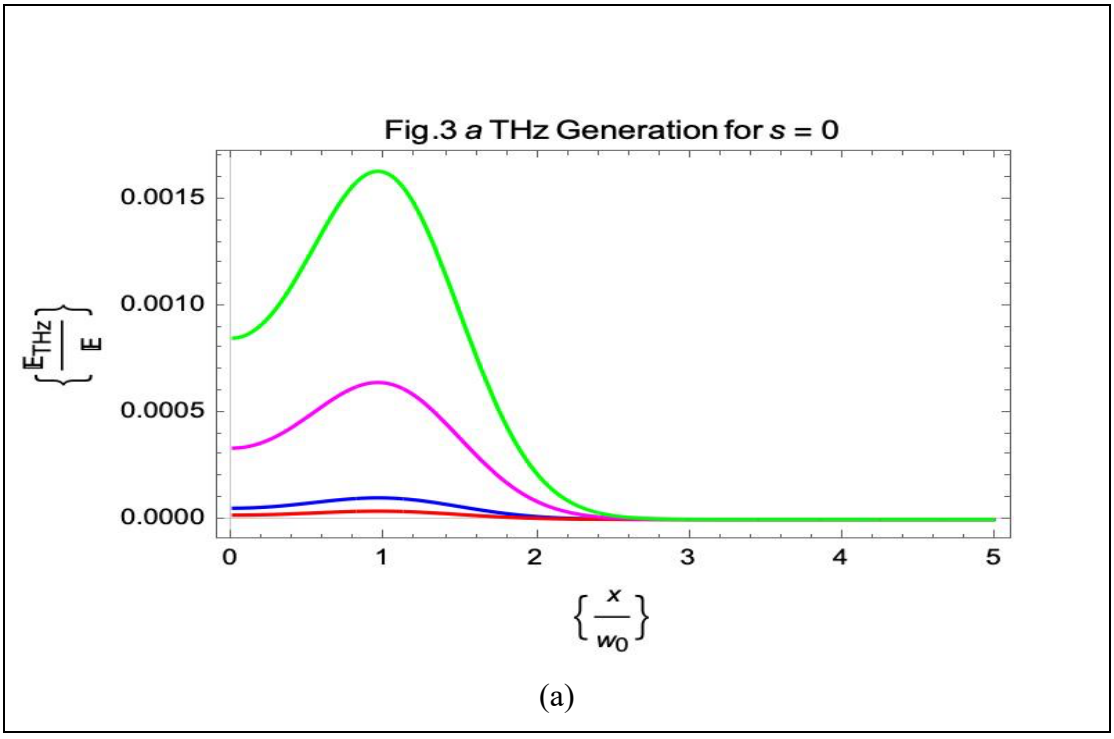

(a)

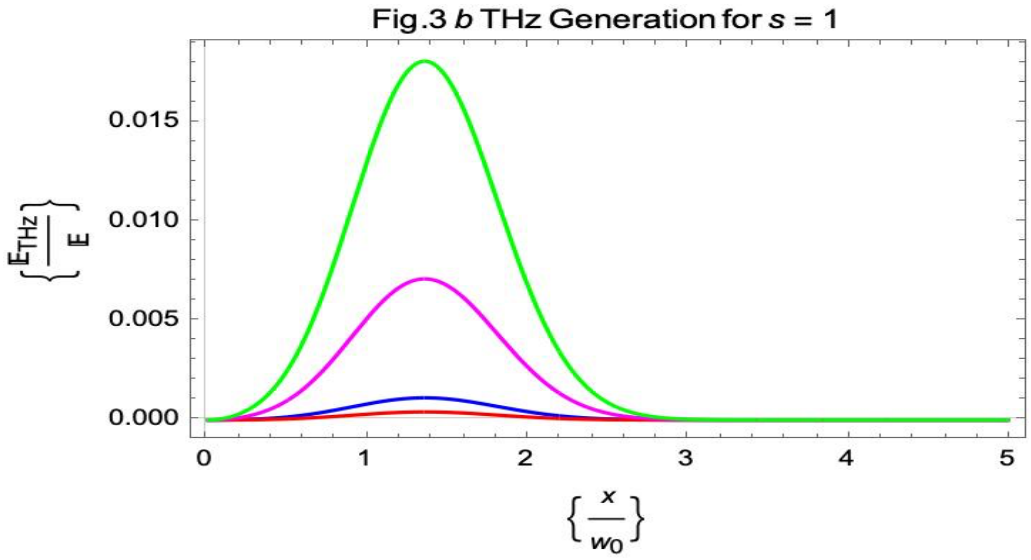

(b)

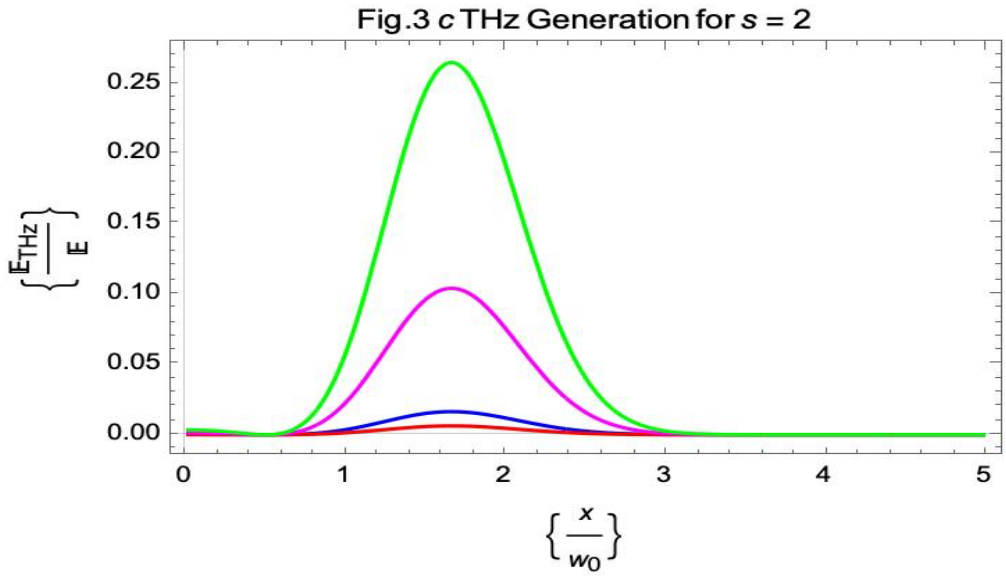

(c)

Fig. 5.3: Contrast of normalized THz amplitude with normalized THz frequency with mode index(a)s= 0, (b) s = 1, (c) s = 2 are shown. For b = 0.0011 (red), b = .0044 (blue), b = .0066 (magenta), b = 0.0099 (green) for decentered parameter a = 2. Other parameters are same as mentioned above.

As the Hermite polynomial mode index value is incremented from 0 to 2, there is an observed increase in the normalised THz amplitude, ranging from around 0.0016 to 0.26. and there is a noticeable shift in the peak towards larger normalized transverse distance values from 0.92 to 1.63. The THz normalized amplitude exhibits an increasing trend as the chirp parameter (b) varies across multiple values, specifically 0.0011 ,0.0044 , 0.0066 and 0.0099.

5.4 Conclusion

This study examines the propagation of two Hermite-cosh-Gaussian chirped laser beams in a collision less under dense plasma medium. An analytical solution is derived to determine the efficiency of terahertz (THz) generation, considering various characteristics such as the normalized THz frequency, normalized transverse distance, and frequency chirp. The resulting solution is then analysed to optimize these parameters, aiming to achieve a tunable and energy-efficient THz source. The normalized THz amplitude exhibits significant values up to 0.8 for normalized transverse distances corresponding to s values of 0, 1, and 2. The findings indicate that as the index value of the Hermite polynomial mode increases from 0 to 2, there is a discernible rise in the normalized amplitude of the THz signal. Additionally, there is an observable displacement of the peak towards higher values of normalized transverse distance

CHAPTER- 6

Enhancing terahertz radiation in slanting density plasma using Gaussian laser beams

6.1 Introduction

In the electromagnetic spectrum, THz waves are located between the microwave and infrared areas, occupying a section of the spectrum that is mostly unknown and significantly underutilised. THz waves have a variety of features that set them apart from other waves, making them extremely promising for a wide range of applications in various sectors. Terahertz vibrations interact with materials differently. They may enter obscure materials like plastics, textiles, and biological tissues. Due to their increased sensitivity to molecular vibrations and rotational transitions, terahertz waves can reveal precise molecule composition and structure[159]. THz radiation cannot ionise atoms or molecules, hence it is non-ionizing[160]. This makes it suitable for many medical and security applications and safe for biological tissues[161], [162]. THz waves accurately photograph subsurface things like clothing and packages. This is useful for non-destructive testing[163], medical diagnostics[164], and security screening[165], [166]. Terahertz waves can enable fast wireless communication networks beyond current technology. Terahertz communication systems could revolutionise data delivery in 6G [167] mobile networks and data-intensive wireless technologies.

Utilising THz waves has enormous promise, but there are several obstacles to overcome, such as effective creation[168], [169], [170], detection, and manipulation[171], [172], [173]. However current studies and technological developments are overcoming these obstacles, opening new applications for THz technology in everything from materials science and security to healthcare and telecommunications. Kumar et al.[174] conducted study on the effects of self-focusing and defocusing of a Gaussian laser beam on the generation of terahertz waves in a large-scale dense array of vertically aligned carbon nanotubes exhibiting anharmonic characteristics. Midha et al.[175] investigated the simultaneous propagation of two Hermite-cosh-Gaussian laser pulses across an under dense plasma medium with a

density profile that increases at an angle. The interaction between laser and plasma displays nonlinear properties, resulting in the generation of THz radiation with a high level of effectiveness. Kumar et al.[176] discovered that the application of a magnetic field, the anharmonic properties of Metallic Carbon Nanotubes, self-focusing, and the diameters of Metallic Carbon Nanotubes all contribute to the increase in the normalised THz amplitude. Kumar et al.[177] presented a method for producing effective terahertz radiation utilising the nonlinear coupling of an amplitude-modulated Gaussian laser beam with a triple-stacked array of anharmonic and rippled carbon nanotubes arranged vertically. Kumar et al.[178] introduced an innovative method to achieve strong, narrowband, and adjustable THz radiation by utilising a nano-sized over dense plasma target, which is exposed to two opposing laser pulses with different frequencies. Chen et al.[179] conducted an experimental study where they successfully proved the creation of coherent terahertz radiation across a wide range of frequencies. This was achieved by colliding laser pulses with gas plasma. Midha et al.[180] conducted a study on the concurrent transmission of two Hermite-Gaussian laser pulses via a collisional plasma medium with an inclined density profile that increases. The interaction between the laser and plasma has nonlinear characteristics, leading to the production of extremely effective terahertz radiation. Singh et al.[181] examined the impact of laser pulse top flatness on the creation of terahertz fields by nonlinear mixing of two lasers that are moving in the same direction through an n-type semiconductor. Ashish et al.[182] described a method for producing THz fields by employing an electron beam that travels in the opposite direction of a laser pulse. Choobini et al.[183] investigated the process of four-wave mixing as a means of producing Terahertz radiation in a magnetised and collisional clustered plasma. Choobini et al.[184] conducted a study on the creation of terahertz radiation using a nonlinear induced electron current density. This was achieved through the interaction of two-color femtosecond laser beams with collisional and magnetised plasma. Milani et al.[185] examined how the spatial and temporal changes in the combination of two Gaussian laser pulses travelling through plasma affect the production of terahertz radiation. Researchers in various fields apply laser-plasma interaction to study certain phenomena, such as self-focusing[176], Wakefield acceleration[186], [187], [188], [189], [190], harmonic generation [191], [192], [193], and THz generation[194], [195], [196].

In this study, I have investigated two Gaussian laser pulses propagating through an under dense collisional plasma with slanting up density profile. Analytical expression for THz efficiency is derived in section II. Using feasible numerical values of parameters, curves are plotted to study the effect of plasma density, collisional frequency and transverse distance on THz generation efficiency in section III. Conclusion of this study is added in section IV.

6.2 Analytical expression for THz efficiency

The electric field of two radially polarized Gaussian laser beams propagating along z-direction is considered as

$$\overrightarrow{E_J}(r,z) = \hat{r}E_0 e^{-\left(r^2/r_0{}^2\right)} e^{i(k_j z-\omega_j t)} \quad (6.1)$$

Where, j= 1,2 corresponding to two different laser beams, r = r (x,y) = $\sqrt{x^2+y^2}$, r_0 is beam waist, k_j is the propagation constant, ω_j is the angular frequency of the propagating laser beam.

The corresponding magnetic field of the laser pulse is $\overrightarrow{B_j}(r,z) = \left(\vec{k}_j \times \overrightarrow{E_j}(r,z)\right)\Big/_{\omega_j}$.

In the initial stage, electrons can be considered at rest so electrons will not experience any magnetic force. So, from the equation of motion $m\, d\vec{V}_j\Big/_{dt} = -e\,\overrightarrow{E_j} - m\vec{V}_j\nu$,

where ν is the collision frequency of collisional plasma, m is the mass of the electron

By solving it, I get the velocity of an electron as $\vec{V}_j = \frac{e\,\overrightarrow{E_j}}{m(i\omega_j-\nu)}$ (6.2)

When these two intense laser beams propagate through plasma, they generate a non-linear ponderomotive force on electrons given by

$$\overrightarrow{F_P}^{NL} = -\frac{m}{2}\left(\overrightarrow{V_1}.\nabla\overrightarrow{V_2}^{*} + \overrightarrow{V_2}^{*}.\nabla\overrightarrow{V_1}\right)$$

By solving, I get

$$\overrightarrow{F_P}^{NL} = \Delta\left\{2\hat{r}\left\{\left(\frac{-2r}{r_0{}^2}\right)\right\} + \{\hat{z}ik\}\right\} e^{i(kz-\omega t)} \quad (6.3)$$

Where, $\Delta = \frac{E_0{}^2 e^2 e^{-\left(2r^2/r_0{}^2\right)}}{2m\,(i\omega_1-\nu)(i\omega_2+\nu)}$, $k = k_1 - k_2$ & $\omega = (\omega_1 - \omega_2)$

From the equation of continuity, for the slanting density profile $n = n_0 e^{k_z z}$

$\frac{\partial(n+n_\omega^{NL})}{\partial t} + \vec{\nabla}.(n + n_\omega^{NL})\vec{V}_\omega^{NL} = 0$

As $n_\omega^{NL} \lll n\ so\ (n + n_\omega^{NL}) \approx n$,

n is constant with time, and a function of z only so, $\frac{\partial(\mathrm{n})}{\partial \mathrm{t}} = 0$

The continuity equation takes the form

$$\frac{\partial n_\omega^{NL}}{\partial t} = -\vec{\nabla}.n\vec{V}_\omega^{NL} \tag{6.4}$$

As both $\vec{V}_\omega^{NL}$ and n_ω^{NL} are produced by $\vec{F}_P^{NL} = \vec{F}_{or}^{NL} e^{i(kz-\omega t)}$

So, both should have the same dependence on z and t.

From the equation of motion $\frac{\partial \vec{V}_\omega^{NL}}{\partial t} = \frac{\vec{F}_P^{NL}}{m} - \nu\vec{V}_\omega^{NL}$ (6.5)

Differentiating equation (5) w.r.t. t

$$\frac{\partial^2 \vec{V}_\omega^{NL}}{\partial t^2} = \frac{1}{m}\frac{\partial \vec{F}_P^{NL}}{\partial t} - \nu\frac{\partial \vec{V}_\omega^{NL}}{\partial t}$$

By putting $\partial/\partial t \equiv -i\omega, \partial/\partial z \equiv ik, \partial n_\omega^{NL}/\partial t = -\vec{\nabla}.n\,\vec{V}_\omega^{NL}$ and solving, we get

$$\Rightarrow \vec{V}_\omega^{NL} = \frac{i\omega\vec{F}_P^{NL}}{m(\omega^2+i\omega\nu)} \tag{6.6}$$

From $\partial n_\omega^{NL}/\partial t = -\vec{\nabla}.n\,\vec{V}_\omega^{NL}$

$$\Rightarrow n_\omega^{NL} = \frac{n_0\vec{\nabla}.(e^{k_z z})\vec{F}_P^{NL}}{m(\omega^2+i\omega\nu)} \tag{6.7}$$

As $n_\omega^L = -\chi_P\vec{\nabla}.(\vec{\nabla}\emptyset_P)/4\pi e$ Where $\chi_P = -\omega_P^2/(\omega^2 + i\omega\nu)$

Using Poisson's equation $\nabla^2\emptyset = 4\pi(n_\omega^L + n_\omega^{NL})e$

We get

$$\Rightarrow \nabla\emptyset = \frac{\omega_P^2 e^{k_z z}\vec{F}_P^{NL}}{e(1+\chi_P)(\omega^2+i\omega\nu)} \qquad \text{As Plasma frequency } \omega_P = \sqrt{4\pi n_0 e^2/m}$$

Linear force

$$\vec{F}_P^L = \mathrm{e}\nabla\emptyset = \frac{\omega_P^2 e^{k_z z}\vec{F}_P^{NL}}{(1+\chi_P)(\omega^2+i\omega\nu)} \tag{6.8}$$

The resultant non-linear oscillatory velocity of electrons by the equation of motion is:

$$\frac{\partial \vec{V}^{NL}}{\partial t} = \frac{\vec{F}_P^{NL}+\vec{F}_P^L}{m} - \nu\,\vec{V}^{NL}$$

By solving we get

$$\Rightarrow \vec{V}^{NL} = \frac{1}{m}\left\{\frac{\omega^2+i\omega\nu-\omega_P^2+\omega_P^2 e^{k_z z}}{(-i\omega+\nu)(\omega^2+i\omega\nu-\omega_P^2)}\right\}\vec{F}_P^{NL} \tag{6.9}$$

Non-linear oscillatory current density $\vec{J}^{NL} = -n_0 e\vec{V}^{NL}/2$,

Putting the value of $\vec{V}^{NL}$ from equation (9) we get,

$$\Rightarrow \vec{J}^{NL} = -\frac{n_0 e}{2m}\left\{\frac{\omega^2+i\omega\nu-\omega_P^2+\omega_P^2 e^{k_z z}}{(-i\omega+\nu)(\omega^2+i\omega\nu-\omega_P^2)}\right\}\vec{F}_P^{NL} \tag{6.10}$$

The equation governing THz generation is given by

$$\Rightarrow \vec{\nabla}.\left(\vec{\nabla}\,\vec{E}_{THz}\right) - \nabla^2\vec{E}_{THz} = \frac{\omega^2}{c^2}\varepsilon\vec{E}_{THz} + \frac{4\pi i\omega}{c^2}\vec{J}^{NL} \quad (6.11)$$

Here, ε is the permittivity of the plasma medium.

In order to neglect higher order derivatives due to fast variation of THz field

$\vec{\nabla}.\left(\vec{\nabla}\vec{E}_{THz}\right) - \nabla^2\vec{E}_{THz} = 0$, So

$$\frac{\omega^2}{c^2}\varepsilon\vec{E}_{THz} = -\frac{4\pi i\omega}{c^2}\vec{J}^{NL}$$

$$\vec{E}_{THz} = \frac{4\pi i}{\varepsilon\,\omega}\left[\frac{n_0 e}{2m}\left\{\frac{\omega^2+i\omega\nu-\omega_P^2+\omega_P^2 e^{k_z z}}{(-i\omega+\nu)\left(\omega^2+i\omega\nu-\omega_P^2\right)}\right\}\right]\vec{F}_P^{NL}$$

Tera hertz efficiency is defined as the ratio of generated THz to the amplitude of laser pulse,

$$\frac{E_{THz}}{E_0} = \frac{4\pi i}{\varepsilon\,\omega}\left[\frac{n_0 e}{2m}\left\{\frac{\omega^2+i\omega\nu-\omega_P^2+\omega_P^2 e^{k_z z}}{(-i\omega+\nu)\left(\omega^2+i\omega\nu-\omega_P^2\right)}\right\}\right]\frac{E_0 e^2 e^{-\left(2r^2/{r_0}^2\right)} e^{i(kz-\omega t)}}{2m\,(i\omega_1-\nu)(i\omega_2+\nu)}\left\{\sqrt{\left(\frac{-4r}{{r_0}^2}\right)^2+k^2}\right\} \quad (6.12)$$

THz efficiency depends on various factors including THz frequency (ω), collisional frequency (ν), transverse distance (r) etc. To obtain optimized THz efficiency source, these parameters should be optimized.

6.3 Result and Discussion

For analytical solution, plasma density is taken from $8.3\times10^{22}m^{-3}$, $8.7\times10^{22}m^{-3}$, $9\times10^{22}m^{-3}$ and $9.5\times10^{22}m^{-3}$. Frequency of a laser pulse is taken as $2.4\times10^{14}\,rad/sec$ while the frequency is other laser pulse is chosen in such a manner that the beat frequency is equal to the frequency of generated THz. The amplitude of electric field is taken as $2\times10^{10}N/C$ which is identical for both the laser pulses. Chosen values of collisional frequency are $\nu = 0, 0.1\,\omega_P, 0.2\,\omega_P,$ and $0.3\,\omega_P$. Chosen values of transverse distance are $0.1\,r_0$, $0.3\,r_0$, $0.5\,r_0$ and $0.7\,r_0$.

6.3.1 Effect of plasma density on THz efficiency

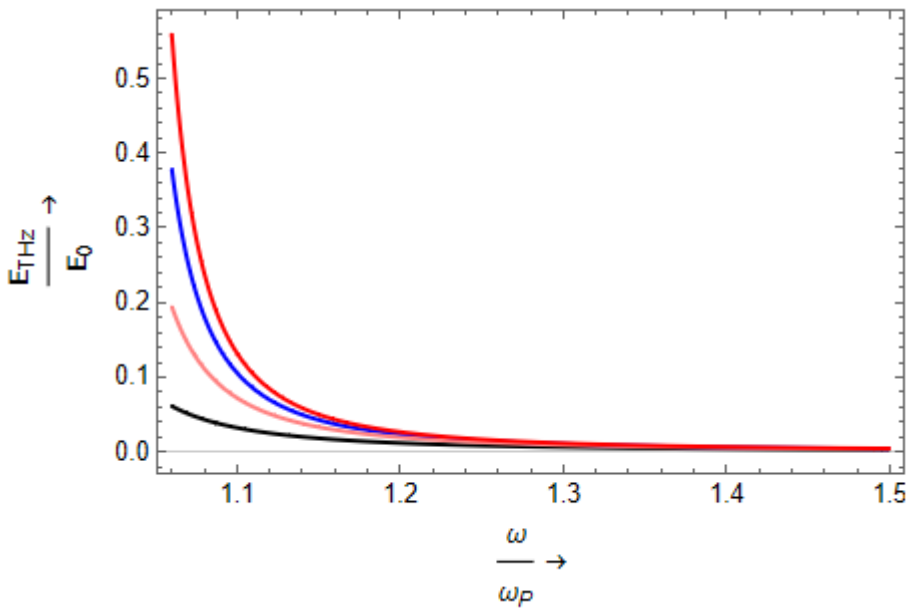

Fig. 6.1: Variation of THz generation efficiency with THz efficiency for different plasma density of $8.3 \times 10^{22} m^{-3}$(red), $8.7 \times 10^{22} m^{-3}$(blue), $9\times 10^{22} m^{-3}$(pink), and $9.5\times 10^{22} m^{-3}$(black). $\omega_1 = 2.4 \times 10^{14}\ rad/sec.\ \nu = 0.01\ \omega_P$, $k_z = 0.5\ k.$

By taking other parameters constant, fig. 6.1 is plotted between THz efficiency and THz frequency for different values of chosen plasma densities. For the chosen values of plasma densities, THz efficiency decreases with increase in plasma density. This variation is due to variation in plasma frequency and collisional frequency with variation in plasma density. As plasma frequency is proportional to square root of plasma density, so with the increase in plasma density, the collisional frequency ($\nu = 0.01\ \omega_P$) also increases and responsible for significant decrease in THz efficiency.

6.3.2 Effect of transverse distance on THz efficiency

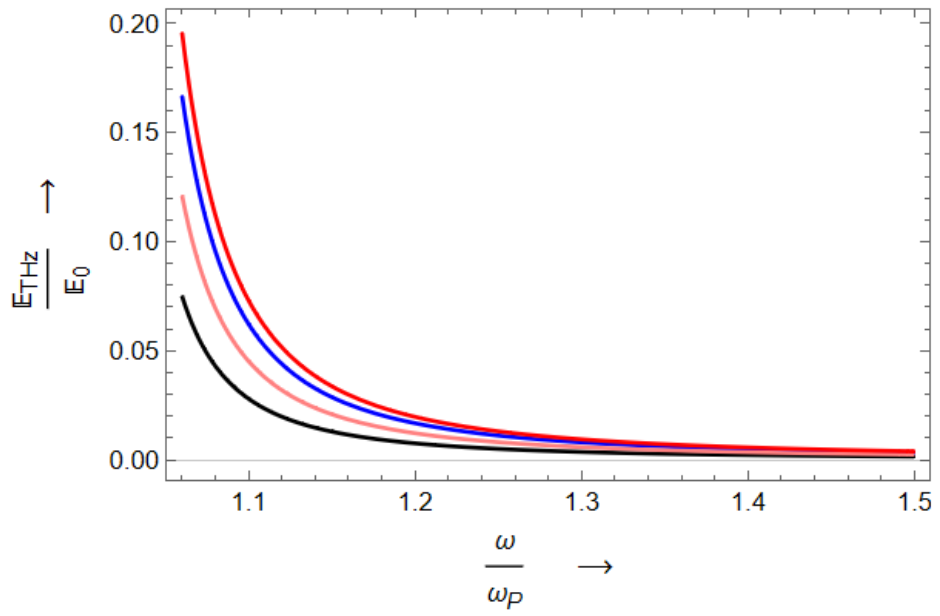

Fig. 6.2: Variation of THz generation efficiency with THz efficiency for different transverse distance of $r = 0.1\ r_0$(red), $0.3\ r_0$(blue), $0.5\ r_0$ (pink), and $0.7\ r_0$ (black). $\omega_1 = 2.4 \times 10^{14}\ rad/sec.\ \nu = 0.01\ \omega_P$, $k_z = 0.5\ k,\ n = 9 \times 10^{22} m^{-3}$.

Fig. 6.2 shows the variation of THz efficiency with THz frequency for different transverse distances. As per analytical solutions, THz efficiency decreases continuously from 0.20 to 0.08 with increase in transvers distance from $r = 0.1\ r_0$ to $r = 0.7\ r_0$. In this study, Gaussian laser pulse profiles are chosen for analytical investigation. In Gaussian distribution of intensity, intensity decreases with increase in transverse distance [197], hence THz efficiency decreases.

Same variation can be seen in fig. 6.3 in which curve is plotted between THz efficiency and transverse distance for THz frequency of $\omega = 1.06\ \omega_P$. For $r > r_0$, THz efficiency becomes almost zero due to significant decrease in laser electric field.

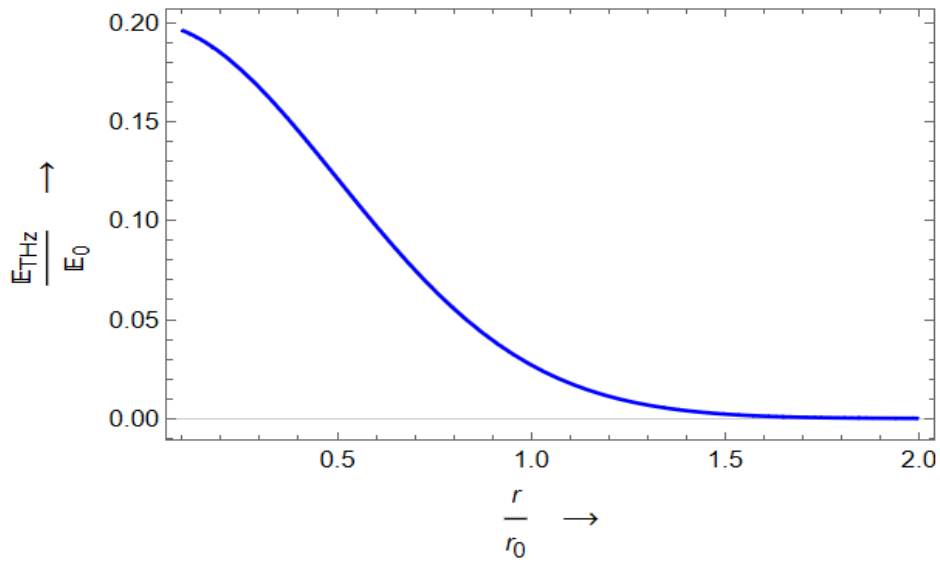

Fig. 6.3: Variation of THz generation efficiency with transverse distance for $\omega_1 = 2.4 \times 10^{14}\ rad/sec.\ \nu = 0.01\ \omega_P,\ k_z = 0.5\ k,\ n = 9 \times 10^{22} m^{-3}$.

6.3.3 Effect of plasma density on THz efficiency

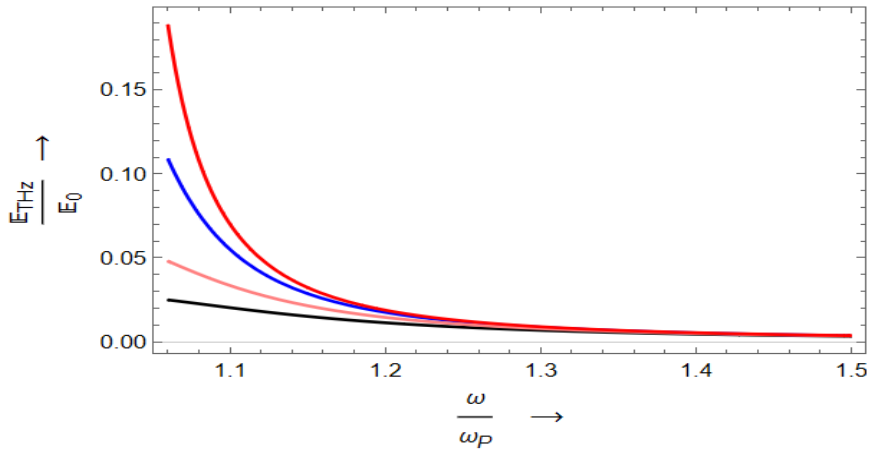

Fig. 6.4: Variation of THz generation efficiency with THz efficiency for different collision frequency of $\nu = 0$ (red), 0.1 ω_P(blue), 0.2 ω_P (pink), and 0.3 ω_P (black). $\omega_1 = 2.4 \times 10^{14}\ rad/sec.\ \nu = 0.01\ \omega_P,\ k_z = 0.5\ k,\ n = 9 \times 10^{22} m^{-3}$.

Fig. 6.4 illustrates the variation of THz efficiency with THz frequency for different collisional frequency of $\nu = 0$, $0.1\,\omega_P$, $0.2\,\omega_P$, and $0.3\,\omega_P$. With the increase in collisional frequency, plasma electrons cannot gain significant energy and loses the energy due to collision with other electrons. With the increase in such collisions, THz conversion efficiency decreases. Same variation can be seen in fig. (5).

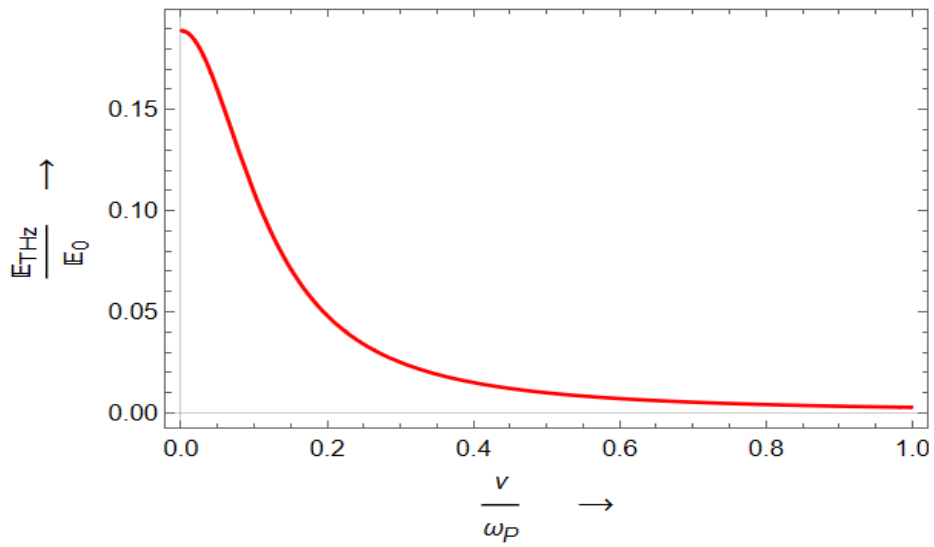

Fig. 6.5: Variation of THz generation efficiency with collisional frequency for $\omega_1 = 2.4 \times 10^{14}\, rad/sec.\, \nu = 0.01\,\omega_P, k_z = 0.5\,k,\ n = 9 \times 10^{22} m^{-3}$, ω = 1.06 ω_P.

The research outcomes of this investigation are in accordance with the research outcomes of Midha et al. [175] . In their study, they investigated the THz efficiency with two Hermite-cosh-Gaussian laser pulses. While I have used Gaussian laser pulse profile.

6.4 Conclusion

This research investigates the amplification of THz radiation in slanting density plasma using Gaussian laser beams. Through the analysis of the interplay between laser beams and plasma, we can determine the most favorable circumstances for achieving the highest possible THz efficiency. The work utilizes analytical techniques to examine the influence of plasma density, collisional frequency, and transverse distance. The results suggest that the interaction between the Gaussian beam characteristics and the plasma

setup is essential for obtaining efficient THz generation. These insights have the potential to facilitate the development of advanced THz sources that have enhanced power and tunability. This could increase the range of practical applications in numerous industries.

CHAPTER- 7

Summary and Conclusion

The terahertz gap refers to the segment of the electromagnetic spectrum situated between microwave and infrared frequencies. This gap presented difficulties and significant opportunities in diverse areas. The use of this elusive spectrum, spanning from around 0.1 to 10 terahertz, has been limited due to technical constraints in the generation, manipulation, and detection of terahertz waves. Nevertheless, the latest breakthroughs in terahertz technology have ignited a wave of curiosity and investigation. The applications of this technology are wide-ranging and cover various fields, such as medical imaging, security screening, communications, and material characterization. Terahertz waves in medical imaging provide non-invasive and high-resolution imaging abilities, which have the potential to significantly transform diagnoses and therapy monitoring. They enhance the ability to detect hidden items with unparalleled accuracy in security settings. In addition, terahertz communication offers extremely high-speed data transfer rates, effectively meeting the increasing need for greater bandwidth in wireless communications. Moreover, the capacity of terahertz spectroscopy to permeate different substances renders it indispensable for the analysis of pharmaceuticals, identification of chemical compounds, and characterization of semiconductors. As scientists strive to close the terahertz gap, the potential for groundbreaking advancements and exploration within this specific band of electromagnetic spectrum is limitless.

Terahertz (THz) waves are produced through laser-plasma interaction by sending two intense laser pulses into a plasma target, with each pulse having a slightly different frequency. This interaction accelerates plasma electrons, leading to the creation of a nonlinear ponderomotive force. As a result, the balance of charged particles in the plasma is disturbed by this non-linear force, causing the formation of non-linear changes in density and fluctuating electric currents. By employing analytical solutions of Maxwell's third and fourth equations, we ascertain the characteristics of THz waves and evaluate the effectiveness of THz conversion.

In this research we examine two HchG laser pulses that propagate together in an under dense plasma with an increasing density profile. The generation of THz radiation is efficiently achieved by the nonlinear phenomena resulting from the interaction between laser and plasma. Analytical research investigates the correlation between THz conversion efficiency and plasma frequency, as well as several laser features such as the Hermite polynomial mode index (s), decentered parameter (b), and collisional frequency. The results indicate that the efficiency of THz conversion decreases as we move further from resonance and becomes almost negligible for normalised THz frequency and normalised collisional frequency values greater than 1.6 and 4, respectively. As the index values of Hermite polynomials (s=0,1,2) increase, the efficiency of THz conversion also increases.

I have also investigated the transmission of two p-polarized chirped laser beams over a hot, collisional, and under dense plasma medium. A mathematical solution is obtained to calculate the effectiveness of THz generation, taking into account different factors such as the relative THz frequency, angle of incidence, collision frequency, relative transverse distance, and frequency modulation. The solution obtained is subsequently examined to optimise these characteristics, with the goal of attaining a customizable and energy-efficient terahertz generator. The normalised amplitude of the terahertz (THz) wave shows substantial values reaching up to 0.8 when the normalised frequency of the THz wave corresponds to a chirp parameter of b = 0.0011. The results suggest that as the chirp parameter value goes from 0.0011 to 0.0099, there is a reduction in the normalised amplitude of the THz signal. The THz amplitude, when normalised, exhibits oscillatory behaviour as the incidence angle varies from zero to 2π. It reaches its maximum value at an incident oblique angle of 45^0 and its minimum value at 225^0.

I have investigated the transmission of two Hermite-cosh-Gaussian chirped laser beams via a plasma medium that is devoid of collisions and has a lower density than usual. A mathematical method is obtained to calculate the efficiency of terahertz (THz) generation, taking into account different factors such as the normalised THz frequency, normalised transverse distance, and frequency chirp. The obtained solution is subsequently examined to optimise these characteristics, with the goal of attaining a customisable and energy-efficient terahertz source. The normalised THz amplitude reaches substantial values of up to 0.8 for normalised transverse distances that

correspond to s values of 0, 1, and 2. The results suggest that as the index value of the Hermite polynomial mode goes from 0 to 2, there is a noticeable increase in the normalised amplitude of the THz signal. Furthermore, there is a noticeable shift of the peak towards larger values of normalised transverse distance.

1. The results of research objective 1 employ novel methods for producing THz fields (such as HchG lasers and slanting density modulation), which have great promise for creating a tunable THz source for use in cancer detection and non-invasive imaging.

2. Findings from the research goal 2 for THz time-domain spectroscopy (THz-TDS), offers theoretical analysis for broadband THz emission, which is very helpful and allows for accurate material characterisation and analysis.

3. Based on the results of research objective 3, scientists can create a highly adjustable THz source for material science and non-destructive testing for material characterisation and quality control by varying the values of the Hermite polynomial mode index and the decentered parameter of the cosh function.

The main goal of this research is to create a source that can generate terahertz (THz) waves with the ability to be adjusted and with a high level of efficiency. The focus of our inquiry involves analysing several laser and plasma characteristics, such as the Hermite polynomial mode index, cosh function, decentered parameter of laser profile, frequency chirp effect, collisional frequency, slanting plasma density modulation, and the utilisation of a static magnetic field. Through the examination of these factors, our objective is to enhance the effectiveness and adjustability of the THz source. The results of this study have great potential for closing the gap in the THz spectrum and creating many opportunities for future research and applications in other industries.

Publication Related to research objectives

Sr. No.	Research Objective	Title of paper	Journal	Date of publication
1	To investigate the efficient THz generation by Hermite-cosh-Gaussian lasers in plasma with slanting density modulation.	Efficient THz generation by Hermite-cosh-Gaussian lasers in plasma with slanting density modulation	Journal of Optics	07 Sept. 2023
2	To investigate the resonant Terahertz radiation by p-polarized chirped laser in hot plasma with slanting density modulation.	Resonant Terahertz radiation by p-polarised chirped laser in hot plasma with slanting density modulation	Journal of Optics	19 June 2023
3	To study THz generation by frequency difference of Hermite cosh Gaussian chirped lasers in magnetized plasma.	Enhanced THz generation by Hermite-cosh-Gaussian chirped laser in static magnetized plasma	Applied Physics B	17 June 2024

Publication detail – Other published work

S.No.	Title of Paper	DOI Number	
1	Optimizing Terahertz emission with Hermite-Gaussian laser beams in collisional slanted up density plasma	https://doi.org/10.1007/s12596-024-01696-2	Journal of Optics
2	Advancements in Efficient Terahertz Generation Techniques for Diverse Applications in spectroscopic studies	https://doi.org/10.1007/s12596-024-01822-0	Journal of Optics
3	Hermite-Gaussian laser modulation for optimal THz emission in collisional homogeneous plasma	https://doi.org/10.1007/s12596-024-01910-1	Journal of Optics
4	Exploring Nonlinear Effects in Terahertz Generation with Hermite-Gaussian Chirp Pulses under Static Magnetic Fields	**https://doi.org/10.1007/s12596-024-01970-3**	Journal of Optics
5	Exploring THz efficiency: Frequency chirp dynamics in Sinh-Gaussian	https://doi.org/10.1007/s12596-024-01963-2	Journal of Optics

	laser-plasma interaction		
6	Parametric analysis of THz wave generation efficiency and plasma density using Sinh-Gaussian beams	https://doi.org/10.1007/s12596-024-01	Journal of Optics
7	Efficient THz generation through laser and plasma parameter optimization with Sinh-Gaussian beams in magnetized plasma	**https://doi.org/10.1007/s12596-024-02031-5**	Journal of Optics
8	Laser-induced THz radiation generation in plasma	https://www.academia.edu/download/84552085/IJRAR1BLP299.pdf	IJRAR
9	Enhancing terahertz radiation in slanting density plasma using Gaussian laser beam	https://doi.org/10.1007/s12596-024-02423-7	Journal of Optics
10	Enhancing electron acceleration with sinh-squared Gaussian pulse under external magnetic fields	https://doi.org/10.1007/s12596-024-01671-x	Journal of Optics
11	Dynamics of terahertz generation in collisional plasma with	https://doi.org/10.1007/s12596-025-02643-5	Journal of Optics

	density modulations using radially polarized lasers		
12	Unravelling chirp dynamics in gaussian laser-plasma interactions for THz wave optimization	https://doi.org/10.1007/s12596-025-02647-1	Journal of Optics
13	Optimization of Terahertz Radiation Generation via Sech-Shaped Laser Pulses in Collisional Homogenous Plasma	https://doi.org/10.1007/s13538-025-01774-1	Brazilian Journal of Physics

Bibliography

[1] B. Ferguson and X.-C. Zhang, "Materials for terahertz science and technology," *Nat Mater*, vol. 1, no. 1, pp. 26–33, 2002.

[2] Y. C. Shen, a T. Lo, P. F. Taday, B. E. Cole, W. R. Tribe, and M. C. Kemp, "Detection and identification of explosives using terahertz pulsed spectroscopic imaging," *Appl Phys Lett*, vol. 86, no. 24, 2005.

[3] M. J. Fitch and R. Osiander, "Terahertz waves for communications and sensing," *Johns Hopkins APL Tech Dig*, vol. 25, no. 4, pp. 348–355, 2004.

[4] J. Orenstein and A. J. Millis, "Advances in the physics of high-temperature superconductivity," *Science (1979)*, vol. 288, no. 5465, pp. 468–474, 2000.

[5] J.-H. Son, "Terahertz electromagnetic interactions with biological matter and their applications," *J Appl Phys*, vol. 105, no. 10, 2009.

[6] H. Zhong, A. Redo-Sanchez, and X.-C. Zhang, "Identification and classification of chemicals using terahertz reflective spectroscopic focal-plane imaging system," *Opt Express*, vol. 14, no. 20, pp. 9130–9141, 2006.

[7] T. Kampfrath *et al.*, "Coherent terahertz control of antiferromagnetic spin waves," *Nat Photonics*, vol. 5, no. 1, pp. 31–34, 2011.

[8] J. A. Fülöp *et al.*, "Efficient generation of THz pulses with 0.4 mJ energy," *Opt Express*, vol. 22, no. 17, pp. 20155–20163, 2014.

[9] M. Shalaby and C. P. Hauri, "Demonstration of a low-frequency three-dimensional terahertz bullet with extreme brightness," *Nat Commun*, vol. 6, no. 1, p. 5976, 2015.

[10] C. Vicario, A. V Ovchinnikov, S. I. Ashitkov, M. B. Agranat, V. E. Fortov, and C. P. Hauri, "Generation of 0.9-mJ THz pulses in DSTMS pumped by a Cr: Mg 2 SiO 4 laser," *Opt Lett*, vol. 39, no. 23, pp. 6632–6635, 2014.

[11] A. Gopal *et al.*, "Characterization of 700 μJ T rays generated during high-power laser solid interaction," *Opt Lett*, vol. 38, no. 22, pp. 4705–4707, 2013.

[12] V. Thakur, N. Kant, and S. Vij, "Effect of cross-focusing of two laser beams on THz radiation in graphite nanoparticles with density ripple," *Phys Scr*, vol. 95, no. 4, p. 45602, 2020.

[13] S. Vij, N. Kant, and V. Thakur, "Resonant enhancement of THz radiation through vertically aligned carbon nanotubes array by applying wiggler magnetic field," *Plasmonics*, vol. 14, pp. 1051–1056, 2019.

[14] A. Mehta and N. Kant, "Terahertz radiation generation driven by the frequency chirped laser pulse in magneto-active plasma," in *Terahertz, RF, Millimeter, and Submillimeter-Wave Technology and Applications XII*, SPIE, 2019, pp. 81–89.

[15] D. J. Cook and R. M. Hochstrasser, "Intense terahertz pulses by four-wave rectification in air," *Opt Lett*, vol. 25, no. 16, pp. 1210–1212, 2000.

[16] A. Proulx, A. Talebpour, S. Petit, and S. L. Chin, "Fast pulsed electric field created from the self-generated filament of a femtosecond Ti: Sapphire laser pulse in air," *Opt Commun*, vol. 174, no. 1–4, pp. 305–309, 2000.

[17] X. Xie, J. Dai, and X.-C. Zhang, "Coherent Control of THz Wave Generation in Ambient Air," *Phys Rev Lett*, vol. 96, no. 7, p. 075005, Feb. 2006, doi: 10.1103/PhysRevLett.96.075005.

[18] A. Houard, Y. Liu, B. Prade, V. T. Tikhonchuk, and A. Mysyrowicz, “Strong enhancement of terahertz radiation from laser filaments in air by a static electric field,” *Phys Rev Lett*, vol. 100, no. 25, p. 255006, 2008.
[19] Z. Zhang *et al.*, “Controllable terahertz radiation from a linear-dipole array formed by a two-color laser filament in air,” *Phys Rev Lett*, vol. 117, no. 24, p. 243901, 2016.
[20] M. Clerici *et al.*, “Wavelength scaling of terahertz generation by gas ionization,” *Phys Rev Lett*, vol. 110, no. 25, p. 253901, 2013.
[21] L.-L. Zhang *et al.*, “Observation of terahertz radiation via the two-color laser scheme with uncommon frequency ratios,” *Phys Rev Lett*, vol. 119, no. 23, p. 235001, 2017.
[22] V. A. Andreeva *et al.*, “Ultrabroad terahertz spectrum generation from an air-based filament plasma,” *Phys Rev Lett*, vol. 116, no. 6, p. 63902, 2016.
[23] V. B. Gildenburg and N. V Vvedenskii, “Optical-to-THz wave conversion via excitation of plasma oscillations in the tunneling-ionization process,” *Phys Rev Lett*, vol. 98, no. 24, p. 245002, 2007.
[24] H.-C. Wu, J. Meyer-ter-Vehn, and Z.-M. Sheng, “Phase-sensitive terahertz emission from gas targets irradiated by few-cycle laser pulses,” *New J Phys*, vol. 10, no. 4, p. 43001, 2008.
[25] M. Chen, A. Pukhov, X.-Y. Peng, and O. Willi, “Theoretical analysis and simulations of strong terahertz radiation from the interaction of ultrashort laser pulses with gases,” *Phys Rev E*, vol. 78, no. 4, p. 46406, 2008.
[26] W.-M. Wang *et al.*, “Strong terahertz pulse generation by chirped laser pulses in tenuous gases,” *Opt Express*, vol. 16, no. 21, pp. 16999–17006, 2008.
[27] K.-Y. Kim, J. H. Glownia, A. J. Taylor, and G. Rodriguez, “Terahertz emission from ultrafast ionizing air in symmetry-broken laser fields,” *Opt Express*, vol. 15, no. 8, pp. 4577–4584, 2007.
[28] A. K. Malik and H. K. Malik, “Tuning and focusing of terahertz radiation by DC magnetic field in a laser beating process,” *IEEE J Quantum Electron*, vol. 49, no. 2, pp. 232–237, 2013.
[29] F. Bakhtiari, S. Golmohammady, M. Yousefi, F. D. Kashani, and B. Ghafary, “Generation of terahertz radiation in collisional plasma by beating of two dark hollow laser beams,” *Laser and Particle Beams*, vol. 33, no. 3, pp. 463–472, 2015.
[30] M. Kumar and V. K. Tripathi, “Resonant terahertz generation by optical mixing of two laser pulses in rippled density plasma,” *IEEE J Quantum Electron*, vol. 48, no. 8, pp. 1031–1035, 2012.
[31] L. Bhasin and V. K. Tripathi, “Terahertz generation via optical rectification of x-mode laser in a rippled density magnetized plasma,” *Phys Plasmas*, vol. 16, no. 10, 2009.
[32] V. B. Pathak, D. Dahiya, and V. K. Tripathi, “Coherent terahertz radiation from interaction of electron beam with rippled density plasma,” *J Appl Phys*, vol. 105, no. 1, 2009.
[33] C. S. Liu and V. K. Tripathi, “Tunable terahertz radiation from a tunnel ionized magnetized plasma cylinder,” *J Appl Phys*, vol. 105, no. 1, 2009.

[34] L. Bhasin and V. K. Tripathi, “Resonant terahertz generation by optical rectification of an amplitude modulated surface plasma wave,” *IEEE J Quantum Electron*, vol. 46, no. 6, pp. 965–969, 2010.
[35] M. Kumar and V. K. Tripathi, “Terahertz radiation from a laser bunched relativistic electron beam in a magnetic wiggler,” *Phys Plasmas*, vol. 19, no. 7, 2012.
[36] M. Kumar, L. Bhasin, and V. K. Tripathi, “Beat excitation of terahertz radiation in a semiconductor slab in a magnetic field,” *Journal of Physics and Chemistry of Solids*, vol. 73, no. 2, pp. 269–274, 2012.
[37] P. Kumar and V. K. Tripathi, “Terahertz surface plasmons excitation by nonlinear mixing of lasers in over ultrathin metal film coated dielectric,” *J Appl Phys*, vol. 114, no. 5, 2013.
[38] P. Kumar and V. K. Tripathi, “Terahertz surface plasmon excitation via nonlinear mixing of lasers in a metal-coated optical fiber,” *Opt Lett*, vol. 38, no. 18, pp. 3475–3477, 2013.
[39] M. Kumar and V. K. Tripathi, “Cherenkov terahertz generation by electron bunches in a dielectric lined resonator,” *IEEE J Quantum Electron*, vol. 49, no. 3, pp. 335–339, 2013.
[40] J. Yoshii, C. H. Lai, T. Katsouleas, C. Joshi, and W. B. Mori, “Radiation from Cerenkov wakes in a magnetized plasma,” *Phys Rev Lett*, vol. 79, no. 21, p. 4194, 1997.
[41] N. Yugami *et al.*, “Experimental observation of radiation from Cherenkov wakes in a magnetized plasma,” *Phys Rev Lett*, vol. 89, no. 6, pp. 065003/1-065003/4, Aug. 2002, doi: 10.1103/PhysRevLett.89.065003.
[42] K. Mori *et al.*, “Directional linearly polarized terahertz emission from argon clusters irradiated by noncollinear double-pulse beams,” *Appl Phys Lett*, vol. 111, no. 24, 2017.
[43] M. Kumar, V. K. Tripathi, and Y. U. Jeong, “Laser driven terahertz generation in hot plasma with step density profile,” *Phys Plasmas*, vol. 22, no. 6, 2015.
[44] A. Mehta, N. Kant, and S. Vij, “Generation of terahertz (THz) radiation by p-polarised lasers beating in hot plasma with surface density ripple,” *Laser Phys Lett*, vol. 16, no. 4, p. 45403, 2019.
[45] P. Varshney, V. Saxena, and V. Sajal, “High power terahertz (THz) radiation generation through the nonlinear interaction of cosh-Gaussian laser beams in cluster plasma,” in *AIP Conference Proceedings*, AIP Publishing, 2019.
[46] A. Mehta, J. Rajput, and N. Kant, “Effect of frequency-chirped laser pulses on terahertz radiation generation in magnetized plasma,” *Laser Phys*, vol. 29, no. 9, p. 95405, 2019.
[47] A. Mehta, J. Rajput, K. Kang, and N. Kant, “Terahertz generation by beating of two chirped pulse lasers in spatially periodic density plasma,” *Laser Phys*, vol. 30, no. 4, p. 45402, 2020.
[48] P. Varshney, V. Sajal, A. Upadhyay, J. A. Chakera, and R. Kumar, “Tunable terahertz radiation generation by nonlinear photomixing of cosh-Gaussian laser pulses in corrugated magnetized plasma,” *Laser and Particle Beams*, vol. 35, no. 2, pp. 279–285, 2017.

[49] S. Vij and N. Kant, “Generation of terahertz radiation by beating of two color lasers in hot clustered plasma with step density profile,” *Plasma Research Express*, vol. 1, no. 2, p. 25012, 2019.
[50] F. Jahangiri, M. Hashida, S. Tokita, T. Nagashima, M. Hangyo, and S. Sakabe, “Enhancing the energy of terahertz radiation from plasma produced by intense femtosecond laser pulses,” *Appl Phys Lett*, vol. 102, no. 19, 2013.
[51] F. Jahangiri, M. Hashida, T. Nagashima, S. Tokita, M. Hangyo, and S. Sakabe, “Intense terahertz emission from atomic cluster plasma produced by intense femtosecond laser pulses,” *Appl Phys Lett*, vol. 99, no. 26, Dec. 2011, doi: 10.1063/1.3672814.
[52] H. K. Midha, V. Sharma, N. Kant, and V. Thakur, “Efficient THz generation by Hermite-cosh-Gaussian lasers in plasma with slanting density modulation,” *Journal of Optics*, Oct. 2023, doi: 10.1007/s12596-023-01413-5.
[53] H. K. Midha, V. Sharma, N. Kant, and V. Thakur, “Resonant Terahertz radiation by p-polarised chirped laser in hot plasma with slanting density modulation,” *Journal of Optics*, Dec. 2023, doi: 10.1007/s12596-023-01563-6.
[54] H. K. Midha, V. Sharma, N. Kant, and V. Thakur, “Enhanced THz generation by Hermite-cosh-Gaussian chirped laser in static magnetized plasma,” *Applied Physics B*, vol. 130, no. 7, p. 130, Jul. 2024, doi: 10.1007/s00340-024-08264-3.
[55] D. Kleppner, “Rereading Einstein on radiation,” *Phys Today*, vol. 58, no. 2, pp. 30–33, 2005.
[56] A. Javan, W. R. Bennett Jr, and D. R. Herriott, “Population inversion and continuous optical maser oscillation in a gas discharge containing a He-Ne mixture,” *Phys Rev Lett*, vol. 6, no. 3, p. 106, 1961.
[57] T. H. Maiman, “Optical and microwave-optical experiments in ruby,” *Phys Rev Lett*, vol. 4, no. 11, p. 564, 1960.
[58] T. H. Maiman, “Stimulated optical radiation in ruby,” 1960.
[59] C. K. N. Patel, “Continuous-wave laser action on vibrational-rotational transitions of C O 2,” *Physical review*, vol. 136, no. 5A, p. A1187, 1964.
[60] J. Hecht, “Short history of laser development,” *Optical engineering*, vol. 49, no. 9, p. 91002, 2010.
[61] X. Huang *et al.*, “A two-dimensional π–d conjugated coordination polymer with extremely high electrical conductivity and ambipolar transport behaviour,” *Nat Commun*, vol. 6, no. 1, p. 7408, 2015.
[62] H. A. Haus, “Mode-locking of lasers,” *IEEE Journal of Selected Topics in Quantum Electronics*, vol. 6, no. 6, pp. 1173–1185, 2000.
[63] M. Abedi-Varaki and N. Kant, “Magnetic field-assisted wakefield generation and electron acceleration by Gaussian and super-Gaussian laser pulses in plasma,” *Modern Physics Letters B*, vol. 36, no. 07, p. 2150604, 2022.
[64] V. Thakur and N. Kant, “Stronger self-focusing of a chirped pulse laser with exponential density ramp profile in cold quantum magnetoplasma,” *Optik (Stuttg)*, vol. 172, pp. 191–196, 2018.
[65] V. Thakur and N. Kant, “Combined Effect of Chirp and Exponential Density Ramp on Relativistic Self-focusing of Hermite-Cosine-Gaussian Laser in Collisionless Cold Quantum Plasma,” *Brazilian Journal of Physics*, vol. 49, no. 1, pp. 113–118, Feb. 2019, doi: 10.1007/s13538-018-00624-7.

[66] V. Thakur and N. Kant, “Stronger self-focusing of cosh-Gaussian laser beam under exponential density ramp in plasma with linear absorption,” *Optik (Stuttg)*, vol. 183, pp. 912–917, Apr. 2019, doi: 10.1016/j.ijleo.2019.03.005.
[67] N. Kant and V. Thakur, “Influence of linear absorption and density ramp on self-focusing of the Hermite-Gaussian chirped pulse laser in plasma,” *Opt Quantum Electron*, vol. 53, no. 1, p. 12, 2021.
[68] V. Thakur, S. Kumar, and N. Kant, “Self-focusing of a Bessel–Gaussian laser beam in plasma under density transition,” *Journal of Nonlinear Optical Physics & Materials*, p. 2350038, 2022.
[69] B. S. Rao, A. Moorti, P. A. Naik, and P. D. Gupta, “Effect of chirp on self-modulation and laser wakefield electron acceleration in the regime of quasimonoenergetic electron beam generation,” *Physical Review Special Topics-Accelerators and Beams*, vol. 16, no. 9, p. 91301, 2013.
[70] S. V Bulanov, F. Pegoraro, A. M. Pukhov, and A. S. Sakharov, “Transverse-wake wave breaking,” *Phys Rev Lett*, vol. 78, no. 22, p. 4205, 1997.
[71] H. K. Dua, N. Kant, and V. Thakur, “Second harmonic generation induced by a surface plasma wave on a metallic surface in the presence of a wiggler magnetic field,” *Brazilian Journal of Physics*, vol. 52, no. 2, p. 44, 2022.
[72] V. Sharma, V. Thakur, and N. Kant, “Second harmonic generation of cosh-Gaussian laser beam in magnetized plasma,” *Opt Quantum Electron*, vol. 52, no. 10, p. 444, Oct. 2020, doi: 10.1007/s11082-020-02559-3.
[73] V. Thakur and N. Kant, “Resonant second harmonic generation by a chirped laser pulse in a semiconductor,” *Optik (Stuttg)*, vol. 130, pp. 525–530, 2017.
[74] V. Thakur, S. Vij, V. Sharma, and N. Kant, “Influence of exponential density ramp on second harmonic generation by a short pulse laser in magnetized plasma,” *Optik (Stuttg)*, vol. 171, pp. 523–528, Oct. 2018, doi: 10.1016/j.ijleo.2018.06.086.
[75] V. Thakur and N. Kant, “Effect of pulse slippage on density transition-based resonant third-harmonic generation of short-pulse laser in plasma,” *Front Phys (Beijing)*, vol. 11, no. 4, p. 115202, Aug. 2016, doi: 10.1007/s11467-016-0563-8.
[76] A. Kargarian, K. Hajisharifi, and H. Mehdian, “Nonlinear absorption of short intense laser pulse in multispecies plasma,” *Phys Plasmas*, vol. 23, no. 8, 2016.
[77] S. Kumar, S. Vij, N. Kant, and V. Thakur, “Resonant excitation of THz radiations by the interaction of amplitude-modulated laser beams with an anharmonic CNTs in the presence of static D.C. electric and magnetic fields,” *Chinese Journal of Physics*, vol. 78, pp. 453–462, Aug. 2022, doi: 10.1016/j.cjph.2022.06.004.
[78] S. Kumar, S. Vij, N. Kant, and V. Thakur, “Resonant terahertz generation by cross-focusing of Gaussian laser beams in the array of vertically aligned anharmonic and magnetized CNTs,” *Opt Commun*, vol. 513, p. 128112, Jun. 2022, doi: 10.1016/j.optcom.2022.128112.
[79] V. Sharma and S. Kumar, “To study the effect of laser frequency-chirp on trapped electrons in laser wakefield acceleration,” in *Journal of Physics: Conference Series*, IOP Publishing, 2022, p. 12097.
[80] T. Tajima, X. Q. Yan, and T. Ebisuzaki, “Wakefield acceleration,” *Rev Mod Plasma Phys*, vol. 4, no. 1, p. 7, Dec. 2020, doi: 10.1007/s41614-020-0043-z.

[81] V. Sharma and V. Thakur, “Enhanced laser wakefield acceleration utilizing Hermite–Gaussian laser pulses in homogeneous plasma,” *Journal of Optics*, pp. 1–9, 2023.
[82] V. Sharma, S. Kumar, N. Kant, and V. Thakur, “Excitation of the Laser wakefield by asymmetric chirped laser pulse in under dense plasma,” *Journal of Optics*, pp. 1–7, 2023.
[83] V. Thakur and N. Kant, “Resonant second harmonic generation in plasma under exponential density ramp profile,” *Optik (Stuttg)*, vol. 168, pp. 159–164, Sep. 2018, doi: 10.1016/j.ijleo.2018.04.073.
[84] V. Thakur, S. Vij, V. Sharma, and N. Kant, “Influence of exponential density ramp on second harmonic generation by a short pulse laser in magnetized plasma,” *Optik (Stuttg)*, vol. 171, pp. 523–528, Oct. 2018, doi: 10.1016/j.ijleo.2018.06.086.
[85] V. Thakur and N. Kant, “Optimization of wiggler wave number for density transition based second harmonic generation in laser plasma interaction,” *Optik (Stuttg)*, vol. 142, pp. 455–462, Aug. 2017, doi: 10.1016/j.ijleo.2017.06.005.
[86] P. H. Siegel, “Terahertz technology in biology and medicine,” *IEEE Trans Microw Theory Tech*, vol. 52, no. 10, pp. 2438–2447, 2004.
[87] Y. Sun, S. Combrié, F. Bretenaker, and A. De Rossi, “Mode locking of the hermite-gaussian modes of a nanolaser,” *Phys Rev Lett*, vol. 123, no. 23, p. 233901, 2019.
[88] V. Sharma, V. Thakur, and N. Kant, “Hermite-cosh-Gaussian laser-induced third harmonic generation in plasma,” *Opt Quantum Electron*, vol. 53, no. 6, p. 281, 2021.
[89] N. Kant, S. Vij, S. K. Chakravarti, J. P. Kushwaha, and V. Thakur, “Relativistic Self-Focusing of Hermite-cosh-Gaussian Laser Beam in Magnetoplasma with Exponential Plasma Density Ramp,” *Commun Theor Phys*, vol. 71, no. 12, p. 1469, 2019, doi: 10.1088/0253-6102/71/12/1469.
[90] N. Kant, A. Singh, and V. Thakur, “Second-harmonic generation by a chirped laser pulse with the exponential density ramp profile in the presence of a planar magnetostatic wiggler,” *Laser and Particle Beams*, vol. 37, no. 4, pp. 442–447, Dec. 2019, doi: 10.1017/S0263034619000739.
[91] A. K. Malik, K. P. Singh, B. P. Singh, S. Chaudhary, and U. Verma, “Terahertz radiation generation by frequency mixing of Hermite–cosh–Gaussian laser beams in density-modulated cold magnetized plasma,” *IEEE Transactions on Plasma Science*, vol. 49, no. 9, pp. 3022–3028, 2021.
[92] T. Qian-Jin, C. Da-Ming, Y. Yong-Ai, and H. Qi-Quan, “Propagation properties of off-axis Hermite–cosh–Gaussian beam combinations through a first-order optical system,” *Chinese Physics*, vol. 15, no. 11, p. 2609, 2006.
[93] M. C. Gurjar, K. Gopal, D. N. Gupta, V. V. Kulagin, and H. Suk, “High-Field Coherent Terahertz Radiation Generation From Chirped Laser Pulse Interaction With Plasmas,” *IEEE Transactions on Plasma Science*, vol. 48, no. 10, pp. 3727–3734, Oct. 2020, doi: 10.1109/TPS.2020.3022903.
[94] A. Varma, S. P. Mishra, A. Kumar, and A. Kumar, “Electron Bernstein wave aided Hermite cosh-Gaussian laser beam absorption in collisional plasma,” *Laser Phys Lett*, vol. 20, no. 7, p. 76001, 2023.

[95] P. Kad, V. Rana, and A. Singh, “Dynamics of Hermite–Gaussian laser beam in plasma and terahertz generation,” *Optik (Stuttg)*, vol. 274, p. 170498, 2023.
[96] A. Kumar, A. Kumar, S. P. Mishra, M. S. Yadav, and A. Varma, “Plasma wave aided heating of collisional nanocluster plasma by nonlinear interaction of two high power laser beams,” *Opt Quantum Electron*, vol. 54, no. 11, p. 753, 2022.
[97] N. Gupta and S. B. Bhardwaj, “Nonlinear interaction of Bessel–Gauss laser beams with plasmas with axial temperature ramp,” *Journal of Optics*, vol. 51, no. 4, pp. 950–959, 2022.
[98] N. Gupta, S. Kumar, and S. B. Bhardwaj, “Stimulated Raman scattering of self focused elliptical q-Gaussian laser beam in plasma with axial temperture ramp: effect of ponderomotive force,” *J Electromagn Waves Appl*, vol. 36, no. 6, pp. 767–786, 2022.
[99] Já. Hebling, K.-L. Yeh, M. C. Hoffmann, and K. A. Nelson, “High-Power THz Generation, THz Nonlinear Optics, and THz Nonlinear Spectroscopy,” *IEEE Journal of Selected Topics in Quantum Electronics*, vol. 14, no. 2, pp. 345–353, 2008, doi: 10.1109/JSTQE.2007.914602.
[100] S. Watanabe, “Terahertz Polarization Imaging and Its Applications,” *Photonics*, vol. 5, no. 4, p. 58, Dec. 2018, doi: 10.3390/photonics5040058.
[101] K. Rikkinen, P. Kyosti, M. E. Leinonen, M. Berg, and A. Parssinen, “THz Radio Communication: Link Budget Analysis toward 6G,” *IEEE Communications Magazine*, vol. 58, no. 11, pp. 22–27, Nov. 2020, doi: 10.1109/MCOM.001.2000310.
[102] A. A. Gowen, C. O’Sullivan, and C. P. O’Donnell, “Terahertz time domain spectroscopy and imaging: Emerging techniques for food process monitoring and quality control,” *Trends Food Sci Technol*, vol. 25, no. 1, pp. 40–46, May 2012, doi: 10.1016/j.tifs.2011.12.006.
[103] S. Kumar, S. Vij, N. Kant, A. Mehta, and V. Thakur, “Resonant terahertz generation from laser filaments in the presence of static electric field in a magnetized collisional plasma,” *The European Physical Journal Plus*, vol. 136, no. 2, p. 148, Feb. 2021, doi: 10.1140/epjp/s13360-021-01089-5.
[104] N. Gupta, “Effect of orbital angular momentum of light on self-action effects of Laguerre Gaussian laser beams in collisionless plasmas,” *Journal of Optics*, vol. 50, no. 3, pp. 466–477, 2021.
[105] S. Kumar, S. Vij, N. Kant, and V. Thakur, “Resonant Terahertz Generation by the Interaction of Laser Beams with Magnetized Anharmonic Carbon Nanotube Array,” *Plasmonics*, vol. 17, no. 1, pp. 381–388, Feb. 2022, doi: 10.1007/s11468-021-01529-z.
[106] S. Kumar, N. Kant, and V. Thakur, “THz generation by self-focused Gaussian laser beam in the array of anharmonic VA-CNTs,” *Opt Quantum Electron*, vol. 55, no. 3, p. 281, Mar. 2023, doi: 10.1007/s11082-023-04562-w.
[107] V. Thakur, S. Vij, N. Kant, and S. Kumar, “THz generation by propagating lasers through magnetized SWCNTs,” *Indian Journal of Physics*, vol. 97, no. 7, pp. 2191–2196, Jun. 2023, doi: 10.1007/s12648-022-02575-x.
[108] S. Kumar, S. Vij, N. Kant, and V. Thakur, “Combined effect of transverse electric and magnetic fields on THz generation by beating of two amplitude-modulated laser beams in the collisional plasma,” *Journal of Astrophysics and Astronomy*, vol. 43, no. 1, p. 30, Jun. 2022, doi: 10.1007/s12036-022-09805-y.

[109] S. Kumar, S. Vij, N. Kant, and V. Thakur, “Interaction of obliquely incident lasers with anharmonic CNTs acting as dipole antenna to generate resonant THz radiation,” *Waves in Random and Complex Media*, pp. 1–13, Dec. 2022, doi: 10.1080/17455030.2022.2155330.
[110] N. Gupta, R. Johari, S. Kumar, S. B. Bhardwaj, and S. Choudhry, “Optical guiding of q-Gaussian laser beams in radial density plasma channel created by two prepulses: ignitor and heater,” *Journal of Optics*, vol. 51, no. 3, pp. 749–760, 2022.
[111] N. Gupta, S. Kumar, S. B. Bhardwaj, S. Kumar, and S. Choudhry, “Nonlinear interaction of quadruple Gaussian laser beams with narrow band gap semiconductors,” *Journal of Optics*, pp. 1–14, 2021.
[112] A. A. Frolov, “Terahertz emission at a p -polarized laser radiation action on plasma,” *Phys Plasmas*, vol. 28, no. 1, Jan. 2021, doi: 10.1063/5.0033225.
[113] X. Xie, J. Dai, and X.-C. Zhang, “Coherent Control of THz Wave Generation in Ambient Air,” *Phys Rev Lett*, vol. 96, no. 7, p. 075005, Feb. 2006, doi: 10.1103/PhysRevLett.96.075005.
[114] M. Hashemzadeh, “Terahertz radiation generation through nonlinear interaction of frequency chirped laser pulses with hot inhomogeneous plasmas,” *Waves in Random and Complex Media*, vol. 32, no. 5, pp. 2279–2296, Sep. 2022, doi: 10.1080/17455030.2020.1849870.
[115] Y. T. Li *et al.*, “Strong terahertz radiation from relativistic laser interaction with solid density plasmas,” *Appl Phys Lett*, vol. 100, no. 25, Jun. 2012, doi: 10.1063/1.4729874.
[116] H. Huang, T. Nagashima, W. Hsu, S. Juodkazis, and K. Hatanaka, “Dual THz Wave and X-ray Generation from a Water Film under Femtosecond Laser Excitation,” *Nanomaterials*, vol. 8, no. 7, p. 523, Jul. 2018, doi: 10.3390/nano8070523.
[117] G.-Q. Liao and Y.-T. Li, “Review of Intense Terahertz Radiation from Relativistic Laser-Produced Plasmas,” *IEEE Transactions on Plasma Science*, vol. 47, no. 6, pp. 3002–3008, Jun. 2019, doi: 10.1109/TPS.2019.2915624.
[118] Z.-M. Sheng, H.-C. Wu, K. Li, and J. Zhang, “Terahertz radiation from the vacuum-plasma interface driven by ultrashort intense laser pulses,” *Phys Rev E*, vol. 69, no. 2, p. 025401, Feb. 2004, doi: 10.1103/PhysRevE.69.025401.
[119] M. Amouamouha, F. Bakhtiari, and B. Ghafary, “Self-focused amplitude modulated super Gaussian laser beam in plasma and THz radiation with high efficiency,” *Results Phys*, vol. 17, p. 103086, Jun. 2020, doi: 10.1016/j.rinp.2020.103086.
[120] H. Hamster, A. Sullivan, S. Gordon, W. White, and R. W. Falcone, “Subpicosecond, Electromagnetic Pulses from Intense Laser-Plasma Interaction,” 1993.
[121] V. Thakur and N. Kant, “Resonant second harmonic generation in plasma under exponential density ramp profile,” *Optik (Stuttg)*, vol. 168, pp. 159–164, Sep. 2018, doi: 10.1016/j.ijleo.2018.04.073.
[122] M. Hashemzadeh, “Terahertz Radiation Generation by Hermite-cosh Gaussian and Hollow Gaussian Laser Beams in Magnetized Inhomogeneous Plasmas,” *Brazilian Journal of Physics*, vol. 53, no. 2, p. 46, Apr. 2023, doi: 10.1007/s13538-023-01261-5.

[123] F. Jahangiri, M. Hashida, T. Nagashima, S. Tokita, M. Hangyo, and S. Sakabe, “Intense terahertz emission from atomic cluster plasma produced by intense femtosecond laser pulses,” *Appl Phys Lett*, vol. 99, no. 26, Dec. 2011, doi: 10.1063/1.3672814.
[124] V. Sharma, V. Thakur, and N. Kant, “Second harmonic generation of cosh-Gaussian laser beam in magnetized plasma,” *Opt Quantum Electron*, vol. 52, no. 10, p. 444, Oct. 2020, doi: 10.1007/s11082-020-02559-3.
[125] F. Bakhtiari, M. Esmaeilzadeh, and B. Ghafary, “Terahertz radiation with high power and high efficiency in a magnetized plasma,” *Phys Plasmas*, vol. 24, no. 7, Jul. 2017, doi: 10.1063/1.4991395.
[126] V. Thakur and N. Kant, “Combined Effect of Chirp and Exponential Density Ramp on Relativistic Self-focusing of Hermite-Cosine-Gaussian Laser in Collisionless Cold Quantum Plasma,” *Brazilian Journal of Physics*, vol. 49, no. 1, pp. 113–118, Feb. 2019, doi: 10.1007/s13538-018-00624-7.
[127] S. Mou *et al.*, “Impact of laser chirp on the polarization of terahertz from two-color plasma,” *Photonics Res*, vol. 11, no. 6, p. 978, Jun. 2023, doi: 10.1364/PRJ.468899.
[128] A. Nguyen, P. G. de A. Martínez, I. Thiele, S. Skupin, and L. Bergé, “THz field engineering in two-color femtosecond filaments using chirped and delayed laser pulses,” *New J Phys*, vol. 20, no. 3, p. 033026, Mar. 2018, doi: 10.1088/1367-2630/aaa470.
[129] L. Zhang, L. Z. Ji, P. Y. Sun, Z. H. Jiao, S. F. Zhao, and G. L. Wang, “Enhanced terahertz generation by controlling electron trajectory with chirp laser field,” *Indian Journal of Physics*, Jul. 2023, doi: 10.1007/s12648-023-02834-5.
[130] X. Xu *et al.*, “Laser-Chirp Controlled Terahertz Wave Generation from Air Plasma,” *Chinese Physics Letters*, vol. 40, no. 4, p. 045201, Apr. 2023, doi: 10.1088/0256-307X/40/4/045201.
[131] Z. Ghayemmoniri, R. N. Siahmazgi, and S. Jafari, “Terahertz radiation generation driven by beating of chirped laser pulses in single-walled carbon nanotubes by applying tapered magnetic field,” *The European Physical Journal D*, vol. 77, no. 3, p. 48, Mar. 2023, doi: 10.1140/epjd/s10053-023-00612-w.
[132] H. Hora, “Self-focusing of laser beams in a plasma by ponderomotive forces,” *Zeitschrift für Physik A Hadrons and nuclei*, vol. 226, no. 2, pp. 156–159, Apr. 1969, doi: 10.1007/BF01392018.
[133] V. Thakur and N. Kant, “Combined Effect of Chirp and Exponential Density Ramp on Relativistic Self-focusing of Hermite-Cosine-Gaussian Laser in Collisionless Cold Quantum Plasma,” *Brazilian Journal of Physics*, vol. 49, no. 1, pp. 113–118, Feb. 2019, doi: 10.1007/s13538-018-00624-7.
[134] P. Sprangle, G. Joyce, E. Esarey, and A. Ting, “Laser wakefield acceleration and relativstic optical guiding,” in *AIP Conference Proceedings*, AIP, 1988, pp. 231–239. doi: 10.1063/1.37621.
[135] V. Thakur and N. Kant, “Optimization of wiggler wave number for density transition based second harmonic generation in laser plasma interaction,” *Optik (Stuttg)*, vol. 142, pp. 455–462, Aug. 2017, doi: 10.1016/j.ijleo.2017.06.005.

[136] R. A. Ganeev, “High-order harmonic generation in a laser plasma: a review of recent achievements,” *Journal of Physics B: Atomic, Molecular and Optical Physics*, vol. 40, no. 22, pp. R213–R253, Nov. 2007, doi: 10.1088/0953-4075/40/22/R01.
[137] V. Thakur and N. Kant, “Effect of pulse slippage on density transition-based resonant third-harmonic generation of short-pulse laser in plasma,” *Front Phys (Beijing)*, vol. 11, no. 4, p. 115202, Aug. 2016, doi: 10.1007/s11467-016-0563-8.
[138] U. Teubner and P. Gibbon, “High-order harmonics from laser-irradiated plasma surfaces,” *Rev Mod Phys*, vol. 81, no. 2, pp. 445–479, Apr. 2009, doi: 10.1103/RevModPhys.81.445.
[139] Y. Ueno and K. Ajito, “Analytical terahertz spectroscopy,” *Analytical Sciences*, vol. 24, no. 2, pp. 185–192, 2008.
[140] Y. H. Tao, A. J. Fitzgerald, and V. P. Wallace, “Non-contact, non-destructive testing in various industrial sectors with terahertz technology,” *Sensors*, vol. 20, no. 3, p. 712, 2020.
[141] D. D. Arnone *et al.*, “Applications of terahertz (THz) technology to medical imaging,” in *Terahertz Spectroscopy and Applications II*, SPIE, 1999, pp. 209–219.
[142] L. W. Casperson and A. A. Tovar, “Hermite–sinusoidal-Gaussian beams in complex optical systems,” *JOSA A*, vol. 15, no. 4, pp. 954–961, 1998.
[143] A. Belafhal and M. Ibnchaikh, “Propagation properties of Hermite-cosh-Gaussian laser beams,” *Opt Commun*, vol. 186, no. 4–6, pp. 269–276, 2000.
[144] S. D. Patil, M. V Takale, S. T. Navare, and M. B. Dongare, “Focusing of Hermite-cosh-Gaussian laser beams in collisionless magnetoplasma,” *Laser and Particle Beams*, vol. 28, no. 2, pp. 343–349, 2010.
[145] V. Nanda, N. Kant, and M. A. Wani, “Self-focusing of a Hermite-cosh Gaussian laser beam in a magnetoplasma with ramp density profile,” *Phys Plasmas*, vol. 20, no. 11, 2013.
[146] V. Nanda and N. Kant, “Enhanced relativistic self-focusing of Hermite-cosh-Gaussian laser beam in plasma under density transition,” *Phys Plasmas*, vol. 21, no. 4, 2014.
[147] S. Kaur, M. Kaur, R. Kaur, and T. S. Gill, “Propagation characteristics of Hermite-cosh-Gaussian laser beam in a rippled density plasmas,” *Laser and Particle Beams*, vol. 35, no. 1, pp. 100–107, 2017.
[148] M. A. Wani, H. S. Ghotra, and N. Kant, “Self-focusing of Hermite-cosh-Gaussian laser beam in semiconductor quantum plasma,” *Optik (Stuttg)*, vol. 154, pp. 497–502, 2018.
[149] A. Varma and A. Kumar, “Electron Bernstein wave aided beat wave of Hermite-cosh-Gaussian laser beam absorption in a collisional nanocluster plasma,” *Optik (Stuttg)*, vol. 245, p. 167702, 2021.
[150] J. Wadhwa and A. Singh, “Generation of second harmonics of intense Hermite–Gaussian laser beam in relativistic plasma,” *Laser and Particle Beams*, vol. 37, no. 1, pp. 79–85, 2019.
[151] H. Hamster, A. Sullivan, S. Gordon, and R. W. Falcone, “Short-pulse terahertz radiation from high-intensity-laser-produced plasmas,” *Phys Rev E*, vol. 49, no. 1, p. 671, 1994.

[152] S. Safari and B. Jazi, “About generation of terahertz radiation due to the nonlinear interaction of Gaussian and Hermite–Cosh–Gaussian laser beams in collisional plasma background: Optimization and field profile controlling,” *IEEE Transactions on Plasma Science*, vol. 47, no. 1, pp. 155–161, 2018.
[153] S. Chaudhary, K. P. Singh, U. Verma, and A. K. Malik, “Radially polarized terahertz (THz) generation by frequency difference of Hermite Cosh Gaussian lasers in hot electron-collisional plasma,” *Opt Lasers Eng*, vol. 134, p. 106257, 2020.
[154] M. Hashemzadeh, “Terahertz Radiation Generation by Hermite-cosh Gaussian and Hollow Gaussian Laser Beams in Magnetized Inhomogeneous Plasmas,” *Brazilian Journal of Physics*, vol. 53, no. 2, p. 46, 2023, doi: 10.1007/s13538-023-01261-5.
[155] S. Safari, A. R. Niknam, F. Jahangiri, and B. Jazi, “Terahertz radiation generation through the nonlinear interaction of Hermite and Laguerre Gaussian laser beams with collisional plasma: field profile optimization,” *J Appl Phys*, vol. 123, no. 15, 2018.
[156] J. Rajput, A. K. Pramanik, P. Kumar, S. S. Gaur, R. Singh, and N. Kant, “Comparative study of electron acceleration by linearly and circularly polarized Hermite-cosh-Gaussian laser pulse in a vacuum,” *Journal of Optics*, vol. 52, no. 2, pp. 642–647, 2023.
[157] X. Wu *et al.*, “Highly efficient generation of 0.2 mJ terahertz pulses in lithium niobate at room temperature with sub-50 fs chirped Ti: sapphire laser pulses,” *Opt Express*, vol. 26, no. 6, pp. 7107–7116, 2018.
[158] J. Li *et al.*, “Efficient terahertz wave generation from GaP crystals pumped by chirp-controlled pulses from femtosecond photonic crystal fiber amplifier,” *Appl Phys Lett*, vol. 104, no. 3, 2014.
[159] P. F. Taday, I. V. Bradley, D. D. Arnone, and M. Pepper, “Using terahertz pulse spectroscopy to study the crystalline structure of a drug: A case study of the polymorphs of ranitidine hydrochloride,” *J Pharm Sci*, vol. 92, no. 4, pp. 831–838, Apr. 2003, doi: 10.1002/jps.10358.
[160] D. S. Sitnikov *et al.*, “Effects of high intensity non-ionizing terahertz radiation on human skin fibroblasts,” *Biomed Opt Express*, vol. 12, no. 11, p. 7122, Nov. 2021, doi: 10.1364/BOE.440460.
[161] D. Crawley, C. Longbottom, V. P. Wallace, B. Cole, D. Arnone, and M. Pepper, “Three-dimensional terahertz pulse imaging of dental tissue,” *J Biomed Opt*, vol. 8, no. 2, p. 303, 2003, doi: 10.1117/1.1559059.
[162] D. Hou *et al.*, “Terahertz spectroscopic investigation of human gastric normal and tumor tissues,” *Phys Med Biol*, vol. 59, no. 18, pp. 5423–5440, Sep. 2014, doi: 10.1088/0031-9155/59/18/5423.
[163] Q. Wang, S. Hameed, L. Xie, and Y. Ying, “Non-destructive quality control detection of endogenous contaminations in walnuts using terahertz spectroscopic imaging,” *Journal of Food Measurement and Characterization*, vol. 14, no. 5, pp. 2453–2460, Oct. 2020, doi: 10.1007/s11694-020-00493-2.
[164] A. Kaur, S. Rani, and B. Kaur, “Ultrasound assisted removal of cadmium ions from wastewater using ionic liquid modified aluminium isopropoxide,” *Agrochimica*, vol. 67, no. 1, pp. 91–102, Aug. 2023, doi: 10.12871/000218572023127.

[165] Y. Takida, K. Nawata, and H. Minamide, “Security screening system based on terahertz-wave spectroscopic gas detection,” *Opt Express*, vol. 29, no. 2, p. 2529, Jan. 2021, doi: 10.1364/OE.413201.
[166] W. R. Tribe, D. A. Newnham, P. F. Taday, and M. C. Kemp, “Hidden object detection: security applications of terahertz technology,” R. J. Hwu, Ed., Apr. 2004, p. 168. doi: 10.1117/12.543049.
[167] W. Jiang *et al.*, “Terahertz communications and sensing for 6G and beyond: A comprehensive review,” *IEEE Communications Surveys & Tutorials*, 2024.
[168] R. P. Sharma, A. Monika, P. Sharma, P. Chauhan, and A. Ji, “Interaction of high power laser beam with magnetized plasma and THz generation,” *Laser and Particle Beams*, vol. 28, no. 4, pp. 531–537, 2010.
[169] L. V. Titova, C. L. Pint, Q. Zhang, R. H. Hauge, J. Kono, and F. A. Hegmann, “Generation of Terahertz Radiation by Optical Excitation of Aligned Carbon Nanotubes,” *Nano Lett*, vol. 15, no. 5, pp. 3267–3272, May 2015, doi: 10.1021/acs.nanolett.5b00494.
[170] J. Singh, S. Rani, H. K. Midha, V. Sharma, and V. Thakur, “Parametric analysis of THz wave generation efficiency and plasma density using Sinh-Gaussian beams,” *Journal of Optics*, Jun. 2024, doi: 10.1007/s12596-024-01988-7.
[171] V. Thakur and S. Kumar, “Terahertz generation in ripple density hot plasma under the influence of static magnetic field,” *Journal of Optics*, Jan. 2024, doi: 10.1007/s12596-023-01588-x.
[172] R. Kumar, K. Gopal, D. Singh, and S. Singh, “Terahertz Field Generation by Beating of Mixed Profile Lasers in Under-Dense Plasma,” *IEEE Transactions on Plasma Science*, pp. 1–9, 2024, doi: 10.1109/TPS.2024.3365824.
[173] K. Gopal, D. N. Gupta, S. Singh, and A. Vijay, “Terahertz radiation generation from amplitude-modulated laser filament interaction with a magnetized plasma,” *Modern Physics Letters B*, Jan. 2024, doi: 10.1142/S0217984924501926.
[174] S. Kumar, N. Kant, and V. Thakur, “THz generation by self-focused Gaussian laser beam in the array of anharmonic VA-CNTs,” *Opt Quantum Electron*, vol. 55, no. 3, p. 281, Mar. 2023, doi: 10.1007/s11082-023-04562-w.
[175] H. K. Midha, V. Sharma, N. Kant, and V. Thakur, “Efficient THz generation by Hermite-cosh-Gaussian lasers in plasma with slanting density modulation,” *Journal of Optics*, Oct. 2023, doi: 10.1007/s12596-023-01413-5.
[176] S. Kumar, V. Thakur, and N. Kant, “Magnetically enhanced THz generation by self-focusing laser in VA-MCNTs,” *Phys Scr*, vol. 98, no. 8, p. 085506, Aug. 2023, doi: 10.1088/1402-4896/ace1ae.
[177] S. Kumar, S. Vij, N. Kant, and V. Thakur, “Nonlinear Interaction of Amplitude-Modulated Gaussian Laser Beam with Anharmonic Magnetized and Rippled CNTs: THz Generation,” *Brazilian Journal of Physics*, vol. 53, no. 2, p. 37, Apr. 2023, doi: 10.1007/s13538-022-01252-y.
[178] M. Kumar, H. S. Song, J. Lee, D. Park, H. Suk, and M. S. Hur, “Intense multicycle THz pulse generation from laser-produced nanoplasmas,” *Sci Rep*, vol. 13, no. 1, p. 4233, Mar. 2023, doi: 10.1038/s41598-023-31427-9.

[179] Y. Chen, Y. He, L. Liu, Z. Tian, and J. Dai, “Interaction of colliding laser pulses with gas plasma for broadband coherent terahertz wave generation,” *Photonics Res*, vol. 11, no. 9, p. 1562, Sep. 2023, doi: 10.1364/PRJ.487934.
[180] H. K. Midha, V. Sharma, N. Kant, and V. Thakur, “Optimizing terahertz emission with Hermite–Gaussian laser beams in collisional slanted up density plasma,” *Journal of Optics*, Mar. 2024, doi: 10.1007/s12596-024-01696-2.
[181] A. P. Singh, K. Gopal, D. N. Gupta, M. Kundu, and P. Varshney, “Laser beat-wave interaction with electron–hole plasmas relevant to terahertz field generation,” *Indian Journal of Physics*, vol. 98, no. 1, pp. 383–389, Jan. 2024, doi: 10.1007/s12648-023-02832-7.
[182] Ashish, K. Gopal, S. Singh, and D. N. Gupta, “High-intensity laser pulse interaction with a counter propagating electron beam for terahertz field generation in magnetized plasmas,” *Opt Quantum Electron*, vol. 55, no. 7, p. 605, Jul. 2023, doi: 10.1007/s11082-023-04889-4.
[183] A. A. M. Choobini and F. M. Aghamir, “Variable laser profiles and polarization states in the wave-mixing scheme for the generation of THz radiation in collisional-magnetized clustered-plasma,” *Phys Plasmas*, vol. 30, no. 12, Dec. 2023, doi: 10.1063/5.0173130.
[184] A. A. M. Choobini and F. M. Aghamir, “Generation of High-Power Terahertz Waves in a Collisional and Magnetized Plasma by Two-Color Femtosecond Laser Beams,” *IEEE Transactions on Plasma Science*, vol. 51, no. 2, pp. 589–597, Feb. 2023, doi: 10.1109/TPS.2022.3227397.
[185] M. R. Jafari Milani, “<scp>THz</scp> generation and spatiotemporal variation of two cross-focused Gaussian laser pulses in plasma,” *Contributions to Plasma Physics*, Apr. 2024, doi: 10.1002/ctpp.202400001.
[186] V. Sharma and V. Thakur, “A comprehensive study of magnetic field-induced modifications in sin-Gaussian pulse-driven laser wakefield acceleration,” *Journal of Optics*, Feb. 2024, doi: 10.1007/s12596-023-01636-6.
[187] V. Sharma and V. Thakur, “Comparative analysis of electron acceleration by Gaussian and cosh-Gaussian laser pulses in homogeneous plasma through laser wakefield acceleration,” *Journal of Optics*, Mar. 2024, doi: 10.1007/s12596-024-01760-x.
[188] V. Sharma and V. Thakur, “Enhanced laser wakefield acceleration utilizing Hermite–Gaussian laser pulses in homogeneous plasma,” *Journal of Optics*, Dec. 2023, doi: 10.1007/s12596-023-01565-4.
[189] V. Sharma, N. Kant, and V. Thakur, “Exploring sin-Gaussian laser pulses for efficient electron acceleration in plasma,” *Opt Quantum Electron*, vol. 56, no. 4, p. 601, Jan. 2024, doi: 10.1007/s11082-023-06262-x.
[190] V. Sharma, N. Kant, and V. Thakur, “Optimizing laser-driven electron acceleration with sinh-squared Gaussian pulses,” *Journal of Optics*, Feb. 2024, doi: 10.1007/s12596-023-01649-1.
[191] V. Thakur and N. Kant, “Resonant second harmonic generation of chirped pulse laser in plasma,” *Optik (Stuttg)*, vol. 129, pp. 239–247, Jan. 2017, doi: 10.1016/j.ijleo.2016.10.068.
[192] V. Thakur and N. Kant, “Resonant second harmonic generation in plasma under exponential density ramp profile,” *Optik (Stuttg)*, vol. 168, pp. 159–164, Sep. 2018, doi: 10.1016/j.ijleo.2018.04.073.

[193] Singh M and Gupta D N, “Relativistic Third-Harmonic Generation of a Laser in a Self-Sustained Magnetized Plasma Channel,” *IEEE J Quantum Electron*, vol. 50, no. 6, pp. 491–496, Jun. 2014, doi: 10.1109/JQE.2014.2320763.
[194] H. K. Midha, V. Sharma, N. Kant, and V. Thakur, “Resonant Terahertz radiation by p-polarised chirped laser in hot plasma with slanting density modulation,” *Journal of Optics*, Dec. 2023, doi: 10.1007/s12596-023-01563-6.
[195] J. Singh, H. K. Midha, S. Rani, V. Sharma, and V. Thakur, “Advancements in efficient Terahertz generation techniques for diverse applications in spectroscopic studies,” *Journal of Optics*, May 2024, doi: 10.1007/s12596-024-01822-0.
[196] H. K. Midha, V. Sharma, N. Kant, and V. Thakur, “Hermite-Gaussian laser modulation for optimal THz emission in collisional homogeneous plasma,” *Journal of Optics*, May 2024, doi: 10.1007/s12596-024-01910-1.
[197] S. Ruschin, E. Yaakobi, and E. Shekel, “Gaussian content as a laser beam quality parameter,” *Appl Opt*, vol. 50, no. 22, p. 4376, Aug. 2011, doi: 10.1364/AO.50.004376.